

Structural Engineering Report No. ST-00-4

**LOCAL FLANGE BENDING AND LOCAL
WEB YIELDING LIMIT STATES IN STEEL
MOMENT-RESISTING CONNECTIONS**

**Sara D. Prochnow, Robert J. Dexter, Jerome F. Hajjar,
Yanqun Ye, and Sean C. Cotton**

November 2000

**Department of Civil Engineering
Institute of Technology
University of Minnesota
Minneapolis, Minnesota 55455**

Abstract

Following the 1994 Northridge Earthquake, connection fractures were detected in approximately 100 steel moment-resisting frame buildings. Observational studies of the damaged buildings directly after the earthquake reported that connections with continuity plates performed better than connections with the stiffeners. This led to a subsequent tendency to over-specify continuity plates and doubler plates. However, not only does this lead to more expensive details, but may also result in an unwanted response of fabrication fractures due to the large residual stresses from the complete joint penetration welds needed by the larger stiffeners. Therefore, the main objective of the research project is to reassess the design criteria and new alternatives for continuity plate and doubler plate detailing in both non-seismic and seismic applications. The research project was divided into three components: monotonically-loaded pull-plate tests focused on the non-seismic behavior of the details, cyclically-loaded cruciform tests to investigate the stiffening details in seismic applications, and finite element analyses to corroborate the experiments and to conduct a parametric study of various stiffening details. This report contains details of the pull-plate tests.

The specific goals of the pull-plate tests were to reassess the non-seismic local web yielding (LWY) and local flange bending provisions (LFB), to determine the required thickness of continuity plates, to investigate the use of fillet welds instead of complete joint penetration (CJP) welds to connect the continuity plates to the column flanges, and to evaluate alternative doubler plate details.

A literature review of past experimental and analytical work related to the design and behavior of continuity plates was conducted and is reported herein. The history of the LWY and LFB equations, which are used in non-seismic design to assess the stiffening that a column requires, were traced back to the founding research of the 1950's and 1960's. Opinions regarding the behavior of continuity plates and the continuity plate welds are summarized from research conducted in the 1940's through current post-Northridge research.

The research project included tests of nine pull-plate specimens, using three column sections (W14x132, W14x145, and W14x159) and various stiffening details. The column sizes were chosen based on a computational parametric study of the need for column stiffening, previous tested column sections, and results from preliminary finite element analyses. The tested stiffening details were continuity plates with half the thickness of the girder flanges (or pull-plates) connected to the column flanges with fillet welds, continuity plates with the full thickness of the pull-plates connected to the column flanges with CJP welds, and a doubler plate box detail. The CJP welds connecting the pull-plates to the column flanges were made using post-Northridge weld details and an E70T-6 weld electrode. The continuity plate and doubler plate welds were made with an E70T-1 weld electrode.

The ultimate failure of all the specimens was fracture of the pull-plate. None of the E70T-6 CJP welds fractured, nor did the welds of the continuity plates or doubler plates. The combined experimental and computational results showed that the equations for LFB and LWY are reasonable and slightly conservative in calculating the need for column stiffening for a non-seismic demand. To better describe the nonlinear behavior in the column web k-line, an LWY equation was determined based upon a quadratic stress distribution in the column web. The LFB bending equation was also examined and augmented to better fit the yield lines seen in the specimens. These equations are presented as potential alternatives to, but not necessarily replacements, for the current equations.

Continuity plates that are only half as thick as the beam flange and are fillet-welded to both the column web and flanges performed satisfactorily. The plates effectively restrained the column section from excessive web yielding or flange bending, and the fillet welds did not fracture. The doubler plate box detail that was CJP welded near the tips of the column flanges performed satisfactorily and provided sufficient stiffness to avoid both LWY and LFB. The detail would be most cost effective when needed to act as both a doubler plate (to eliminate excessive panel zone deformation) and a continuity plate (to restrain from exceeding the LWY and LFB limit states).

Acknowledgements

Funding for this research was provided by the American Institute of Steel Construction and the University of Minnesota. In-kind funding and materials were provided by LeJeune Steel Company, Minneapolis, Minnesota and Braun Intertec, Minneapolis, Minnesota. Supercomputing resources were provided by the Minnesota Supercomputing Institute.

I would like to thank my advisors, Dr. Robert D. Dexter and Dr. Jerome F. Hajjar for their guidance in this research. My fellow graduate student research partners, Sean C. Cotton and Yanqun Ye, deserve recognition for their collaborative efforts. I would also like to thank Dr. Theodore V. Galambos of the University of Minnesota and Lawrence A. Kloiber of LeJeune Steel Company for their assistance in designing, detailing, and fabricating the test specimens. Special acknowledgement goes to Paul M. Bergson who gladly suffered my lack of lab experience.

Any opinions, findings, and conclusions or recommendations expressed in this material are those of the author and do not necessarily reflect the views of the sponsors.

Table of Contents

Abstract	i
Acknowledgements	iii
Table of Contents	iv
List of Figures	vi
List of Tables	xiv
1 Introduction	1
1.1 Research Objectives.....	3
1.2 Organization of the Report.....	4
2 Background of Continuity Plate Design Provisions	6
2.1 Definition of the Limit States.....	6
2.2 Opinions Regarding Continuity Plate Behavior and Design.....	19
3 Experimental Procedure	25
3.1 Parametric Study of Continuity Plate Requirements	25
3.1.1 Definitions of Parameters.....	25
3.1.2 Results of Continuity Plate Parameter Study.....	30
3.1.3 Conclusions of Continuity Plate Parametric Study.....	33
3.2 Specimen Selection.....	34
3.2.1 Pull-Plate Specimen Selection Procedure.....	34
3.2.2 Pull-Plate Specimen Justification.....	47
3.2.2.1 Preliminary Finite Element Analyses to Predict Specimen Behavior.....	47
3.2.2.2 Specimen Parameter Discussion.....	54

3.3 Specimen Design.....	56
3.3.1 Specimen Connection Description.....	56
3.3.2 Weld Description.....	63
3.4 Material Properties.....	64
3.4.1 Steel Material Properties.....	64
3.4.2 Weld Material Testing.....	70
3.5 Testing Procedure.....	72
3.6 Instrumentation Plan.....	73
4 Specimen Behavior and Interpretation of Results.....	80
4.1 Definition of Failure Modes and Yield Mechanisms	81
4.2 Effect of Eccentric Loading	84
4.3 Comparison of Specimens and Finite Element Analysis.....	87
4.4 Specimen Behavior.....	97
4.4.1 Local Web Yielding.....	100
4.4.2 Local Flange Bending.....	112
4.4.3 Column Stiffener Behavior.....	131
4.4.3.1 Continuity Plates.....	131
4.4.3.2 Doubler Plate Box Detail.....	134
5 Summary and Conclusions.....	139
5.1 Summary.....	139
5.2 Conclusions.....	141
Appendix A.....	144
References.....	241

List of Figures

2.1	Local Web Yielding Definitions [after (AISC, 1937)].....	7
2.2	Local Web Yielding Definitions [after (AISC, 1999b)].....	12
2.3a	Illustrations of Local Flange Bending.....	13
2.3b	Illustration of Local Flange Bending.....	13
2.4	Column Flange Model [after (Graham et al., 1960)].....	16
3.1	One-Quarter Symmetric Finite Element Model of Pull-Plate Specimen.....	48
3.2	Finite Element Mesh of Unstiffened Specimens [after (Ye et al., 2000)]	49
3.3	Stress-Strain Curve of A992 Steel [after (Ye et al., 2000)].....	50
3.4	Comparison of Strain in Web vs. Load for Possible Pull-Plate Specimens..	51
3.5	Comparison of Strain in Web vs. Load for Possible Pull-Plate Specimens...	52
3.6	Comparison of Strain in Column Flange vs. Load for Possible Pull-Plate Specimens.....	52
3.7	Comparison of Strain in Column Flange vs. Load for Possible Pull-Plate Specimens.....	53
3.8	Comparison of Flange Separation vs. Load for Possible Pull-Plate Specimens.....	53
3.9	Specimens 1-LFB and 2-LFB.....	58
3.10	Doubler Plate Fillet Weld on Specimens 1-LFB and 2-LFB.....	58
3.11	Specimens 1-LWY, 2-LWY, and 3-UNST.....	59
3.12	Specimens 1-HCP and 1B-HCP.....	60
3.13	Specimen 1-FCP.....	61
3.14	Specimen 1-DP.....	62
3.15	CJP Weld Connecting Pull-Plate to Column Flange.....	64
3.16	Location of CVN Coupons.....	67
3.17	Rockwell Hardness Values B-Scale of W14x132.....	69
3.18	Rockwell Hardness Values B-Scale of W14x145.....	69

3.19	Rockwell Hardness Values B-Scale of W14x159.....	70
3.20a	Longitudinal Cross-Section of CJP and Fillet Welds of Specimen 1-HCP...	71
3.20b	Transverse Cross-Section of CJP and Fillet Welds of Specimen 1-HCP....	71
3.21a	Longitudinal Cross-Section of CJP and Fillet Welds of Specimen 2-LFB...	72
3.21b	Transverse Cross-Section of CJP and Fillet Welds of Specimen 2-LFB.....	72
3.22a	Longitudinal Cross-Section of CJP and Fillet Welds of Specimen 3-UNST.	72
3.22b	Transverse Cross-Section of CJP and Fillet Welds of Specimen 3-UNST...	72
3.23	Instrumentation Plan of Specimens 1-LFB and 2-LFB.....	76
3.24	Instrumentation Plan of Specimens 1-LWY, 2-LWY, and 3-UNST.....	77
3.25	Instrumentation Plan of Specimens 1-HCP, 1B-HCP and 1-FCP.....	78
3.26	Instrumentation Plan of Specimen 1-DP.....	79
4.1	Finite Element Strain Distribution along the k-line in the Column Web at 450 kips.....	83
4.2	Full-Width vs. Narrow-Width Regions of Continuity Plates.....	84
4.3	Comparing Specimen Elongation with and without Eccentric Loading.....	86
4.4	Location of Specimen Elongation LVDTs.....	86
4.5	Comparison of Flange Separation Measurements Before and After Misalignment Correction.....	87
4.6	Experimental and FEM Results of Specimen 2-LWY Specimen Elongation.....	91
4.7	Experimental and FEM Results of Specimen 2-LWY Pull-Plate Strain.....	91
4.8	Experimental and FEM Results of Specimen 2-LWY Flange Separation....	92
4.9	Experimental and FEM Results of Specimen 2-LWY Column Web Strain..	92
4.10	Experimental and FEM Results of Specimen 2-LWY Column Flange Strain.	93
4.11	Experimental and FEM Results of Specimens 1-HCP and 1B-HCP Specimen Elongation.....	94
4.12	Experimental and FEM Results of Specimens 1-HCP and 1B-HCP Specimen Pull-Plate Strain.....	94

4.13	Experimental and FEM Results of Specimens 1-HCP and 1B-HCP Specimen Flange Separation.....	95
4.14	Experimental and FEM Results of Specimens 1-HCP and 1B-HCP Specimen Column Web Strain.....	95
4.15	Experimental and FEM Results of Specimens 1-HCP and 1B-HCP Specimen Column Flange Strain.....	96
4.16	Experimental and FEM Results of Specimens 1-HCP and 1B-HCP Specimen Continuity Plate Strain.....	96
4.17	Load-Deformation Curves for Five Specimens and Pull-Plate Coupon.....	98
4.18	Whitewash Yield Patterns of Specimen 1-LWY.....	101
4.19	Specimen 2-LWY 40° Angle Yield Lines.....	101
4.20	Strain Distribution in the Column k-line at 1.5% Specimen Elongation.....	103
4.21	Stress Distributions in the Column k-line.....	108
4.22	Comparing k-line Stress Distributions of Specimen 1-LWY.....	109
4.23	Comparing k-line Stress Distributions of Specimen 2-LWY.....	110
4.24	Comparing k-line Stress Distributions of Specimen 3-UNST.....	110
4.25	Gap between Column Web and Doubler Plates of Specimen 2-LFB.....	113
4.26	Yield Lines on Inside Face of Column Flange under Pull-Plate of Specimen 2-LFB.....	114
4.27	Yield Lines on Outside Face of Column Flange Radiating Out from Center of Specimen 1-LFB.....	115
4.28a	Illustrations of Local Flange Bending	116
4.28b	Illustrations of Local Flange Bending	116
4.29	Longitudinal Strain on the Inside Face of Column Flanges at 1.5% Specimen Elongation.....	117
4.30	Transverse Strain on the Inside Face of the Column Flanges at 1.5% Specimen Elongation.....	118
4.31	Column Flange Separation along Column Length at 1.5% Specimen Elongation.....	120

4.32	Separation of Column Flanges Transverse to Column Length at 1.5% Specimen Elongation.....	121
4.33	Specimen 1-LWY Flange Separation in Longitudinal Direction.....	122
4.34	Specimen 1-LWY Flange Separation in Transverse Direction.....	122
4.35	Assumed Yield Line Pattern of Column Flange Due to LFB.....	128
4.36	Yield Line Patterns on Half-Thickness Continuity Plates.....	132
4.37	Continuity Plate Strain Distribution along Full-Width of Plate at 1.5% Specimen Elongation.....	133
4.38	Continuity Plate Strain Distribution along Narrow-Width of Plate at 1.5% Specimen Elongation.....	134
4.39	Strain Distributions in the Column k-line and Doubler Plate of Specimen 1-DP at 0.6% and 1.5% Specimen Elongation.....	136
A.1	LVDT Names and Locations.....	147
A.2	Column Web Strain Gage Names and Locations.....	148
A.3	Column Flange Strain Gage Names and Locations.....	149
A.4	Continuity Plate Strain Gage Names and Locations.....	150
A.5	Doubler Plate Strain Gage Names and Locations.....	151
A.6	Pull-Plate Strain Gage Names and Locations.....	152
A.7	Load vs. Overall LVDT Displacement of Specimen 1-LFB.....	153
A.8	Load vs. Flange LVDT Displacement of Specimen 1-LFB.....	154
A.9	Load vs. Top Pull-Plate Gages of Specimen 1-LFB.....	155
A.10	Load vs. Bottom Pull-Plate Gages of Specimen 1-LFB.....	156
A.11	Load vs. Column Flange Gages in the Longitudinal Direction of Specimen 1-LFB.....	157
A.12	Load vs. Column Flange Gages in the Transverse Direction of Specimen 1-LFB.....	158
A.13	Load vs. Column Flange Gages in the xy Direction of Specimen 1-LFB....	159
A.14	Load vs. Overall LVDT Displacement of Specimen 2-LFB.....	160
A.15	Load vs. Flange LVDT Displacement of Specimen 2-LFB.....	161

A.16	Load vs. Top Pull-Plate Gages of Specimen 2-LFB.....	162
A.17	Load vs. Bottom Pull-Plate Gages of Specimen 2-LFB	163
A.18	Load vs. Column Flange Gages in the Longitudinal Direction of Specimen 2-LFB.....	164
A.19	Load vs. Column Flange Gages in the Transverse Direction of Specimen 2-LFB.....	165
A.20	Load vs. Column Flange Gages in the xy Direction of Specimen 2-LFB....	166
A.21	Load vs. Overall LVDT Displacement of Specimen 1-LWY.....	167
A.22	Load vs. Flange LVDT Displacement of Specimen 1-LWY.....	168
A.23	Load vs. Top Pull-Plate Gages of Specimen 1-LWY.....	169
A.24	Load vs. Bottom Pull-Plate Gages of Specimen 1-LWY.....	170
A.25	Load vs. Column Web k-line Gages in Columns 3 and 4 of Specimen 1-LWY.....	171
A.26	Load vs. Column Web k-line Gages in Columns 5 and 6 of Specimen 1-LWY.....	172
A.27	Load vs. Column Web Mid-Depth Gages of Specimen 1-LWY.....	173
A.28	Load vs. Column Flange Gages in the Longitudinal Direction of Specimen 1-LWY.....	174
A.29	Load vs. Column Flange Gages in the Transverse Direction of Specimen 1-LWY.....	175
A.30	Load vs. Overall LVDT Displacement of Specimen 2-LWY.....	176
A.31	Load vs. Flange LVDT Displacement of Specimen 2-LWY.....	177
A.32	Load vs. Top Pull-Plate Gages of Specimen 2-LWY.....	178
A.33	Load vs. Bottom Pull-Plate Gages of Specimen 2-LWY.....	179
A.34	Load vs. Column Web k-line Gages in Columns 3 and 4 of Specimen 2-LWY.....	180
A.35	Load vs. Column Web k-line Gages in Columns 5 and 6 of Specimen 2-LWY.....	181
A.36	Load vs. Column Web Mid-Depth Gages of Specimen 2-LWY.....	182

A.37	Load vs. Column Flange Gages in the Longitudinal Direction of Specimen 2-LWY.....	183
A.38	Load vs. Column Flange Gages in the Transverse Direction of Specimen 2-LWY.....	184
A.39	Load vs. Overall LVDT Displacement of Specimen 3-UNST.....	185
A.40	Load vs. Flange LVDT Displacement of Specimen 3-UNST	186
A.41	Load vs. Top Pull-Plate Gages of Specimen 3-UNST	187
A.42	Load vs. Bottom Pull-Plate Gages of Specimen 3-UNST.....	188
A.43	Load vs. Column Web k-line Gages in Columns 3 and 4 of Specimen 3-UNST.....	189
A.44	Load vs. Column Web k-line Gages in Columns 5 and 6 of Specimen 3-UNST.....	190
A.45	Load vs. Column Web Mid-Depth Gages of Specimen 3-UNST.....	191
A.46	Load vs. Column Flange Gages in the Longitudinal Direction of Specimen 3-UNST.....	192
A.47	Load vs. Column Flange Gages in the Transverse Direction of Specimen 3-UNST.....	193
A.48	Load vs. Column Flange Gages in the xy Direction of Specimen 3-UNST..	194
A.49	Load vs. Overall LVDT Displacement of Specimen 1-HCP.....	195
A.50	Load vs. Flange LVDT Displacement of Specimen 1-HCP.....	196
A.51	Load vs. Top Pull-Plate Gages of Specimen 1-HCP.....	197
A.52	Load vs. Bottom Pull-Plate Gages of Specimen 1-HCP.....	198
A.53	Load vs. Column Web k-line Gages in Columns 3 and 4 of Specimen 1-HCP.....	199
A.54	Load vs. Column Web k-line Gages in Columns 5 and 6 of Specimen 1-HCP.....	200
A.55	Load vs. Column Web Mid-Depth Gages of Specimen 1-HCP.....	201
A.56	Load vs. Column Flange Gages in the Longitudinal Direction of Specimen 1-HCP.....	202

A.57	Load vs. Column Flange Gages in the Transverse Direction of Specimen 1-HCP.....	203
A.58	Load vs. Column Flange Gages in the xy Direction of Specimen 1-HCP....	204
A.59	Load vs. Continuity Plate Gages in Rows 1 and 4 of Specimen 1-HCP.....	205
A.60	Load vs. Continuity Plate Gages in Row 2 of Specimen 1-HCP.....	206
A.61	Load vs. Continuity Plate Gages in Row 3 of Specimen 1-HCP.....	207
A.62	Load vs. Overall LVDT Displacement of Specimen 1B-HCP.....	208
A.63	Load vs. Flange LVDT Displacement of Specimen 1B-HCP.....	209
A.64	Load vs. Top Pull-Plate Gages of Specimen 1B-HCP.....	210
A.65	Load vs. Bottom Pull-Plate Gages of Specimen 1B-HCP.....	211
A.66	Load vs. Column Web k-line Gages in Columns 3 and 4 of Specimen 1B-HCP.....	212
A.67	Load vs. Column Web k-line Gages in Columns 5 and 6 of Specimen 1B-HCP.....	213
A.68	Load vs. Column Web Mid-Depth Gages of Specimen 1B-HCP.....	214
A.69	Load vs. Column Flange Gages in the Longitudinal Direction of Specimen 1B-HCP.....	215
A.70	Load vs. Continuity Plate Gages in Row 1 of Specimen 1B-HCP.....	216
A.71	Load vs. Continuity Plate Gages in Row 2 of Specimen 1B-HCP.....	217
A.72	Load vs. Continuity Plate Gages in Row 3 of Specimen 1B-HCP.....	218
A.73	Load vs. Overall LVDT Displacement of Specimen 1-FCP.....	219
A.74	Load vs. Flange LVDT Displacement of Specimen 1-FCP.....	220
A.75	Load vs. Top Pull-Plate Gages of Specimen 1-FCP..	221
A.76	Load vs. Bottom Pull-Plate Gages of Specimen 1-FCP.....	222
A.77	Load vs. Column Web k-line Gages in Columns 3 and 4 of Specimen 1-FCP.....	223
A.78	Load vs. Column Web k-line Gages in Columns 5 and 6 of Specimen 1-FCP.....	224
A.79	Load vs. Column Web Mid-Depth Gages of Specimen 1-FCP.....	225

A.80	Load vs. Column Flange Gages in the Longitudinal Direction of Specimen 1-FCP.....	226
A.81	Load vs. Continuity Plate Gages in Row 1 of Specimen 1-FCP.....	227
A.82	Load vs. Continuity Plate Gages in Row 2 of Specimen 1-FCP.....	228
A.83	Load vs. Continuity Plate Gages in Row 3 of Specimen 1-FCP.....	229
A.84	Load vs. Overall LVDT Displacement of Specimen 1-DP.....	230
A.85	Load vs. Flange LVDT Displacement of Specimen 1-DP.	231
A.86	Load vs. Top Pull-Plate Gages of Specimen 1-DP.....	232
A.87	Load vs. Bottom Pull-Plate Gages of Specimen 1-DP.....	233
A.88	Load vs. Column Web k-line Gages in Columns 3 and 4 of Specimen 1-DP.....	234
A.89	Load vs. Column Web k-line Gages in Columns 5 and 6 of Specimen 1-DP.....	235
A.90	Load vs. Column Web Mid-Depth Gages of Specimen 1-DP.....	236
A.91	Load vs. Column Flange Gages in the Longitudinal Direction of Specimen 1-DP.....	237
A.92	Load vs. Doubler Plate Box Detail Gages in Columns 3 and 4 of Rows 1 and 3 of Specimen 1-DP.....	238
A.93	Load vs. Doubler Plate Box Detail Gages in Columns 5 and 6 of Rows 1 and 3 of Specimen 1-DP.....	239
A.94	Load vs. Doubler Plate Box Detail Gages in Row 2 of Specimen 1-DP.....	240

List of Tables

3.1	Girder-to-Column Combinations Meeting the SCWB Criterion.....	31
3.2	Properties of Possible Unstiffened Pull-Plate Specimens.....	47
3.3	Nominal Column Resistance and Demands.....	51
3.4	Actual and Nominal Flange and Web Thicknesses	63
3.5	Steel Tension Coupon Test Properties.....	66
3.6	CVN Values of Column Sections.....	68
4.1	Specimen Results.....	99
4.2	Material Dimensions and Yield Strengths for Specimens Analyzing LWY.	105
4.3	Comparison of LWY Equations and Experimental Results.....	106
4.4	Test-to-Predicted Ratios for LWY Equations.....	111
4.5	Comparison of LFB Equations and Experimental Results.....	125
4.6	Statistical Description of Equation 4.4 Variables.....	129
4.7	Comparison of LFB Failure Loads.....	130

Chapter 1

Introduction

Girder-to-column flange welds fractured in approximately 100 steel moment-frame connections during the 1994 Northridge earthquake. These welds fractured primarily because of low fracture toughness of weld metal combined with a backing bar forming a notch at the weld root and weld root defects (Fisher et al., 1997; FEMA, 2000b). Subsequently, there has been a tendency to be overly conservative in the design and detailing of these connections. In some situations, continuity plates and web doubler plates have been specified when they are unnecessary and, when they are necessary, thicker continuity plates have been specified than would be required. The specified type of welds have often been complete joint penetration (CJP) welds to join the continuity plates to the column flanges, even though the use of more economical fillet welds may have sufficed.

The tendency to be overly conservative with column stiffeners in seismic applications in particular is understandable since they do have a significant effect on the stress and strain distribution in the connection and on connection performance. For example, Roeder (1997) observed that girder-to-column joints with modest continuity plates and/or doubler plates performed better in cyclic loading tests than joints without such reinforcement. Also, it has been observed from finite element analyses of these joints that there is a decrease in stress concentration at the middle of the girder flange-to-column flange welds when continuity plates are used (Roeder, 1997; El-Tawil et al., 1998).

The design criteria for these limit states are provided in Section K1 of Chapter K of the American Institute of Steel Construction (AISC) Load and Resistance Factor

Design (LRFD) Specification for Structural Steel Buildings (AISC, 1999b). There are additional more stringent provisions in the requirements for Special Moment Frames (SMF) in the AISC Seismic Provisions for Structural Steel Buildings (1992). However, the 1997 AISC Seismic Provisions (AISC, 1997) removed all design procedures related to continuity plates, requiring instead that they be proportioned to match those provided in the tests used to qualify the connection.

As part of the SAC Joint Venture research program, guidelines and an advisory were published (FEMA, 1996a; FEMA, 1996b) that pertained to these column reinforcements in seismic zones. For example, the guidelines called for continuity plates at least as thick as the beam flange that must be joined to the column flange in a way that fully develops the strength of the continuity plate, i.e., this encourages the use of CJP welds. However, the SAC 100% draft guideline document (FEMA, 2000b) has reestablished design equations to determine whether continuity plates are required and, if so, what thickness is required.

The present non-seismic provisions that govern the need for and the design of continuity plates are based on two limit states: local web yielding (LWY) and local flange bending (LFB). Continuity plates are only needed if the beam flange force exceeds the resistance to LWY or LFB. The resistance equations for LWY and LFB are largely based on experimental research that was conducted by Sherbourne and Graham (1957) and Graham et al. (1960) in conjunction with limit load and buckling analyses of Parkes (1952) and Wood (1955).

Recent research has revealed that excessively thick continuity plates are unnecessary. El-Tawil et al. (1998) performed parametric finite element analyses of girder-to-column joints. They found that continuity plates are increasingly effective as the thickness increases to about 60% of the girder flange. However, continuity plates more than 60% of the girder flange thickness brought diminishing returns.

Furthermore, over-specification of column reinforcement may actually be detrimental to the performance of connections. As continuity plates are made thicker and attached with highly restrained CJP welds, they are sometimes causing cracking during fabrication. CJP welds have also been specified for the attachment of continuity plates to

the web, where fillet welds have traditionally been adequate. Yee et al. (1998) performed finite element analyses comparing fillet welded and CJP welded continuity plates. Based on principal stresses extracted at the weld terminations, it was concluded that fillet welded continuity plates may be less susceptible to cracking during fabrication than if CJP welds are used.

1.1 Research Objectives

The research described in this paper is part of an ongoing project sponsored by AISC to reassess the design provisions for column stiffeners for non-seismic and seismic conditions, and to investigate new alternative column stiffener details. The project includes three components: monotonically-loaded pull-plate experiments to investigate the need for and behavior of transverse stiffeners, cyclically-loaded cruciform girder-to-column joint experiments to investigate panel zone behavior and local flange bending as well as innovative doubler plate and continuity plate details (Cotton et al., 2001), and parametric finite element analyses to corroborate the experiments and assess the performance of various transverse stiffener and doubler plate details (Ye et al., 2000).

The test matrices for this project were designed by examining all practical combinations of girder and column sizes to identify which girder-to-column joints satisfy the limit states of LFB, LWY, web crippling, and panel zone yielding, as well as which combinations satisfy the strong-column/weak-beam (SCWB) provisions, according to AISC non-seismic and seismic provisions (AISC, 1997; AISC, 1999b). A parametric study was then conducted using three-dimensional nonlinear continuum finite element analysis (FEM) to model the behavior of these connections and the performance of various transverse stiffener and doubler plate details. These analyses permitted the behavior of these connections to be characterized in detail. Criteria were established to identify the limit states of LWY and LFB for stiffened and unstiffened specimens. The results of the parametric study showed that web crippling did not control the need for column stiffening in any of the practical combinations of girder and column sizes, and therefore was not further investigated in the research program. The results of the finite

element analyses and the comprehensive investigation of the limit states for all girder and column combinations were then coupled with the results of past experiments to establish the test matrices for the present project.

Nine laboratory experiments were conducted with pull-plates (simulating a girder flange) attached to column sections for the study of localized flange bending and web yielding, investigating both common and new alternatives for detailing. These monotonic tests focus on the non-seismic behavior, with some consideration given to seismic design as well. Additional experiments are then being conducted on five full-scale cyclic girder-to-column joint subassemblies. These tests will focus on seismic behavior, although they will provide useful information for non-seismic design as well. The scope of this research is limited to investigation of hot-rolled wide-flange steel sections. All column sections are made of A992 steel, and all stiffening material is made of A572 Grade 50 steel.

1.2 Organization of the Report

This thesis is divided into five chapters. Chapter 2 summarizes the history of the LWY and LFB limit states. It traces the equations back to their respective origins and how they have been altered over the years. Chapter 2 also includes opinions of researchers regarding continuity plate design and behavior.

Chapter 3 contains information about the experimental procedure. This chapter includes the results of a computational parametric study that examined continuity plate requirements as related to the current AISC non-seismic and seismic provisions (AISC, 1997; AISC, 1999b) for LWY, LFB, and web crippling. Also included is a description of the specimen selection procedure and justification for the chosen specimen sizes. Each specimen design is also detailed, including the steel grades, weld types, and electrodes. The chapter continues with a description of the ancillary testing conducted on the column sections, plate material, and weld metal to establish their material characteristics.

Chapter 3 concludes with a description of the testing procedure and instrumentation plan for all nine pull-plate specimens.

Chapter 4 contains the results of the pull-plate tests and comparison to the finite element analyses. This chapter defines the possible failure modes and yield mechanisms of the specimens. The behavior of the specimens is compared to the failure modes, yield mechanisms, and the current equations for LWY and LFB. Equations are developed in order to better describe the LWY and LFB behavior of the specimens. These equations are presented as potential alternatives to, but not necessarily replacements for, the current equations.

Chapter 5 summarizes and presents conclusions of the research project, particularly the behavior of the specimens in comparison to the LWY and LFB limit states and the behavior of the stiffening details. Appendix A contains the strain gage and LVDT data for all nine pull-plate tests of this research.

Chapter 2

Background of Continuity Plate Design Provisions

The AISC LRFD Specification (1999b) includes a number of limit states related to concentrated forces. Three of these limit states that are applicable to concentrated flange forces delivered by a girder in a girder-to-column moment connection are used to determine the need for transverse stiffeners (continuity plates). These are:

- Local web yielding
- Local flange bending
- Local web crippling

The developments of the provisions for local web yielding and local flange bending are discussed below in detail. Web crippling is discussed only briefly because it almost never controls for column shapes subjected to beam flange forces in moment frame connections. For example, in every column shape except W12x50 or W10x33, local web yielding and local flange bending will give a lower allowable transverse flange force than the web crippling limit state (AISC, 1999b).

2.1 Definition of the Limit States

Local Web Yielding

The 1937 AISC Steel Construction Specification (AISC, 1937) was the first design guide to formulate a criterion for web crippling. At that time, the term “web crippling” referred to both of what are known today as two distinct limit states, i.e., local

web yielding and local web crippling. The specification stated that “beams should be designed so the compression stress in the web at the toe of the fillet ... shall not exceed 24 kips per square inch.” (AISC, 1937). The equations were given as:

$$\frac{R}{t_{cw}(N + 2k)} \leq 24,000 \text{ psi, for interior condition} \quad (\text{Section 19h, 1937})$$

$$\frac{R}{t_{cw}(N + k)} \leq 24,000 \text{ psi, for end conditions} \quad (\text{Section 19h, 1937})$$

where:

R = concentrated load

t_{cw} = thickness of column web

N = length of bearing surface (taken as the thickness of the girder flange)

k = distance from outer face of flange to web toe of fillet

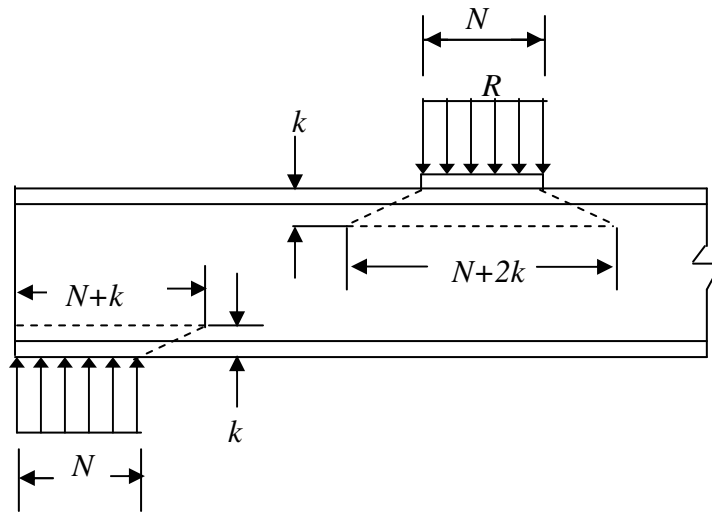


Figure 2.1: Local Web Yielding Definitions [after (AISC, 1937)]

As shown in Figure 2.1, the equations were based on a stress gradient of 1:1 (i.e., a 45° slope of stress distribution on the column web). The 1937 specification was written for one type of steel, and maximum strengths were given for this one steel type for

different loading situations. For web yielding, the maximum strength of the steel was taken to be 24,000 psi. No references were given for the reasons for the value of 24,000 psi or for the slope of the stress distribution.

In 1957, Sherbourne and Jensen (1957) tested nine two-sided direct-welded girder-to-column connections (cruciform tests) that resulted in proposed changes to the stress distribution of the local web yielding equations. In all nine tests, the girder used was a 16WF36, while the column shapes varied between 8WF31 and 12WF99. Besides column size, another variable was the type of stiffener tested. The connections were tested by applying an axial load on the columns and an incrementally increasing monotonic load on the girders. The column axial stress was kept constant at 14.5 ksi. A downward load was applied to each girder at a distance of 4 feet from the column flange face in four equal increments up to the working load of 23.5 kips. The test results showed that the 1:1 gradient of stress distribution that was currently being used in LWY equations was too conservative. A 2:1 slope was still somewhat conservative, but more representative of actual connection behavior. Changes to the LWY equations were proposed:

$$\sigma = \frac{R}{t_{cw}(N + 4k)} \quad \text{for interior conditions} \quad (2.1)$$

$$\sigma = \frac{R}{t_{cw}(N + 2k)} \quad \text{for end conditions} \quad (2.2)$$

where:

σ = stress that the column web is able to resist

The test results verified the proposed equations. When the specimens tested had a column web thickness greater than the thickness proposed by the new LWY equations, the column web did not yield. When the experimental webs were thinner than what was required by the proposed equations, the webs failed by web crippling.

In 1960, Graham et al. (1960) analyzed cruciform and four-way (three-dimensional) connections and the need for column stiffening. Four cruciform tests

without stiffeners and 11 pull-plate tests were performed to investigate column web yielding. The cruciform tests were the four unstiffened experiments previously summarized by Sherbourne and Graham (1957). The 11 pull-plate tests consisted of eleven column stubs (approximately 3 feet in length) compressed at the flanges between two plates representing the girder compression flanges. The loading history for both the cruciform and the pull-plate tests were the same: a constant column axial load was applied followed by statically increasing loads on the girders (or plates representing the compression flanges of the girders). The tests showed that the 2:1 stress gradient, proposed by Sherbourne and Jensen (1957) was still too conservative, and that a 2.5:1 stress gradient would be more acceptable.

To corroborate the experimental test results, Graham et al.(1960) used the theoretical work of Parkes (1952), who developed a theory for the distribution of elastic stresses along the column “k-line” due to a transverse concentrated force on a girder flange. A plot of the normalized stress in the column web versus the normalized distance from the girder compression flange was created. The theoretical curve represented the stress distribution until first yielding, i.e., the elastic resistance of the column web in the compression region.

Graham also plotted the experimental test results of the four cruciform tests and 11 pull-plates tests, normalized by Parkes’ method. All but one of the test results had approximately the same non-dimensionalized stress ratio. The test results represent the inelastic resistance of the column web after some yielding. Because the area under the elastic curve (from Parkes) was greater than the area under the inelastic curve (the Graham data), the stress distribution proposed by Graham et al. (1960) of 2.5:1 was considered to be conservative. Hence, the stress distribution of 2.5:1 proposed by Graham et al. (1960) is a more accurate but still conservative measure.

The LWY equation remained the same until the AISC Allowable Stress Design (ASD) Specification 8th Edition (AISC, 1978). The 1937 equations (AISC, 1937) were valid for only one type of steel, whereas the ASD equations (AISC, 1978) were based on the nominal yield strength of the column web. The ASD specification continued to use a stress gradient of 1:1 and required that the resistance of the column be greater than the

total service load from the compression flange of the girder, acting over a distance $(N+2k)$. A factor of safety of 1.33 was chosen. Consequently, the LWY equations (AISC, 1978) became:

$$\frac{R}{t_{cw}(N+2k)} \leq 0.75F_{yc} \quad \text{for interior conditions} \quad (\text{Section 1.10.10, 1978})$$

$$\frac{R}{t_{cw}(N+k)} \leq 0.75F_{yc} \quad \text{for end conditions} \quad (\text{Section 1.10.10, 1978})$$

where:

F_{yc} = yield strength of the column

The ASD Specification 9th Edition (AISC, 1989) was the first ASD Specification to characterize a difference between local web yielding and local web crippling. Local web yielding was defined as yielding of the web material directly beneath the load and is common in stocky webs. Local web crippling was defined as crumpling of the web into buckled waves near the flange-web juncture. It is often the controlling failure mode for slender webs. Each limit state had unique requirements.

The ASD 9th edition (1989) used the stress gradient proposed by Graham et al. (1960) of 2.5:1. In the process of changing the LWY equation from the 8th edition (AISC, 1978) to reflect the less conservative stress gradient, the factor of safety was increased. The slope became 2.5:1, while the factor of safety became 1.5. The equations are as follows:

$$\frac{R}{t_{cw}(N+5k)} \leq 0.66F_{yc} \quad \text{for interior conditions} \quad (\text{Equation K1-2, 1989})$$

$$\frac{R}{t_{cw}(N+2.5k)} \leq 0.66F_{yc} \quad \text{for end conditions} \quad (\text{Equation K1-3, 1989})$$

The specification for web crippling was governed by a different relationship, which also had to be satisfied:

$$R = 67.5t_{cw}^2 \left[1 + 3 \left(\frac{N}{d_c} \right) \left(\frac{t_{cw}}{t_{cf}} \right)^{1.5} \right] \sqrt{F_{yc} \frac{t_{cf}}{t_{cw}}} \quad \text{(Equation K1-4, 1989)}$$

where:

d_c = column depth

t_{cf} = column flange thickness

All three editions of the AISC Load and Resistance Factor Design (LRFD) Specification (AISC, 1986, 1993, 1999b) have used a 2.5:1 stress gradient, and references were made to Graham et al. (1960) to account for the choice of stress gradient. The latest edition of the AISC LRFD Specification will be referenced (AISC, 1999b). The LWY equations in the LRFD specification can be manipulated and shown to be essentially the same as the ASD 9th Edition equations (Salmon and Johnson, 1996). The following derivation is outlined for just the LWY equation for interior conditions, but applies with slight modification for the end conditions.

Equation (K1-2, 1989) is the ASD equation for LWY interior conditions, stated below:

$$\frac{R}{t_{cw}(N + 5k)} \leq 0.66F_{yc} \quad \text{for interior conditions} \quad (2.3)$$

Equation 2.3 is equivalent to:

$$\frac{R}{t_{cw}(N + 5k)} \leq \frac{F_{yc}}{1.5} \quad (2.4)$$

The following variables are then defined:

$$\text{critical stress} = f_c = \frac{R}{A_c}$$

$$FS = \text{factor of safety} = 1.5 = FS = \frac{\gamma}{\phi}$$

where:

R = total service load

A_c = critical area for LWY with the 2.5:1 stress gradient = $(5k+N)t_{cw}$.

γ = average overload factor

ϕ = resistance factor

Substituting into Equation 2.4

$$f_c \leq \frac{R_n}{FS * A_c} = \frac{R_n \phi}{A_c \gamma} \quad (2.5)$$

The general format for the LRFD provisions is $\phi R_n \geq \Sigma \gamma_i Q_i = R_u$, where:

R_n = nominal resistance

Q_i = service load for load case i

R_u = total factored load

The LRFD strength relationship is then reformulated by dividing by γ

$$\frac{\phi R_n}{\gamma} \geq \Sigma \frac{\gamma_i Q_i}{\gamma} = \frac{R_u}{\gamma} = R \quad (2.6)$$

Equations 2.5 and 2.6 may be combined to get the LRFD equation for LWY (see Figure 2.2)

$$R_u < \phi R_n = \phi(5k + N)F_{yc}t_{cw} \quad \text{for interior conditions} \quad (\text{Equation K1-2, 1999b})$$

$$R_u < \phi R_n = \phi(2.5k + N)F_{yc}t_{cw} \quad \text{for end conditions} \quad (\text{Equation K1-3, 1999b})$$

where:

$$\phi = 1.0$$

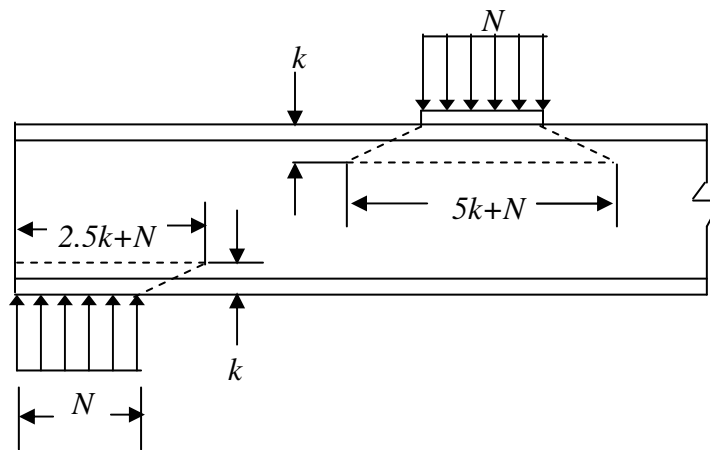
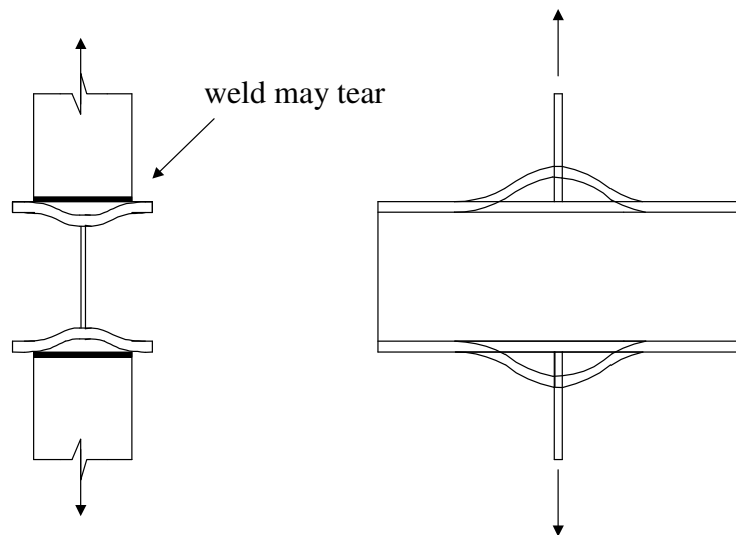


Figure 2.2: Local Web Yielding Definitions [after (AISC, 1999b)]

If either Equation K1-2 or K1-3 is breached, then stiffeners are required that are capable of resisting the portion of the demand that the column cannot resist.

Local Flange Bending

Local flange bending (LFB) occurs when the girder flange in a connection pulls or pushes and bends the outstanding column flanges. As force is applied to the column flange (without continuity plates), the deflection of the flange is not uniform across the entire flange. At the ends of the column flanges, the girder and column flanges bend together. However, at the middle of the column flange, the column web restrains the deformation, particularly when the web has not yielded. Figures 2.3a and b are schematic views of the bending of the column section, showing LFB in only two dimensions from two perspectives. However, the bending is actually a more complicated three-dimensional deformation, combining both of the bending directions.



Figures 2.3a and b: Illustrations of Local Flange Bending

Currently, the AISC LRFD Specification (AISC, 1999b) requires that the factored strength of column flanges exceed the concentrated transverse force applied by the girder flange across the column flange. The factored strength of the column flange is given as:

$$\phi R_n = \phi 6.25 t_{cf}^2 F_{yc} \quad (\text{Equation K1-1, 1999b})$$

where:

$$\phi = 0.9$$

If the concentrated transverse girder force is larger than the column flange strength, then a pair of transverse stiffeners (continuity plates) extending at least one-half of the depth the web is required to resist the portion of the girder demand that the column flange is unable to resist. According to the AISC Specification (1999b), the thickness of the each continuity plate must be greater than one-half the thickness of the girder flange

load and greater than its width times $1.79\sqrt{\frac{F_y}{E}}$.

The 8th and 9th Editions of the AISC ASD Specification (AISC, 1978, 1989) require a pair of stiffeners opposite the tension flange if:

$$t_{cf} < 0.4 \sqrt{\frac{P_{bf}}{F_{yc}}} \quad (\text{Equation K1-1, 1989})$$

where:

$$P_{bf} = \frac{5}{3} (\text{service-level force from beam flange}) \text{ if force is live + dead load, or}$$

$$P_{bf} = \frac{4}{3} (\text{service-level force from beam flange}) \text{ if force is live + dead + (wind or earthquake).}$$

When terms are rearranged, the ASD Equation gives essentially the same requirements as the LRFD Equation. These two equations were generated in 1960 from cruciform and pull-plate connection tests by Graham et al. (1960). Graham used his experimental results along with mathematical and geometrical approximations of the connection to determine the LFB equation. The column flange that was attached to the tensile girder flange (pull-plate) was approximated as two half-flange plates on either side of the column web, plus a thicker center portion of the flange between the fillet

extremities. The column flange plates were assumed to have a length of $12t_{cf}$, where t_{cf} is the column flange thickness. The force of the girder tension flange was approximated as a line load on each plate. A summary of this derivation follows.

Using plastic analysis, the bending resistance of the column flange is $c_1 F_{yc} t_{cf}^2$, where c_1 is a coefficient depending on the width of the column and girder flanges, the extent of two-way bending, the distance between the column fillet extremities, and the boundary conditions (Graham et al., 1960). The boundary conditions are shown in Figure 2.4. The value of c_1 is given by:

$$c_1 = \frac{\left(\frac{4}{\beta} + \frac{\beta}{\eta} \right)}{\left(2 - \frac{\eta}{\lambda} \right)} \quad (2.7)$$

where the following variables are defined and shown in Figure 2.4:

$$\beta = \frac{12t_{cf}}{q} \quad (2.8)$$

$$\eta = \frac{\beta}{4} \left(\left(\sqrt{\beta^2 + 8\lambda} \right) - \beta \right) \quad (2.9)$$

$$\lambda = \frac{h}{q} \quad (2.10)$$

$$q = \frac{b_{cf}}{2} - \frac{m}{2}$$

$$h = \frac{b_{gf}}{2} - \frac{m}{2}$$

b_{cf} = column flange width

b_{gf} = girder flange width

$m = t_{cw} + 2(k - t_{cf}) \approx k_1$ [k_1 was not used at the time, because the dimension was not yet

tabulated in the AISC Manual (AISC, 1950)]

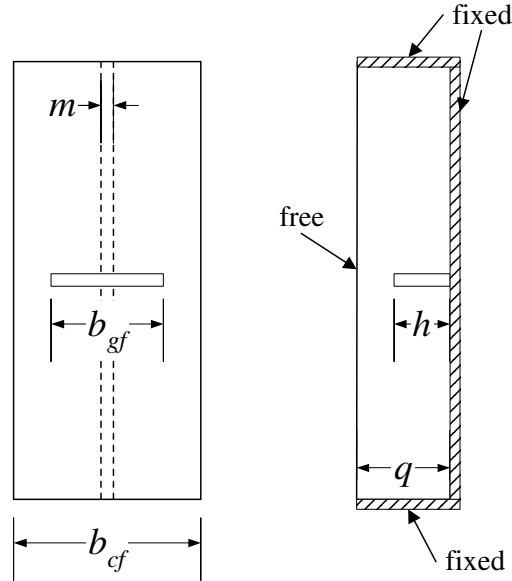


Figure 2.4: Column Flange Model [after (Graham et al., 1960)]

Graham et al. (1960) stated that for the wide flange columns and girders commonly used in the 1950's, c_I varied between 3.5 and 5. To be conservative, $c_I = 3.5$ was used to calculate the resistance for the two plates (or one column flange) in bending, which was thus equal to $7\sigma_y t_{cf}^2$.

The thicker center portion of the column flange between the fillet extremities resists a girder flange force of $\sigma_y t_{gf} m$, where m is the distance between the fillet extremities (shown in the Figure 2.4). Therefore, to develop the full yield strength of the girder tension flange, the resistance of the column flange must be at least equal to:

$$F_{yg} A_{gf} = F_{yc} t_{gf} m + 7F_{yc} t_{cf}^2 \quad (2.11)$$

where:

F_{yg} = girder yield strength

A_{gf} = column flange area = $b_{gf} t_{gf}$

t_{gf} = column flange thickness

Graham et al. (1960) used engineering judgment to conservatively reduce the resistance of the column flange by 20%. Therefore, the resistance becomes:

$$F_{yg} A_{gf} = 0.8(F_{yc} t_{gf} m + 7F_{yc} t_{cf}^2) \quad (2.12)$$

Assuming that the yield strength of the column and girder are the same, Equation 2.12 reduces to:

$$t_{cf}^2 = \frac{A_{gf}}{7} \left(1.25 - \frac{m}{b_{gf}} \right) \quad (2.13)$$

Graham used girder and column sizes from the 1953 AISC Manual (AISC, 1953) to determine that m/b_{gf} varies from 0.15 to 0.20. To be conservative, $m/b_{gf} = 0.15$ was used. The minimum column thickness then reduced to:

$$t_{cf} = 0.396\sqrt{A_{gf}} \approx 0.4\sqrt{b_{gf} t_{gf}} \quad (2.14)$$

Thus, if $t_{cf} < 0.4\sqrt{b_{gf} t_{gf}}$, stiffeners are needed.

To achieve more general applicability for any type of steel with a given yield strength, the ASD 8th and 9th Editions (AISC, 1978, 1989) altered the equation so as to include the concentrated load (service load level) for a given girder flange:

$$t_{cf} < 0.4\sqrt{\frac{P_{bf}}{F_{yc}}} \quad (2.15)$$

The LRFD Specification (1999b) used the same Graham equation and generalized it in terms of nominal strength, R_n (Salmon and Johnson, 1996). The factored flange force, P_{bf} , cannot exceed the design strength ϕR_n . Consequently, Graham's equation for LFB [Equation (2.11)] rewritten in terms of R_n is:

$$R_n = 7t_{cf}^2 F_{yc} + t_{gf} m F_{yc} \quad (2.16)$$

where:

$$m = t_{gf} + 2(k - t_{cf}) \quad (2.17)$$

Again, to be conservative a 20% reduction of nominal strength was observed.

Thus:

$$R_n = 0.8(7t_{cf}^2 F_{yc} + t_{gf} m F_{yc}) \quad (2.18)$$

Referring to the tests from Graham et al. (1960), the minimum value of

$\frac{t_{gf} m F_{yc}}{R_n} = 0.15$ was used. Thus, the flange column thickness requirement reduces to:

$$t_{cf} \geq \sqrt{\frac{R_n}{7F_{yc}}(1.25 - 0.15)} \cong 0.4 \sqrt{\frac{R_n}{F_{yc}}} \quad (2.19)$$

Solving for the nominal strength yields the LRFD expression for LFB:

$$\phi R_n = \phi \left(\frac{t_{cf}}{0.4} \right)^2 F_{yc} = \phi 6.25 t_{cf}^2 F_{yc} \quad (\text{Equation K1-1, 1999b})$$

where:

$$\phi = 0.90$$

FEMA (2000b), resulting from the research of the SAC Joint Venture, uses the LFB equation and a seismic girder demand to calculate the need for continuity plates. The guidelines state that unless proven with tested connections, continuity plates are required if the thickness of the column flange is less than either of the two following equations:

$$t_{cf} < 0.4 \sqrt{1.8 b_{gf} t_{gf} \left(\frac{F_{yg}}{F_{yc}} \right)} \quad (2.20)$$

$$t_{cf} < \frac{b_{gf}}{6} \quad (2.21)$$

Equation 2.20 is similar to Equation 2.15, but with the seismic demand of the girder flange taken as $1.8F_{yg}b_{gf}t_{gf}$ to account for strain hardening and focusing of the girder moment into the girder flanges near the welds. Equation 2.21 is an additional criterion proposed by Ricles et al. (2000), described in Section 2.2.

2.2 Opinions Regarding Continuity Plate Behavior and Design

The objective of the testing done by Sherbourne and Jensen (1957) and Graham et al. (1960) was to investigate column web and flange behavior in moment-resisting frame connections and to create design specification provisions for the connection design involving stiffeners. The outcome of the research generated guidelines for the use and sizing of continuity plates. The continuity plate thickness was determined by the required demand and design strength of the column.

Since then, several researchers have examined the behavior of moment-resisting connections with and without continuity plates, and have recommended various methods of sizing continuity plates. Since the 1994 Northridge earthquake, the trend in continuity plate design for seismic moment frames has been to require stiffeners with the full thickness of the larger girder flange framing into the connection, regardless of demand. Furthermore, continuity plates were often previously fillet welded to the column web and flanges. After the Northridge earthquake, despite the fact that no failures can be attributed to the use of fillet-welded continuity plates, it has been typical to use full-penetration welds to join the continuity plates to the column flanges, and often to the web as well.

The following is a summary of past researchers' opinions regarding continuity plate design:

- Johnson (1959) reported three different series of tests all subjected to monotonic loading. The first series of tests (1959a) consisted of 15 fully-welded connections with and without continuity plates. The results of the tests showed that continuity plates should be used in moment-resisting connections. The author concluded that

not enough tests were conducted to provide definite new continuity plate specifications. However, it was determined that the stiffeners should not be larger than the girder flanges, and fillet welds were adequate to connect the continuity plates to the column flanges for non-seismic design. The second series of tests by Johnson (1959b) were 16 moment-resisting connections that consisted of considerably larger column and girder sizes than previously tested. The outcome of the series expanded on his previous results. He concluded that the continuity plates should be half the width of the girder flange and about the same thickness, and that fillet welds were still sufficient to connect the stiffeners to the column flanges. The third series of tests (1959c) included 22 pull-plate tests examining continuity plates. Johnson concluded that the specimens with the thicker continuity plates were able to withstand a much greater load, and that the fillet welds attaching the continuity plates to the column flanges were still adequate.

- Popov et al. (1986) performed a series of cyclic half-scale cruciform tests to verify the design criteria for girder-to-column connections in seismic conditions. Tests were performed with and without continuity plates. The results of the tests showed that, for two connections consisting of the same column and girders, when continuity plates were added the inelastic girder rotation was greatly increased. Yielding and buckling of the stiffeners was witnessed when the girders were within the strain-hardening range. Thus, the researchers concluded that designing stiffeners on the basis of nominal yielding in beam flanges was unconservative. Also, the test results led to the conclusion that stiffeners were essential even when the column flanges were 1.25 in. thick. Regarding the continuity plate welds, recommendations were made to use full-penetration welds to attach the continuity plates to the column flanges, rather than fillet welds. In two of the eight connections, the welds attaching the continuity plates to the column were made using fillet welds all-around. In one of these specimens, the connection between the column flange and continuity plate failed prematurely.
- Tremblay et al. (1995) outlined the characteristics of the seismic design provisions (AISC, 1992), summarized reconnaissance site visits of several connections after the

Northridge earthquake, and compared the observed behavior to the expected performance. From observation of actual performance, the authors contended that the presence of continuity plates may have played a role in mitigating weld failures. The buildings with the continuity plates had fewer weld failures, which suggested that the flexibility of the column flanges could have resulted in local overstressing of the welds. Tremblay et al. (1995) recommended the use of continuity plates in all connections designed for seismic zones.

- Kaufmann et al. (1996a, 1996b) tested several fully welded girder-to-column connections. The connections varied the type of welding electrodes used in the girder-to-column CJP weld. Each of the connections contained continuity plates joined to the column flanges and webs with 5/8 in. fillet welds. The results of the tests showed that fully welded connections that used electrodes with higher toughness values and continuity plates can act in a ductile manner.
- Roeder (1997) performed detailed finite element analyses for critical joints of pre-Northridge connections. These local analyses showed that transverse strains in the girder and column flange are restrained by the surrounding steel, and are therefore susceptible to hydrostatic tensile stress and potential cracking. The author also showed that continuity plates may decrease the hydrostatic stress at the girder-to-column interface, which then may affect the likelihood of weld cracking. Roeder gave no recommendations on the most effective size of continuity plates in moment-resisting frames.
- Engelhardt et al. (1997) tested three welded flange-bolted web moment connections under cyclic load to failure. The connections were then repaired and retested. The test results showed that repairing connections by using high toughness weld metal makes the connection behave adequately under dynamic cyclic loads. The authors recommended changing the CJP welds between column web and continuity plate to 5/16 in. fillet welds. However, it was recommended that complete joint penetration welds be used to attach the continuity plate to the column flanges.
- Welding of the continuity plates to the column flanges creates a highly-restrained configuration and generates tremendous tensile residual stresses. Since it became

customary to use thicker welds, i.e. groove welds, and thicker continuity plates, a number of fractures of the k-line region of the column web were occurring during fabrication (Tide, 1999). The AISC Advisory for the k-line Region (1997) recommended that the welds for continuity plates should stop before the “k” area. The Advisory defined the “k” area as the “region extending from approximately the midpoint of the radius of the fillet into the web approximately 1 to 1-½ inches beyond the point of tangency between the fillet and web”. The Advisory recommended that all the welds should be fillet welds and/or partial penetration welds, which are proportioned to transfer stress to the column web.

- Yee et al. (1998) performed finite-element simulations on connections with continuity plates, which were attached by complete joint penetration (CJP) groove welds or fillet welds. The analyses resulted in higher stresses occurring when the stiffeners were attached with CJP groove welds. This led to the recommendation that fillet welds should be used to avoid brittle fracture. The analyses showed that the weld type strongly influenced the restrained stresses.
- El-Tawil et al. (1998) performed finite element analyses on the geometry of the cantilever Berkeley specimen PN3, which consisted of a W36x150 beam connected to a W14x257 column (SAC, 1996). This connection was used in four different analyses involving continuity plates; one with no continuity plates and three with different stiffener thicknesses: 0.5 in., 0.75in., and 0.94 in. The girder flange thickness was 0.94 in. The results of the analyses supported the FEMA-267 (FEMA, 1995) and FEMA-267A (FEMA, 1996) provisions, which required continuity plates as thick as the thicker girder flange in all connections designed for seismic zones. However, the analyses concluded that continuity plates with thicknesses less than 60% of the girder flange thickness resulted in very similar stress and strain distributions compared to the results of those with continuity plates as thick as the girder flanges.
- Dexter and Melendrez (2000) tested over 40 pull-plate tests with 100 ksi yield strength pull plates to investigate the through-thickness strength of the column flanges. Most of the specimens had fillet-welded continuity plates. These fillet-

welded continuity plates performed adequately provided they were detailed in accordance with the AISC Advisory (AISC k-line Advisory, 1997). Many of the specimens had continuity plate fillet welds, which encroached on the k-line region in violation of the recommendation of the Advisory (AISC k-line Advisory, 1997). In one case where the fillet welds encroached on the k-line, the k-line fractured, although at a load that exceeded any realistic girder force. Also, the only test conducted without continuity plates resulted in the only failure of the column flange material, although this also occurred at a force much higher than a typical girder flange could deliver.

- Bjorhovde et al. (1999) tested a series of one-sided cruciform tests with relatively weak panel zones. These specimens had fillet-welded continuity plates that met criteria of the AISC Advisory (AISC K-Line Advisory, 1997). The continuity plates performed adequately in these tests.
- Engelhardt (1999) made preliminary recommendations for the design and detailing of reduced beam section (RBS) moment connections based on available experimental data on the connections. All of the successful tests of RBS connections used continuity plates that were CJP welded (using an electrode with a rated CVN of at least 20 ft-lb at -20 deg F) to the column flanges and webs. The recommendations included avoiding welding continuity plates to the column in the “k-line” region. However, removing backing bars was not recommended. None of the RBS tests omitted continuity plates, however, so it is unclear what conditions require continuity plates. Engelhardt recommended using continuity plates with thicknesses similar to the beam flange thickness in all RBS connections, until more tests are done.
- Ricles et al. (2000) conducted four cruciform tests that focused on the need for continuity plates. The connections consisted of W36x150 girders, W14x398 or W27x258 columns with and without continuity plates, and doubler plates on both sides of the column web. The continuity plates were attached to the column flanges with CJP welds. The tests showed that continuity plates improve performance of the connections, but that satisfactory behavior can be achieved if the column flanges are

heavy enough. An additional equation for defining continuity plate requirements was proposed. If:

$$t_{cf} \geq b_{gf}/5.2 \quad \text{no continuity plates are required} \quad (2.22)$$

$$b_{gf}/5.2 \geq t_{cf} \geq b_{gf}/7 \quad \text{continuity plates are required with} \quad (2.23)$$

thicknesses equal to half the girder flange thickness

$$t_{cf} < b_{gf}/7 \quad \text{continuity plates are required with a} \quad (2.24)$$

thickness equal to the girder flange thickness.

- Roeder discussed the results of the SAC research in FEMA (2000f). The continuity plate requirements presented were the same equations as the AISC Seismic Provisions (AISC, 1992). Continuity plates are required if:

$$t_{cf} < 0.4 \sqrt{\frac{P_{gf}}{F_{yc}}} \quad (2.25)$$

where:

$$P_{gf} = 1.8t_{gf}b_{gf}F_{yg} \quad (2.26)$$

The equations (Equations 2.22-2.24) presented in the research by Ricles et al. (2000) were also included in FEMA (2000f) as possible additions to the continuity plate requirements. However, since the tests of Ricles et al. (2000) showed that Equations 2.25 and 2.26 provided a conservative measure of the continuity plate requirements, Roeder concluded that it was appropriate to return to the requirements of the 1992 Seismic Specification (AISC, 1992).

In summary, there is some consensus that continuity plates may be fillet-welded and may not always be required in non-seismic connections. However, there is strong consensus that continuity plates are required for connections in seismic zones, although there are differing opinions on the required width and thickness of the plate and on the type of weld that should be used to connect the stiffener to the column flange.

Chapter 3

Experimental Procedure

This chapter describes the specimen selection, specimen design, instrumentation, and testing procedure for the pull-plate tests. The specimen selection was based on a parametric study of continuity plate requirements, past research, and how well the specimens tested the realistic range of relevant parameters. The specimen design description includes details of connection design, material properties, and welding specifications. The description of the specimen instrumentation plans includes justification of strain gage and LVDT placement in order to define specimen failure modes and to compare these tests with previous research, current design specifications, and possible augmentations to the design equations.

3.1 Parametric Study of Continuity Plate Requirements

3.1.1 Definitions of Parameters

To aid in specimen selection for the pull-plate tests, a study of the parameters affecting continuity plate requirements was performed to analyze interior girder-to-column connections accounting for three different limit states: local flange bending (LFB), local web yielding (LWY), and local web crippling (LWC) (AISC, 1999b). The pull-plate tests were used primarily to investigate the design provisions for continuity plates for connections in non-seismic zones, although some consideration was given to seismic detailing as well. As such, the girder-to-column connections were also checked for compliance with the strong-column weak-beam (SCWB) criterion of the AISC Seismic Provisions (AISC, 1997). The table of section properties used in this study

contained values for 211 wide-flange sections (AISC, 1995). At first, the three failure modes were analyzed for all 44,521 possible girder-to-column combinations. However, to limit the possible combinations to a reasonable number, and to adhere to AISC (1997) to permit some consideration of seismic design, the parametric study was limited only to girder-to-column combinations commonly used in moment frames. These common sections included all W14 columns and girders ranging from W24 to W36. Both 50 ksi and 65 ksi column materials were considered, to include the possibility of using girder-to-column combinations of A572 Grade 50 and 65, A992, and A913 steel. All girder steel was assumed to be grade 50. All stiffener material strength was assumed to be 50 ksi.

For each of the three failure modes, the relationship between the factored nominal strength of the column and the required strength demand from the girder flange force was examined. If the girder flange force were greater than the nominal column strength, then a continuity plate (CP) would be needed.

The connections were examined for compliance with both non-seismic and seismic design provisions. The differences between the two provisions are the calculation of the required strength demand (AISC, 1992; AISC, 1997; AISC, 1999b), and the calculations for the SCWB criterion (AISC, 1997).

For the non-seismic provisions, the girder-to-column combination is not required to meet the SCWB criterion. The required strength demand, R_u , was calculated as:

$$R_u = F_{yg}A_{gf} \quad (3.1)$$

where:

F_{yg} = girder yield strength

A_{gf} = girder flange area

For seismic design considerations, the required strength demand was calculated as:

$$R_u = 1.8F_{yg}A_{gf} \quad (3.2)$$

The 1.8 factor is a result of a 1.3 strain hardening factor and the assumption that the plastic modulus of the girder flange is 70% of the plastic modulus of the girder to account for the focusing of the girder moment into the flanges. The pull-plate tests were designed to impart as large a girder flange force as possible on the column. However, a study of more than 20,000 tensile test samples of A992 and A572 Grade 50 structural steel (Dexter et al., 2000) resulted in an upper bound tensile-to-yield strength ratio of 1.5. Therefore, for these pull-plate tests, achieving a pull-plate strength that is 1.8 times the girder flange force is not possible; a peak strength of 1.4 to 1.5 of the pull-plate yield strength is a more reasonable expectation. The pull-plate tests thus impart on the column a peak demand that includes the effects of strain hardening (assuming a strain hardening factor of 1.3) plus some effect of the focusing of the girder moment into the girder flanges.

For the seismic provisions, the girder-to-column combination must meet the SCWB criterion as specified by the AISC Seismic Provision (1997) for Special Moment Frame (SMF) and Intermediate Moment Frame (IMF) structures, which is calculated as:

$$\frac{\sum_{column} M_{pc}}{\sum_{girder} M_{pg}} > 1.0 \quad (3.3)$$

$$\sum_{column} M_{pc} = \sum_{column} Z_c \left(F_{yc} - \frac{P_{uc}}{A_g} \right) \quad (3.4)$$

$$\sum_{girder} M_{pg} = \sum_{girder} (1.1R_y M_p + M_v) \quad (3.5)$$

where:

M_{pc} = column plastic moment

M_{pg} = girder plastic moment

Z_c = column plastic section modulus

F_{yc} = yield strength of the column

P_{uc}/A_g = required axial stress of column; axial stresses of 0, 10, 20 and 40 ksi were used to examine the effects of extreme axial stresses (0 and 40 ksi) and more typical axial stresses

$R_y = 1.1$ for rolled shapes made from A572/50, A992, A572/65 or A913 steel

M_p = nominal plastic moment of the girder

M_v = moment due to shear amplification

(Any variables not defined here are defined in Chapter 2.)

For this study, the additional moment due to shear amplification from the location of the plastic hinge to the column centerline, M_v , was not included, since the shear at the joint cannot be accurately calculated because the girder span is unknown. Neglecting this will not greatly affect the results, because if the plastic hinge forms at the column face, then the value of M_v is small.

Girder-to-column configurations meeting this SCWB criterion (for a particular axial stress) would be considered for this study to be permissible for Special Moment Frame (SMF) and Intermediate Moment Frame (IMF) applications, while those configurations failing this check, even at a column axial stress of zero, were considered permissible for Ordinary Moment Frame (OMF) or non-seismic configurations.

A third factored girder demand was also calculated, since for the pull-plate tests the seismic girder demand (Equation 3.2) resulted in a force larger than the ultimate tensile strength of the pull-plates (which was made of A572/50 steel) times the area of the pull-plates. Also, the current AISC Seismic Provisions (AISC, 1997) do not define a girder demand for continuity plate design, but indicate that the engineer should design the continuity plates according to how they were detailed in tests of similar connections. However, the provisions do identify a girder demand in order to check the strong-column weak-beam criterion. The girder demand in this case is calculated as:

$$R_u = 1.1R_y F_{yg} A_{gf} \quad (3.6)$$

The calculation of the girder demand takes into account strain-hardening of the girder with a more realistic 1.1 factor and includes an overstrength factor of the shapes.

For the research program, this definition for the girder demand was used to consider possible seismic demands on the columns.

The three different limit states associated with continuity plate requirements are briefly defined below (AISC, 1999b). If the column demand, R_u , were greater than the factored column strength, ϕR_n , then a continuity plate would be needed. For all three of these limit states, and for non-seismic (Equation 3.1) and seismic (Equation 3.6) values of R_u , the ratios of $\frac{\phi R_n}{R_u}$ were calculated to show what percentage of the flange force that the column could resist.

Local Web Yielding

$$\phi R_n = \phi(5k + N)F_{yc}t_{cw} \quad (3.7)$$

where:

$$\phi = 1.0$$

R_n = nominal resistance

k = distance from outer face of flange to web toe of fillet

N = length of bearing surface (taken as the thickness of the girder flange)

t_{cw} = thickness of column web

Local Flange Bending

$$\phi R_n = \phi 6.25 t_{cf}^2 F_{yc} \quad (3.8)$$

where:

$$\phi = 0.90$$

t_{cf} = column flange thickness

Local Web Crippling

$$\phi R_n = 135t_{cw}^2 \left[1 + 3 \left(\frac{N}{d_c} \right) \left(\frac{t_{cw}}{t_{cf}} \right)^{1.5} \right] \sqrt{\frac{F_{yc} t_{cf}}{t_{cw}}} \quad (3.9)$$

where:

$$\phi = 0.75$$

d_c = column depth

3.1.2 Results of Continuity Plate Parameter Study

The results of the study indicated which girder-to-column combinations need continuity plates. Only the combinations consisting of W14 columns and W24 to W36 girders are considered herein. The results are separated for non-seismic and seismic provisions. For seismic design considerations, the girder-to-column combinations are required to meet the SCWB criterion. Determining which girder-to-column combinations met this criterion severely restricted the number of sections that were possible for use in seismic design. Depending on the assumed column axial stress (0, 10, 20, or 40 ksi) and the column yield strength, the number of specimens eliminated by this check varied widely, but was always over 50% of the 1824 seismic moment frame combinations. For a column strength of 50 ksi and no column axial stress, the number of possible girder-to-column combinations decreased from the total number of combinations, 2204, to 574 combinations that met the SCWB criterion. For axial stresses of 0, 10 ksi, 20 ksi, and 40 ksi, the number of SCWB combinations decreased to 560, 422, 279, and 12, respectively. Similarly, for 65 ksi column strength, the number of SCWB combinations decreased to 739, 644, 490, and 195 as the axial stress was increased from 0 to 40 ksi.

A typical range of column sizes that had been previously tested by other researchers (SAC, 1996; Kaufmann et al., 1996a, 1996b; Dexter and Melendrez, 2000, Stojadinovic et al., 1999) includes W14x120, W14x145, W14x176, W14x257, and W14x311 sections. Table 3.1 gives an overview of the number of typical seismic girder-to-column combinations that met the SCWB criterion for these column sections and W24 to W36 girder sections.

Table 3.1: Girder-to-Column Combinations Meeting the SCWB Criterion

	50 ksi Column Strength		65 ksi Column Strength	
	10 ksi Axial Stress	20 ksi Axial Stress	10 ksi Axial Stress	20 ksi Axial Stress
W14x120	0	0	1	0
W14x145	0	0	3	1
W14x176	2	0	7	3
W14x257	9	3	19	12
W14x311	15	7	27	19

Local Web Yielding

For the investigation of LWY in conjunction with the seismic provisions, the equations for nominal strength from the AISC LRFD Specification (1999b) are used, since the 1997 AISC Seismic Provisions include no nominal strength equations (AISC, 1997). In the study for seismic design, only girder-to-column combinations that met the SCWB criterion were considered. The axial stresses of 10 and 20 ksi represent an approximate range of typical column axial stresses. For an axial stress of 10 ksi and a column strength of 65 ksi, 6% of the girder-column combinations that met SCWB criterion needed continuity plates. For the same axial stress and a column strength of 50 ksi, 3% of the SCWB combinations needed continuity plates. For an axial stress of 20 ksi and 65 ksi column strength, only 1.5% of the SCWB combinations needed continuity plates. For a 20 ksi axial stress and 50 ksi column strength, none of the 279 SCWB girder-to-column combinations needed continuity plates. These are significant results, since it shows that few of the connections designed to meet SCWB specifications would need continuity plates.

Compared to seismic design, fewer of the girder-column combinations designed for non-seismic zones need continuity plates. This is due to the smaller required strength demand. Considering the limited column and girder sections in this study, for a column of 50 ksi steel, it is possible to use a column as small as a W14x132 section and not need

continuity plates. Using 65 ksi column steel, the smallest possible section decreases to a W14x109.

Local Flange Bending

The results of the LFB study are similar to those for the LWY investigation. The LFB study showed that for connections meeting the SCWB criterion (i.e., seismic design), fewer of the columns need continuity plates, compared to LWY. In fact, there are no girder-to-column combinations using a W14 column and W24 to W36 girders that would require a continuity plate to meet LFB criteria, but would not need one to meet LWY criteria. In other words, the LWY failure mode always controls over LFB. Of course, connections may include doubler plates to mitigate panel zone yielding, in which case LWY is avoided. However, continuity plates may still be required for LFB.

The results from the non-seismic portion of the study follow the same trends as the seismic portion. Fewer columns need continuity plates compared to LWY, and there are no girder-column combinations that require continuity plates for LFB that do not require them for LWY. Thus, LWY controls the need for continuity plates in non-seismic regions also.

Local Web Crippling

The results from the LWC study followed the same trends as for the LWY and LFB failure modes. For seismic provisions, even fewer of the girder-column combinations that met the SCWB criterion needed continuity plates compared to the number of combinations that needed continuity plates to satisfy the LFB limit state. For a 65 ksi column strength, none of the SCWB connections required continuity plates regardless of the column axial stress considered. For a 50 ksi column strength, only 10 of the combinations needed continuity plates, and this was for the case of no column axial stress. The LWY limit state thus clearly controls the need for continuity plates in the unstiffened sections of this study.

The trends of the results for LWC in non-seismic zones are consistent with the non-seismic results for LWY and LFB. There are fewer connections that need continuity

plates for local web crippling in non-seismic zones compared to seismic areas. Also, LWY controls the need for continuity plates in non-seismic design considerations over both LWC and LFB.

3.1.3 Conclusions of Continuity Plate Parametric Study

Several general conclusions can be made regarding the results of this study:

- For seismic design, meeting the SCWB criterion significantly limits the number of possible girder-column combinations. For the girder and column sizes considered here (W14 columns and W24 to W36 girders), approximately 20% of the possible connections met the SCWB criterion. For 50 ksi column strength and axial stresses of 0, 10, 20, and 40 ksi, the lightest columns that met the SCWB criterion were W14x132, W14x159, W14x211, and W14x550, respectively. For 65 ksi column strength and an axial stress of 0 ksi, columns as light as a W14x99 section met the SCWB criterion.
- For non-seismic and seismic design considerations, the LWY limit state controls the need for continuity plates. A SCWB connection would need a continuity plate or web doubler plate to stiffen the column to prevent web yielding before a continuity plate would be needed for local flange bending or web crippling.
- The LWY study showed that for a column strength of 50 ksi and an axial stress of 10 ksi, approximately 3% of the girder-column combinations that met SCWB criterion would need continuity plates. For an axial stress of 20 ksi and 50 ksi column strength, none of the 279 girder-column SCWB combinations would need continuity plates. The LFB study showed that even fewer SCWB combinations breached this limit state.

3.2 Specimen Selection

3.2.1 Pull-Plate Specimen Selection Procedure

To establish specimen sizes for investigating continuity plate needs and detailing, several factors were used to limit the number of possible girder-column combinations that would be tested. The limiting factors were grouped into six categories.

- Commonly used girder and column sizes
- SCWB criterion
- Testing equipment capacity
- Recently tested sizes
- Girder compact section width-to-thickness ratio
- Study of relevant parameters

The first five factors were used to eliminate most of the possible girder-column combinations. A study of the pertinent parameters involving local web yielding and local flange bending was then used to select the final specimens for testing. The following section is an outline of the process used to select the pull-plate test specimens.

Commonly Used Girder and Column Sizes

The complete list of column and girder sizes was reduced to section sizes that are commonly used in moment frames. The columns were limited to W14 nominal section sizes and the girders were restricted to sizes ranging from W24 to W36. The column and girder sizes were further limited by considering only sizes that are commonly made in the United States. This eliminated seven of the heaviest W14 column sizes. These two restrictions created a list of 22 possible columns and 76 possible girders.

SCWB Criterion

The testing is aimed at developing continuity plate provisions for both non-seismic and seismic design considerations. For design of Special Moment Frames (SMF) and Intermediate Moment Frames (IMF) in seismic zones, the SCWB criterion (AISC, 1997) must be met. This criterion further restricts the possible girder-column

combinations. Two key variables of the SCWB criterion for the column, including column yield strength and column axial stress, were previously discussed in detail. In order to identify a range of appropriate specimen sizes in seismic zones, a yield strength of 50 ksi and an axial stress of 10 ksi were considered. An axial stress of 10 ksi was used for this selection criterion to be representative of an approximate lower bound typical column axial stress seen in practice.

Testing Equipment Capacity

The capacities of the equipment available for testing were also used as limiting criteria. The pull-plate tests were performed using a 600 kip testing machine. Therefore in order to develop the full demand of the girder flange, only girders with ultimate strength flange forces less than 600 kips could be used. The flange force, R_u , was calculated as $R_u = 1.1R_y F_y t_{gf} b_{gf}$, where $F_y = 50$ ksi. This criterion eliminated the heaviest girders of each nominal size and limited the number of possible girders to 17.

Attempts were made to coordinate the girder sizes tested in the pull-plate tests with the sizes used in the full-scale cyclic cruciform tests (Cotton et al., 2001). For the cruciform tests, laboratory capabilities enable testing of 11-foot girders (representing the span from the column face to the girder inflection point) attached to a 14-foot column section. Of the 17 girder sections that met the requirement of the 600 kip machine for the pull-plate specimens, nine were thus available for consideration for the cruciform tests.

Recently Tested Sizes

Consideration of recently tested sizes provided a guideline for selecting specimens that may be compared. The list of most commonly tested sizes includes the following columns and girders: W14x120, W14x145, W14x176, W14x257, W14x311, W14x398, W24x68, W27x94, W30x99, and W36x150 (e.g., SAC, 1996; Kaufmann et al., 1996a, 1996b; Leon et al., 1998; Stojadinovic et al., 1999; Dexter and Melendrez, 2000).

Width-to-Thickness Ratios

The girders were also examined for compliance of the compact section width-to-thickness ratio, λ_p , provision of the AISC Seismic Provisions (AISC, 1997). The

provision states that for girders $\lambda_p = \frac{b_f}{2t_f} \leq \frac{52}{\sqrt{F_y}}$. For a girder yield strength of 50 ksi,

this restricted the list to five possible girders. It is interesting to note that a W30x99 girder does not meet the seismic width-to-thickness ratio for 50 ksi steel, yet this section has been used in several recent experimental cyclically loaded tests (SAC, 1996; Stojadinovic et al., 1999). For these tests, the researchers assumed a yield strength of 36 ksi for the girders, for which the girder section does meet the width-to-thickness ratio. However, since this shape has proven to have good cyclic response in many of the tests, a relaxation the flange local buckling to the non-seismic ratio (AISC, 1993) of

$\frac{b_f}{2t_f} \leq \frac{65}{\sqrt{F_y}}$ is being considered (Iwankiw, 1999). All nine of the girders that had passed

the previously listed restrictions have width-to-thickness ratios that meet the non-seismic provision.

The width-to-thickness ratios of the columns were also considered. The seismic

specification (AISC, 1997) states that if the ratio of $\frac{\sum_{column} M_{pc}}{\sum_{girder} M_{pg}} \leq 1.25$, then $\frac{b_f}{2t_f} \leq \frac{52}{\sqrt{F_y}}$,

otherwise $\frac{b_f}{2t_f} \leq \frac{65}{\sqrt{F_y}}$. For the remaining possible column sizes and a yield strength of

50 ksi, all the columns passed the width-to-thickness ratio. The ratios ranged between 2.9 and 7.1.

Study of Relevant Parameters

A number of parameters were considered to verify the LWY and LFB equations and to propose standards for the use and sizing of continuity plates in moment-resisting frames. The parameters considered included:

- Column web thickness, t_{cw}
 - Column flange thickness, t_{cf}
 - Girder flange area, A_{gf}
 - Continuity plate size, A_{st}
 - Continuity plate welds
- Column Web Thickness

The majority of the past research of the effects of column web thickness on local web yielding was done by Sherbourne and Jensen (1957) and Graham et al. (1960) (see Chapter 2). Sherbourne and Jensen (1957) statically tested nine cruciform connections with girder tip loads monotonically applied in the same direction, using five different stiffener designs: no stiffeners, horizontal plate, vertical plate, split WF, and doubler plate. Five column sizes and one girder size were used in the connections. The column web thicknesses ranged from 0.288 in. to 0.580 in. In the four unstiffened connection tests (A-series), stress concentrations were located in the column webs opposite the girder flanges. Two of the unstiffened tests had significantly thinner column webs and flanges than the other two, and the connections failed by local web yielding. The two connections (B-series) with horizontal stiffeners (continuity plates) had flange and web thicknesses similar to the thinner A-series tests. Test B1 used a continuity plate approximately the same thickness as the girder flange, while test B2 used a continuity plate with about one-half the thickness. The B-series tests performed adequately, and were able to develop the full girder plastic moment. There was no evidence of overstress in the column webs or continuity plates, except for a few strain lines in the thinner continuity plates. It is unknown how much thinner these stiffeners could have been made and still have served their purpose.

Graham et al. (1960) also analyzed cruciform and four-way (i.e., three-dimensional) connections and the need for column stiffening to avoid local web yielding. Four cruciform tests without stiffeners and 11 compressive and 11 tensile pull-plate tests were performed to determine the column local web yielding criterion. The four cruciform tests were the unstiffened tests (A-series) performed by Sherbourne and Jensen

(1957). The compressive pull-plate tests consisted of 11 column stubs (approximately 3 feet in length) compressed at the flanges between two plates representing the girder compression flanges. No stiffeners were used. The columns tested had web thicknesses that ranged from 0.294 in. to 0.510 in. and “k” values that ranged from 1.063 in. to 1.438 in. The compressive load was continued until the column web failed by web crippling, which occurred well after web yielding. The compressive load at specimen failure was above the maximum nominal tensile strength of the pull-plate in all but one of the specimens, which had the thinnest web.

Two compressive pull-plate tests were also conducted on connections with continuity plates. The specimens consisted of a 12WF40 column section with a ¼ in. thick continuity plate and a 14WF61 column section with 3/8 in. thick continuity plate. These two column sections had the thinnest webs (0.294 in. and 0.378 in.) of the tested sections. As expected, the stiffened specimens failed at a higher load than the unstiffened tests. The loads at ultimate failure of the tests were 102.5 kips and 137.5 kips for the unstiffened tests and 172 kips and 282 kips for the stiffened specimens. Graham et al. (1960) compared the experimental results to the calculations using the proposed formula for local web yielding for interior conditions:

$$\sigma = \frac{R}{t_{cw}(N + 4k)} \quad (3.10)$$

The comparison showed that when Equation 3.10 predicted that a connection would need continuity plates, either the unstiffened connection failed by local web yielding or the stiffened connection behaved adequately. Using Equation 3.10, the average stress that the columns of the 11 compressive specimens resisted was approximately 50 ksi. The combinations of the pull-plate demand and web thicknesses of these 11 pull-plate tests enabled examination of the column web yielding behavior.

The girder (pull-plate)-column combinations of the current research program should have similarly high nominal column web stress values (calculated from Equation 3.10) in order to describe the local web yielding behavior of column sections that are commonly used today.

- Column Flange Thickness

The primary research that investigated the effects of column flange thickness on local flange bending, which led to the development of the current LFB equations was done by Graham et al. (1960), as discussed in Chapter 2. Along with the 11 compressive pull-plate tests done by Graham et al, 11 tensile pull-plate tests were conducted. These tests used tensile girder flanges to apply the force to the column flange. No continuity plates were used. The 11 tests varied two factors, column flange thickness and girder tension flange (pull-plate) thickness. The columns tested had flange thicknesses ranging from 0.3125 in. to 1.313 in. All of the connections failed because of excessive straining in the area close to the column fillet and the center of the weld, as a result of the outward bending of the column flanges.

Verification of the LFB equation is worthwhile, since the equation was developed from tests that consisted of columns and girders having a much lower yield strength than currently used today, and all the connections consisted of columns with fairly thin flanges. Also, approximations based on sizes from a range of girder-to-column combinations were used to simplify the LFB equation. For example, the original LFB equation contained the term $\frac{t_{gf} m F_{yw}}{R_n}$, and it was determined from the Graham et al. (1960) that the minimum value of this term was 0.15. This simplification is still used in the current LFB equation (AISC, 1999b).

The current research program was aimed at testing commonly used column section sizes that would reassess the approximated variables of the LFB equation with current material properties.

- Girder Flange Area

In the 11 tensile pull-plate tests performed by Graham et al. (1960), a group of tests consisted of the same column shape with varying tensile girder flange areas. The results of the tests showed that as the girder flange (pull-plate) area was increased, the

failure load of the connection also increased. No tests were conducted to investigate the effects of the girder flange area when continuity plates were included in the connection.

In the proposed test matrix, the girder flange area will be kept constant in order to focus the effects of the column flange thicknesses and continuity plate thicknesses on the limit states.

- Stiffener Details

Graham et al. (1960) developed equations to size continuity plates, which were based on the theory that the continuity plates would resist the force equal to the difference between the required demand strength of the girder flange and the factored design strength of the column. The equation was created with the assumption that the continuity plates had the same total width as the girder flanges and that the continuity plates, girders, and columns all had the same yield strength. As discussed in Chapter 2, for the compression region of the connection, the force required of the continuity plates was defined as:

$$F_{yst} A_{st} = b_{gf} t_{gf} F_{yg} - F_{yc} t_{cw} (5k + N) \quad (3.11)$$

where:

F_{yst} = yield strength of the continuity plates (stiffener)

A_{st} = area of continuity plates = $t_{st} b_{st}$

t_{st} = continuity plate thickness

b_{st} = continuity plate thickness

Therefore, the required thickness of the continuity plates was:

$$t_{st} = \frac{b_{gf} t_{gf} - t_{cw} (5k + N)}{b_{bf}} \quad (3.12)$$

Using plate buckling analysis by Haaijer (1958), a further limitation for slenderness of the continuity plates was defined by Graham et al. (1960) as:

$$t_{st} \geq \frac{b_{st}}{16} \quad (3.13)$$

Two connections with continuity plates were tested by Graham et al. (1960) to validate the continuity plate thickness equation. One connection used a continuity plate with the same thickness as the girder flange thickness. The second connection used a continuity plate that was one-half the thickness of the girder flange. The tests confirmed that the equations to size continuity plates were reasonable and somewhat conservative. The tests showed no evidence that the half-thickness continuity plates were overstressed. However, only two connections were tested, and the two specimens consisted of different column sizes.

The Allowable Stress Design (ASD) Specification, 8th and 9th Editions (1978, 1989) adopted the continuity plate equations of Graham et al. (1960) for non-seismic design. The equations were generalized to size the area of the continuity plate, A_{st} , instead of just the thickness, and to incorporate different yield strengths of the girder, column, and continuity plates. The minimum continuity plate area was calculated from the following formula whenever the calculated value of A_{st} was positive:

$$A_{st} = \frac{P_{bf} - F_{yc} t_{cw} (5k + N)}{F_{yst}} \quad (3.14)$$

where:

P_{bf} = factored girder flange force

= force delivered by the flange multiplied by 5/3 when the force is due to live and dead load only, or by 4/3 with the force is due to live and dead load in conjunction with wind or earthquake forces

The ASD Specifications (1978, 1989) also required that the continuity plates meet the following criteria:

- The width of each stiffener plus one-half the thickness of the column web must be greater than one-third the width of the flange delivering the concentrated force
- The thickness of the stiffeners must be greater than $t_{bf}/2$

- The weld joining the stiffeners to the column web must be of sufficient size to carry the force in the stiffener caused by the unbalanced moments on opposite sides of the column

The AISC LRFD Specification (AISC, 1999b) uses the same basic equations for the area requirements for the continuity plates:

$$A_{st} = \frac{R_{ust}}{\phi F_{yst}} \quad (3.15)$$

where:

$$\phi = 0.90$$

R_{ust} = required force the continuity plate must resist:

$$R_{ust} = P_{uf} - \phi R_{n \min} \quad (3.16)$$

P_{uf} = factored girder flange force (required strength)

$\phi R_{n \min}$ = the lesser of the column design strengths for LFB and LWY

Similar to the 1978 and 1989 Specifications, the 1999 AISC Specification has requirements for the continuity plate width and thickness. The continuity plate width plus one-half the thickness of the column web must be greater than or equal to one-third of the width of the girder flange delivering the concentrated force.

$$b_{st} \geq \frac{W - t_{cw}}{2} \quad (3.17)$$

where:

$$W = \frac{2b_{gf}}{3} \quad (3.18)$$

The minimum thickness of the continuity plates is defined as:

$$t_{s \min} = \frac{t_{gf}}{2} \geq 1.79 \sqrt{\frac{F_{yst}}{E}} \quad (3.19)$$

where the last term is the limiting width-thickness ratio for unstiffened compression elements (Table B5.1, AISC, 1999b). The 1999 LRFD Specification does not give equations to size the welds connecting the continuity plates to the column flanges or web. The specification states that the welds joining the continuity plates to the column flanges

should be develop the welded portion of the stiffener. The welds connecting the continuity plates to the column web need to be appropriately sized in order to transmit the unbalanced forces.

After the Northridge earthquake, the FEMA Interim Guidelines Advisory No. 1 (FEMA, 1996a) recommended that continuity plates be used in all seismic moment resisting frames, and that the thickness of the plates be at least equal to the thickness of the girder flange. The commentary gave insight into determining the thickness of the continuity plate but gave no recommendations. It stated that the thickness of the continuity plates should not be overly thick, because the thick welds would contribute to high restraint and cause residual stresses in the column. However, eliminating the continuity plates would cause column flange bending and web yielding.

The AISC Seismic Provisions (AISC, 1997) removed all guidelines for sizing continuity plates. The specification simply stated that, for special moment frames, “continuity plates shall be provided to match the tested connection” (AISC, 1997). The commentary expanded on the statement by citing post-Northridge tests, which showed that even when continuity plates of substantial thickness were used, the inelastic strains across the weld of the beam flange to the column flange were substantially higher opposite the column web than at the flange tips. The stress distributions of these tests showed that the provisions of continuity plate sizing from earlier specifications were unjustified.

AISC published a design guide of continuity plate provisions as part of the Steel Design Guide Series (AISC, 1999a). The Design Guide (AISC, 1999a) recommends using the required continuity plate area equations as defined in the 1999 AISC LRFD Specification [Equations (3.14) and (3.15)].

The Design Guide requires different continuity plate widths and thicknesses for low-seismic and high-seismic applications. For low-seismic considerations, the minimum width of each continuity plate is defined as given in the 1999 AISC Specification [Equations (3.16) and (3.17)]. In high-seismic applications, the minimum width should be successfully tested before it is specified for design. Currently, qualifying

cyclic tests have used continuity plates with widths equal to or slightly greater than the girder flange, or the same as the full width of the column flange.

The thickness of the continuity plates was also differentiated for low and high seismic applications. In low-seismic zones, the minimum thickness of each continuity plate was the same as the 1999 AISC Specification [Equation (3.18)]. However, another limitation for full depth continuity plates that included the dimension of the clips was added:

$$t_{st} \geq \frac{(R_{ust})_1 + (R_{ust})_2}{0.9 * 0.6 F_{yst} (l - 2 * clip)(2)} \quad (3.20)$$

where:

R_{ust} = required strength of the continuity plates; the subscripts 1 and 2 indicate the forces at each end of the continuity plate

l = continuity plate length

$clip$ = continuity plate corner clip dimension

In high-seismic zones, AISC (1999a) indicates that the thickness of each continuity plate that is specified should be previously tested. Currently, most qualifying tests have used continuity plates with thicknesses equal to the girder flange thicknesses.

FEMA (2000b) indicates that when continuity plates are required for two-sided connections the thickness should be equal to the thickness of the girder flange and should conform to Section K1.9 of the AISC LRFD Specification (AISC, 1999b). The commentary states that following the Northridge earthquake, the lack of continuity plates contributed to failure of the connections, which was the reason FEMA-267A (FEMA, 1996) required continuity plates in all connections. However, Ricles et al., (2000) confirmed that if the column flange is sufficiently thick, continuity plates might not be necessary.

Doubler plates were also stiffer details that were parameters of this research program. The doubler plate detail, in which the doubler plates are flush against the column web, is a detail more prevalent in seismic design, and will be examined in more depth in Cotton et al. (2001). However, the behavior of the doubler plate box detail, in

which the doubler plates are welded to the column flanges near the tip of the flanges, is examined to act as both a doubler plate and a continuity plate. This detail was first tested cyclically by Bertero et al. (1973) and is included in AISC Seismic Provisions (AISC, 1997). The detail will be described further in Section 3.3.1.

An objective of the current research program was to reassess stiffener details. Past research of Graham et al. (1960) looked at two fairly small column sizes, 8WF31 and 12WF40, with full-thickness and half-thickness continuity plates, respectively. The results of the research stated that the half-thickness continuity plates were not overstressed. However, the current design guidelines and provisions recommend full-thickness continuity plates in seismic design applications. The current research program is focused on comparing the behaviors a common column-girder (pull-plate) combination with different continuity plate thicknesses. The doubler plate box detail was examined by Bertero et al. (1963) under cyclically loading applications. This research program tested the detail under monotonic loading, as well as under cyclic load (Cotton et al., 2001), using modern material and larger member sizes.

- *Continuity Plate Welds*

The history of the provisions for continuity plate welds is not as detailed as for the continuity plate thickness. As outlined in Section 2.2, several researchers have made recommendations for weld types and sizes. However, no tests have been done for the sole purpose of testing continuity plate welds. The results of the research created little consensus regarding whether fillet welds or CJP welds should be used to connect the continuity plates to the column flanges. The final design recommendations by SAC (FEMA, 2000c) required the use of CJP welds unless otherwise shown. Fillet welds are allowed to connect the continuity plates to the column webs, and must be sized in order to transmit the shear capacity of the net length of the plates.

The AISC Design Guide Series (AISC, 1999a) recommended procedures for sizing the weld connecting the continuity plate to the column flanges. In low-seismic applications, the weld must develop the strength of the welded portion of the continuity

plate. This can be accomplished by using double-sided fillet welds, double-sided partial penetration welds with fillet weld reinforcement, or complete joint penetration groove welds. The required weld size for double-sided fillet welds is:

$$w_{\min} = \frac{0.9F_{yst}t_{st}}{0.75(1.5 * 0.6F_{EXX})\sqrt{2}} = \frac{0.943F_{yst}t_{st}}{F_{EXX}} \quad (3.23)$$

where:

w_{\min} = minimum fillet weld size

F_{EXX} = welding electrode specified minimum strength

If the continuity plate is required only for a compressive flange force, the minimum weld size for double-sided fillet welds is:

$$w_{\min} = \frac{R_{ust}}{0.75(1.5 * 0.6F_{EXX})(b_{st} - clip)(2)\sqrt{2}} = \frac{0.542R_{ust}}{F_{EXX}(b_{st} - clip)} \quad (3.24)$$

In high seismic zones, the weld must develop the strength of the welded portion of the continuity plate. If using double-sided fillet welds, the required weld size is given by Equation (3.23).

Proposed Pull-Plate Specimens

Based on the presented selection criteria and relevant test parameters, a test matrix of possible connection sizes was created as shown in Table 3.2.

Table 3.2: Properties of Possible Unstiffened Pull-Plate Specimens

	Column	W14x120	W14x132	W14x145	W14x159	W14x176
	t_{cw}	0.590	0.645	0.680	0.745	0.830
	t_{cf}	0.940	1.030	1.090	1.190	1.310
	SCWB? (with a 10 ksi axial load)	No	No	No	No	No
Seismic*	LWY	0.39	0.44	0.48	0.56	0.66
	LFB	0.37	0.44	0.50	0.59	0.72
	LWC	0.50	0.60	0.67	0.80	0.99
Non- seismic*	LWY	0.70	0.79	0.86	1.01	1.19
	LFB	0.66	0.80	0.89	1.06	1.29
	LWC	0.90	1.08	1.20	1.44	1.78
1.1R_y*	LWY	0.58	0.66	0.72	0.84	0.99
	LFB	0.55	0.66	0.74	0.89	1.07
	LWC	0.75	0.90	1.00	1.20	1.48

* The values in the table are the ratio of $\frac{\phi R_n}{R_u}$, which show the percentage of the flange force the column can resist. Equations (3.1), (3.2), and (3.6) were used to determine R_u for non-seismic and seismic design, respectively, while Equations (3.7), (3.8), and (3.9) were used to calculate ϕR_n for LWY, LFB, and LWC, respectively.

3.2.2 Pull-Plate Specimen Justification

The specimen sizes were designed taking into consideration the relevant parameters, as previously discussed, and finite element analyses. The column sections proposed were selected in order to test a variety of column flange thicknesses and column web thicknesses. The following parameter discussion explains how the specimens were selected and how they tested the relevant parameters.

3.2.2.1 Preliminary Finite Element Analyses to Predict Specimen Behavior

In order to select the specimen sizes for experimental research, finite element models were built for several different connections and the results were compared. Not

only was the finite element method used to help determine the appropriate specimen sizes, but it was also used to select the length of the column stub. Details of the finite element models are given in Ye et al. (2000).

Models were built using W14x120, W14x132, W14x145, and W14x159 column sections. One-quarter of each specimen was used in the finite element model. There are two planes of symmetry: a horizontal plane passing through the mid-depth of the column web and a vertical plane passing through the mid-plane of the column web, as shown in Figure 3.1. All four of the connections consisted of unstiffened sections and pull-plates representing a W27x94 girder flange. Actual nominal dimensions of a W27x94 flange are $t_{gf} = 0.745$ in. and $b_{gf} = 9.995$ in. The pull-plates were constructed as $\frac{3}{4}$ in. by 10 in. plates. The columns were built using nominal section dimensions (AISC, 1995).

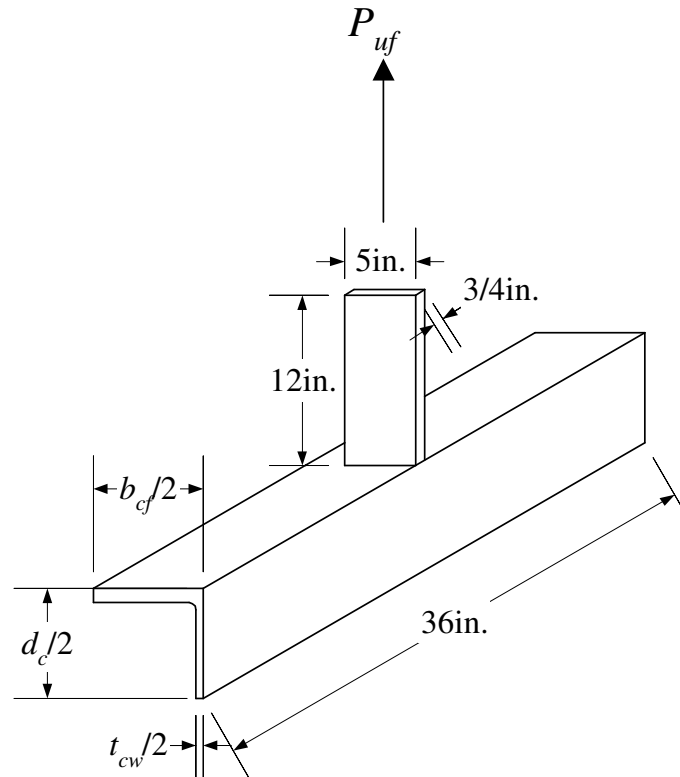


Figure 3.1: One-Quarter Symmetric Finite Element Model of Pull-Plate Specimen

The unstiffened pull-plate model typically consisted of 4725 nodes and 3273 elements, as shown in Figure 3.2. Generally, the mesh consisted of four layers of elements through the thickness of the pull plate, the column web, and the continuity plate;

three layers of elements through the column flange thickness; 17 elements along the half width of the column flange; and 11 elements along the half depth of the column web. However, at areas of high stress concentrations, such as directly below the pull-plate in the column k-line, smaller elements were used to more accurately define the behavior of the specimens. A mesh refinement study [details can be found in (Ye, et al., 2000)] was conducted on an unstiffened specimen with a 2 ft column stub length, refining the mesh everywhere where high stress and strain gradients were observed. The results of the study indicated the coarser mesh to be sufficient for the analysis.

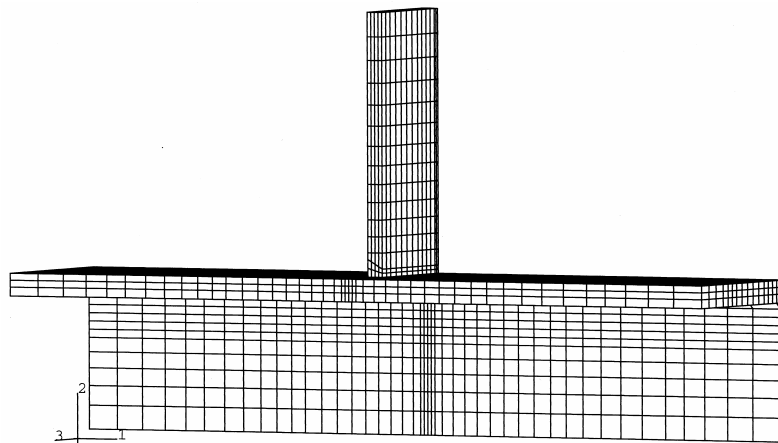


Figure 3.2: Finite Element Mesh of Unstiffened Specimens [after (Ye et al., 2000)]

The models were constructed using A992 column sections and A572 Gr. 50 plate material for the pull-plates. For the preliminary finite element analyses, the nominal minimum specified yield strength of 50 ksi was used for all column sections and plate material. The input data for the finite element models were simplified piecewise linear stress-strain curves based on the results of tensile tests conducted by Frank on a sampling of currently rolled shapes (FEMA, 2000d). Figure 3.3 shows this stress-strain curve, based on Frank's research, for the A992 steel used in the preliminary finite element models. The curve was defined by the nominal yield strength F_{yn} (e.g., 50 ksi for A992 steel) and by the nominal yield strain $\epsilon_{yn}=F_{yn}/E$, where E is Young's modulus, which was taken as 29,000 ksi.

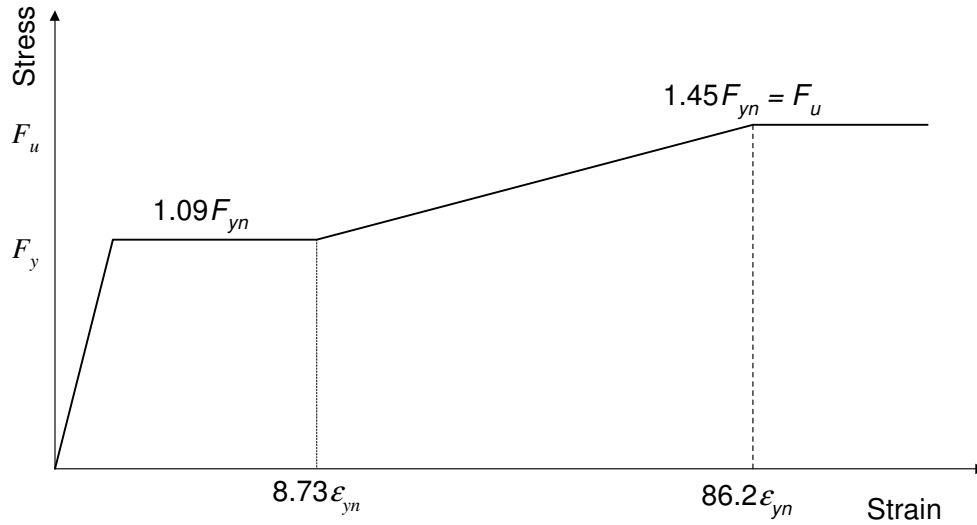


Figure 3.3: Stress-Strain Curve of A992 Steel [after (Ye et al., 2000)]

The stress-strain curve of the weld metal was similar to that of the base metal, except that a shorter yield plateau and more gradual strain-hardening progression were used. A yield strength of 75 ksi and a tensile strength of 80 ksi was used in the finite element models.

For specimen selection, the behavior of the finite element models was compared, including key comparisons at five different locations: one measurement of flange displacement and two strain measurements at two locations in the column flanges and column webs. The behavior at these five locations is compared in Figures 3.4 through 3.8. The comparisons in the figures are reported at a load of approximately 400 kips. This load level was chosen since it is greater than the nominal yield strength of the pull-plates (equal to 375 kips, calculated by Equation 3.1 using F_{yg} equal to 50 ksi), and is also greater than the loads that the columns can resist for either LWY or LFB (calculated by Equation 3.7 and Equation 3.8). Table 3.3 contains the load levels (in kips) that the limit states for LWY and LFB are breached for the four column sections that were considered.

Table 3.3: Nominal Column Resistance and Demands

	W14x120	W14x132	W14x145	W14x159
LWY (Eq. 3.7)	262 kips	296 kips	323 kips	380 kips
LFB (Eq. 3.8)	249 kips	298 kips	334 kips	398 kips
Non-seismic Demand (Eq. 3.1)	375 kips			
Seismic Demand (Eq. 3.6)	~ 450 kips			

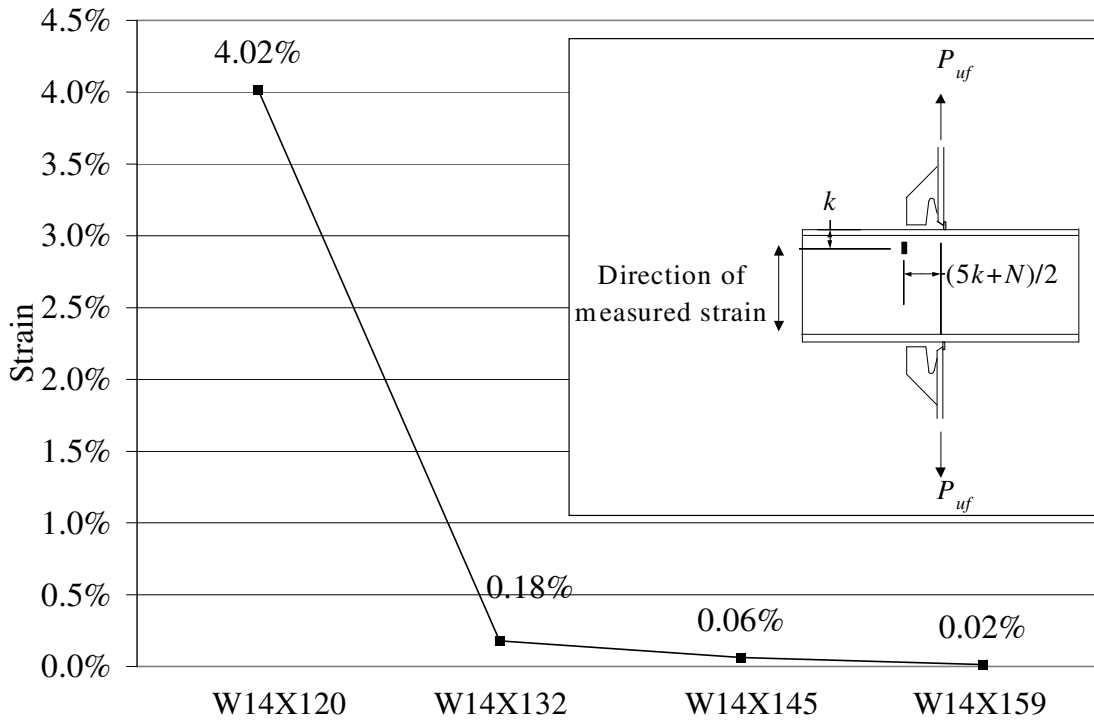


Figure 3.4: Comparison of Strain in Web vs. Load for Possible Pull-Plate Specimens

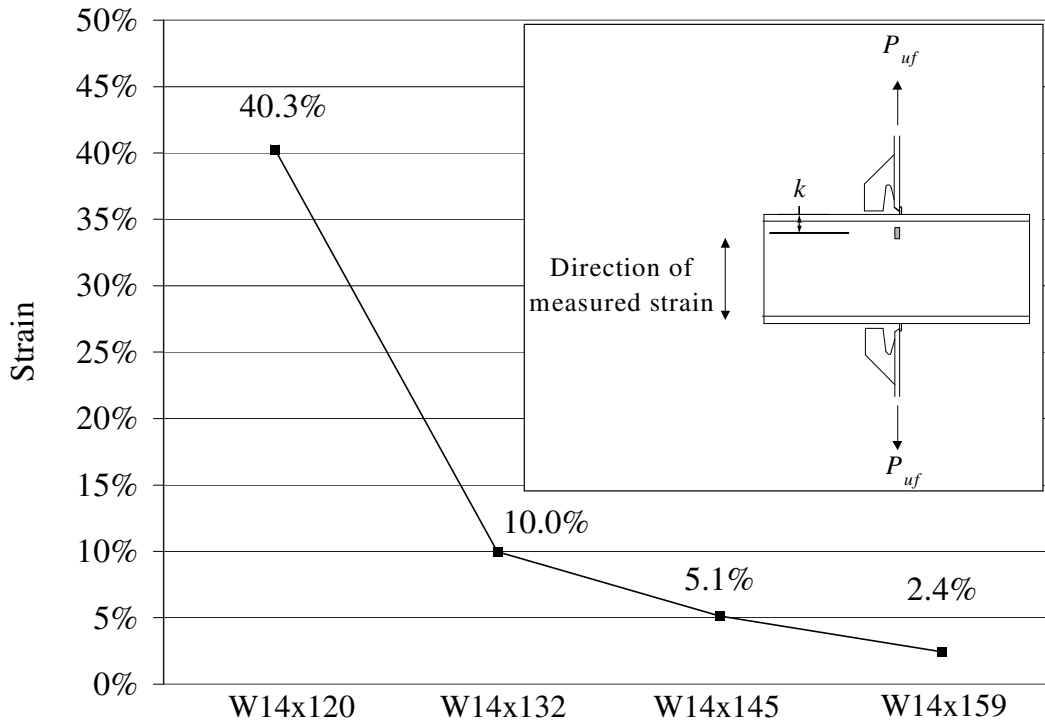


Figure 3.5: Comparison of Strain in the Web vs. Load for Possible Pull-Plate Specimens

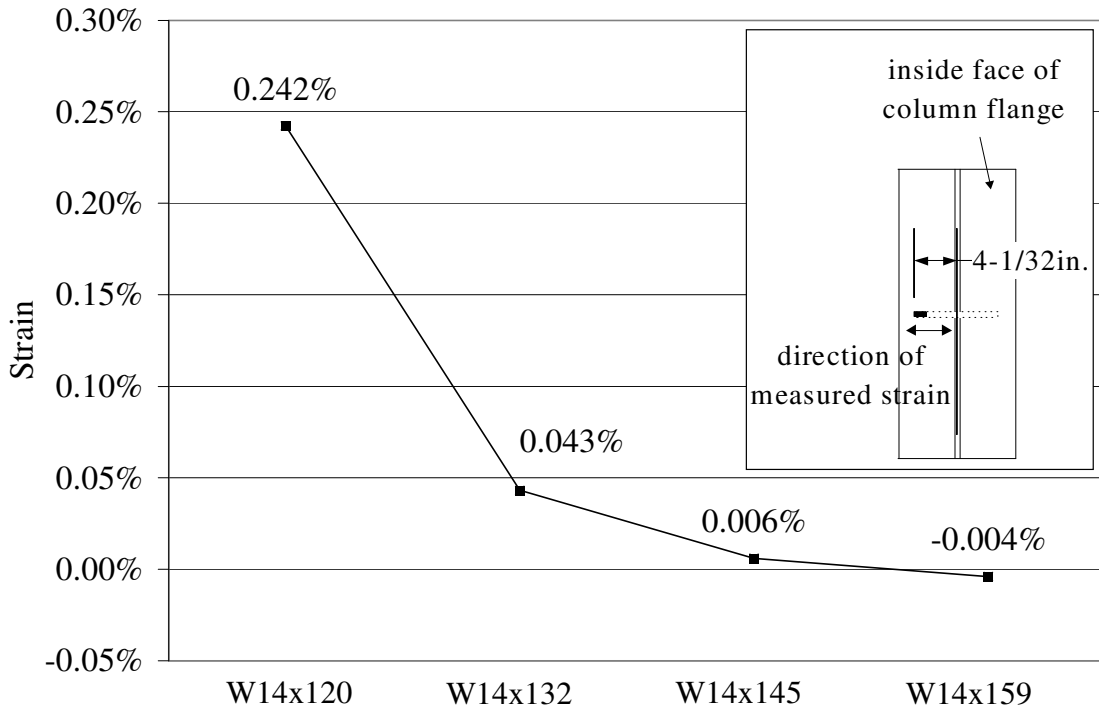


Figure 3.6 Comparison of Strain in Flange vs. Load for Possible Pull-Plate Specimens

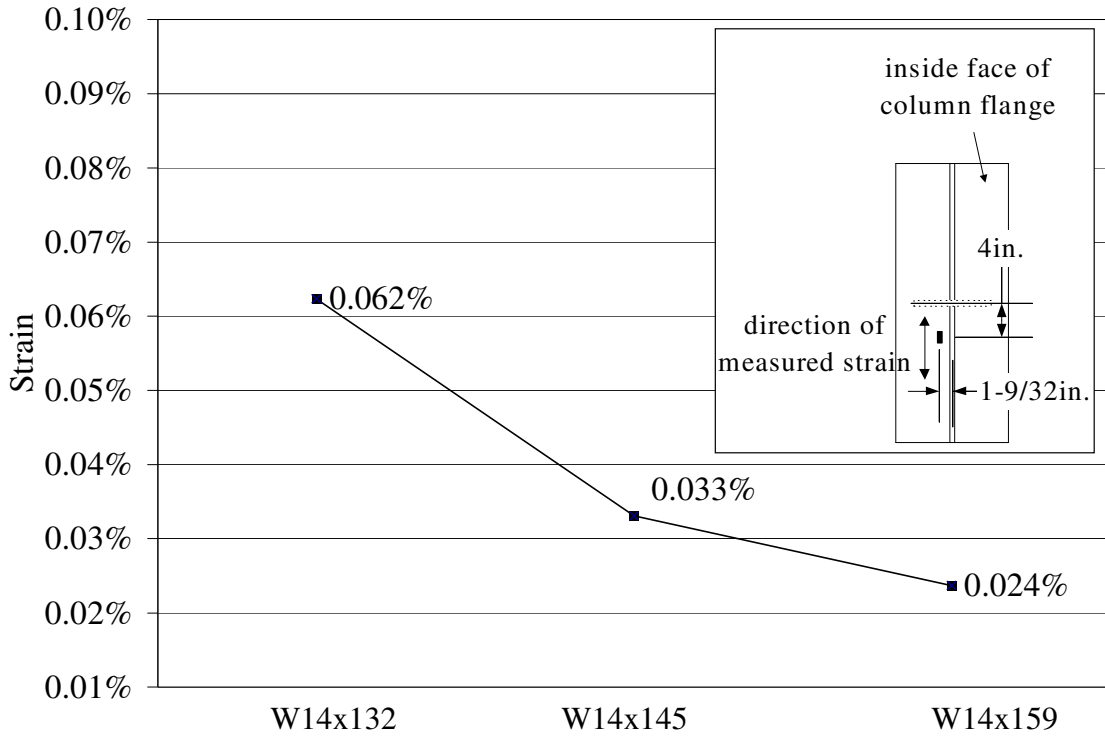


Figure 3.7: Comparison of Strain in Flange vs. Load for Possible Pull-Plate Specimens

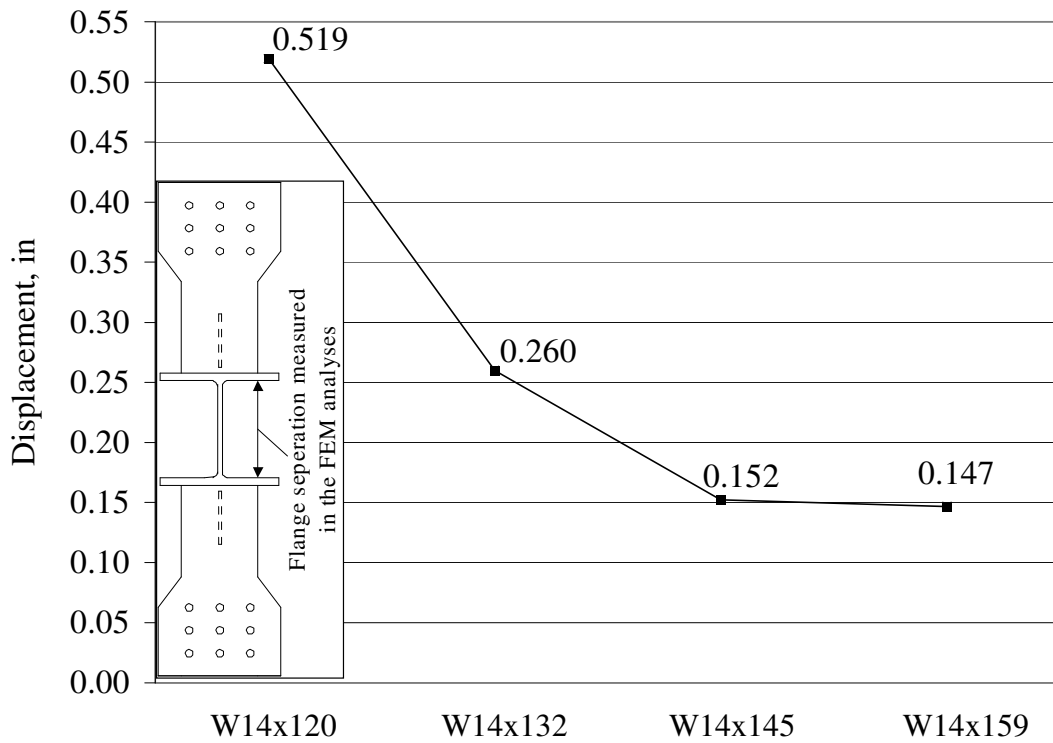


Figure 3.8: Comparison of Flange Separation vs. Load for Possible Pull-Plate Specimens

As can be seen in all the figures, there is a considerably larger change in displacement or strain measurement between the W14x120 and W14x132 column sections than when comparing the other sections. Figure 3.4 shows that at 400 kips the predicted strain in the column web in the direction of loading at a distance of $(5k+N)/2$ from the column length centerline was approximately 4% strain for the W14x120 section. As shown in Figure 3.5, at the column centerline, the corresponding web the strain was about 40%. These are extreme values, and clearly the specimen would have exceeded the LWY limit state. The same figures show that the W14x132 had much more reasonable behavior, but still would likely fail by LWY. The strain at a distance of $(5k+N)/2$ was predicted as 0.18% (approximately equal to the yield strain), and at the centerline the value was 10%. According the AISC LRFD Specification (AISC, 1999b), all of the lightest three sections needed continuity plates for non-seismic applications. Therefore, since the W14x132 needed stiffeners according to the specifications and the finite element analyses predicted a reasonable possibility of LWY failure, it was chosen as the smallest section to test the LWY limit state.

Also, since the difference in the behavior of the column webs so closely resembled the difference in the behavior of the column flanges, the LFB limit state was tested using the same sections. Therefore, the W14x132 column section was predicted to exceed both the LWY and LFB limit states, while the W14x145 was predicted to behave adequately. A W14x159 section was also tested unstiffened to insure testing of a column that exhibited little tendency toward failure. In addition, a W14x132 and a W14x145 were tested with doubler plates to mitigate LWY, so as to focus on the distinction in the LFB response of these specimens. Four stiffened W14x132 specimens, described more in the next sections, completed the test matrix.

3.2.2.2 Specimen Parameter Discussion

- *Column Web Thickness*

The column webs from the three proposed column sections ranged from 0.645 in. to 0.745 in. In comparison, the cruciform tests by Sherbourne and Jensen (1957)

consisted of columns with web thicknesses ranging between 0.288 in. and 0.580 in, and Graham et al. (1960) tested 11 pull-plate tests with web thicknesses in a similar range, 0.294 in. to 0.510 in. The web thicknesses tested in this research program represent realistic column sizes used currently. Considering the girder demand, the pull-plate specimens tested by Graham et al. (1960) had column web stresses (calculated from Equation 3.10) of approximately 50 ksi, as stated in Section 3.2.1. This web stress value was great enough to examine the web yielding behavior. The column sections in this research program had nominal column web stress values of approximately 70 ksi, which also enable examination of the local web yielding behavior.

- Column Flange Thickness

The purpose of investigating the effect of the column flange thickness was to verify the local flange bending equation developed by Graham et al. (1960). The 11 pull-plate tests by Graham et al. (1960) had flange thicknesses varying between 0.3125 in. and 1.313 in. The upper end of this range of flange thicknesses is not unreasonable for non-seismic design. However, for seismic provisions regarding SCWB, columns with thin flanges will not meet the strong column criterion. Therefore, to provide some consideration of these results for seismic design, the test matrix consists of columns with a range of flange thicknesses from 1.03 in. to 1.19 in.

- Girder Flange Area

The specimens all include a pull-plate whose dimensions are that of the tensile girder flange of a W27x94. This girder section was chosen because it is commonly used today. To insure consistency in the demand placed on the columns, the girder flange area was not a variable in this study.

- Stiffener Details

While AISC (AISC, 1999b) indicates that continuity plates need not be used in all connections, previous tests and analysis (Popov et al., 1986, Tremblay et al., 1995, Roeder, 1997) have resulted in recommendations that continuity plates should be used in

all moment-resisting frames in seismic zones. However, the appropriate thickness of the continuity plates has not yet been solidified. El-Tawil (1998) performed finite element analyses to determine the needed thickness of continuity plates. In addition, alternative doubler plate details, which avoid welding in the column k-lines, were investigated. Four specimens were selected to contribute to recommendations by testing W14x132 columns with a half-thickness continuity plates, full-thickness continuity plates, and the doubler plate box detail. The specimen with the half-thickness continuity plates was repeated to verify the results.

- *Continuity Plate Welds*

The test specimens were designed to help determine if fillet welds or CJP welds are needed to adequately connect the continuity plates to the column flanges. The majority of the past research (Popov et al., 1986; Engelhardt et al., 1997; Engelhardt, 1999) in this area has determined that complete joint penetration welds should be used. However, no tests have been done for the sole purpose of determining if fillet welds are inadequate. Yee et al. (1998) performed finite element analyses and determined that fillet welds would be sufficient for the continuity plate welds. The pull-plate experiments further contribute to this past research.

3.3 Specimen Design

The following sections contain a description of the specimens in the research program. The complete dimensions of each specimen connection, stiffener details, and weld sizes will be described.

3.3.1 Specimen Connection Description

The following is a list of all nine specimens. For all the specimens, pull-plates with the approximate dimensions of W27x94 girder flanges were used. All columns were

made of A992 steel. The pull-plates and all stiffener plates were made of A572 Grade 50 steel.

1. Specimen 1-LFB: W14x132 without continuity plates, with doubler plates
2. Specimen 2-LFB: W14x145 without continuity plates, with doubler plates
3. Specimen 1-LWY: W14x132 without any stiffeners
4. Specimen 2-LWY: W14x145 without any stiffeners
5. Specimen 3-UNST: W14x159, without any stiffeners
6. Specimen 1-HCP: W14x132, with half-thickness continuity plates and fillet welds
7. Specimen 1B-HCP: repeat of 1-HCP to verify results
8. Specimen 1-FCP: W14x132, with full-thickness continuity plates and CJP welds
9. Specimen 1-DP: W14x132, with doubler plate box detail

Specimens Focused on Local Flange Bending

The first two specimens were designed to test the cusp of the LFB behavior. Preliminary finite element analyses (as discussed in Section 3.2.2.1) concluded that a connection consisting of a W14x132 with doubler plates to stiffen the web would exceed the LFB limit state, and a similar specimen with a W14x145 column would not exceed the limit state. Neither specimen met the SCWB criterion for any level of column axial stress. Figure 3.9 is a drawing of both specimens 1-LFB and 2-LFB. The specimens had doubler plates fillet-welded flush to the column webs in order to eliminate web yielding and isolate the LFB behavior. The doubler plates were sized on the basis of the AISC Seismic Provisions (AISC, 1997), assuming a W27x94 girder section and accounting for panel zone yielding so as to provide consistency in the design philosophy used in the cyclic tests of Cotton et al. (2001). The doubler plates were ½ in. thick beveled A572 Gr. 50 plates fillet-welded to the column flange to avoid welding in the column k-line. Not only did the doubler plates act to isolate the flange bending behavior, but they also tested one of the alternative doubler plate welding details included in the 1997 AISC Seismic Provisions (AISC, 1997) (shown in Figure 3.10).

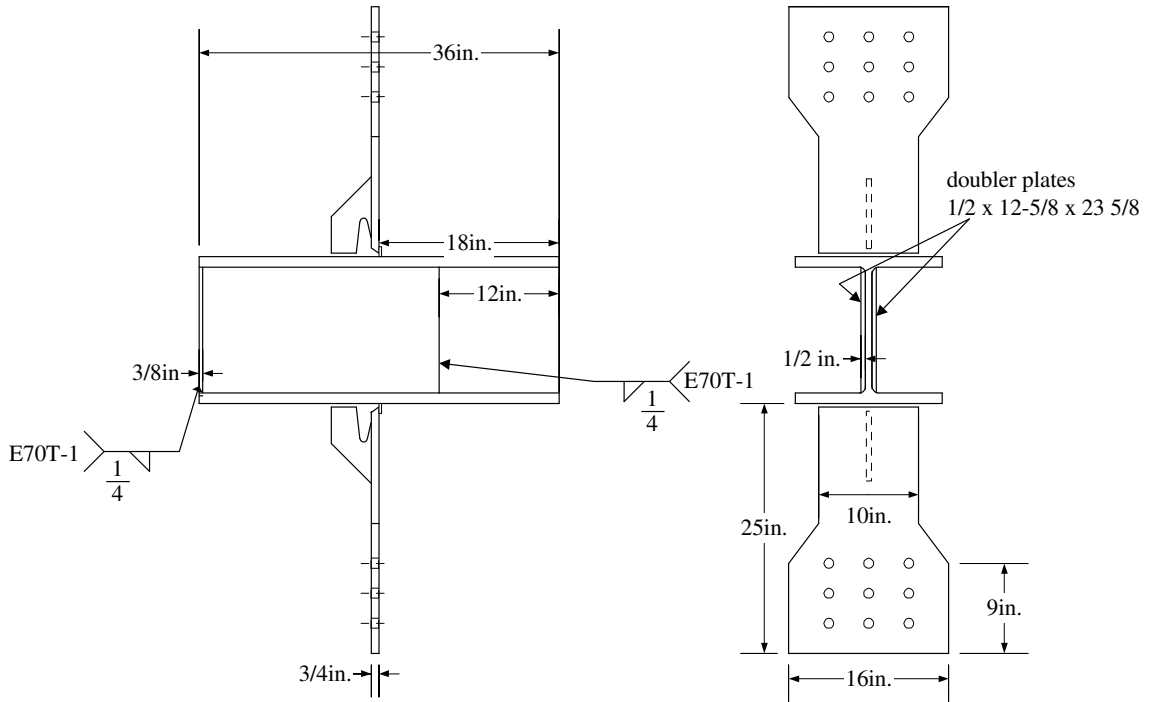


Figure 3.9: Specimens 1-LFB and 2-LFB

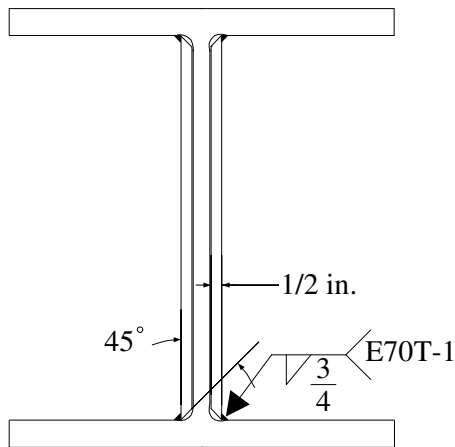


Figure 3.10: Doubler Plate Fillet Weld on Specimens 1-LFB and 2-LFB

Specimens Focused on Local Web Yielding

Shown in Figure 3.11 are Specimens 1-LWY, 2-LWY, and 3-UNST, which were designed to examine LWY behavior. The specimens did not meet the SCWB criterion and needed continuity plates for both LWY and LFB, but were tested completely

unstiffened. The finite element analyses (as described in Section 3.2.2.1) resulted in the conclusion that the unstiffened W14x132 specimen (1-LWY) would exceed both the limit states of LWY and LFB and the unstiffened W14x145 specimen (2-LWY) would not exceed either limit state. (See Table 3.3 for the values for column resistance and girder demand.) Specimen 3-UNST was an unstiffened W14x159 column section that did not meet the SCWB criterion, and did not need continuity plates for LWY or LFB for non-seismic demand. This specimen was tested in order to compare the behavior of the under-reinforced specimens that did need continuity plates.

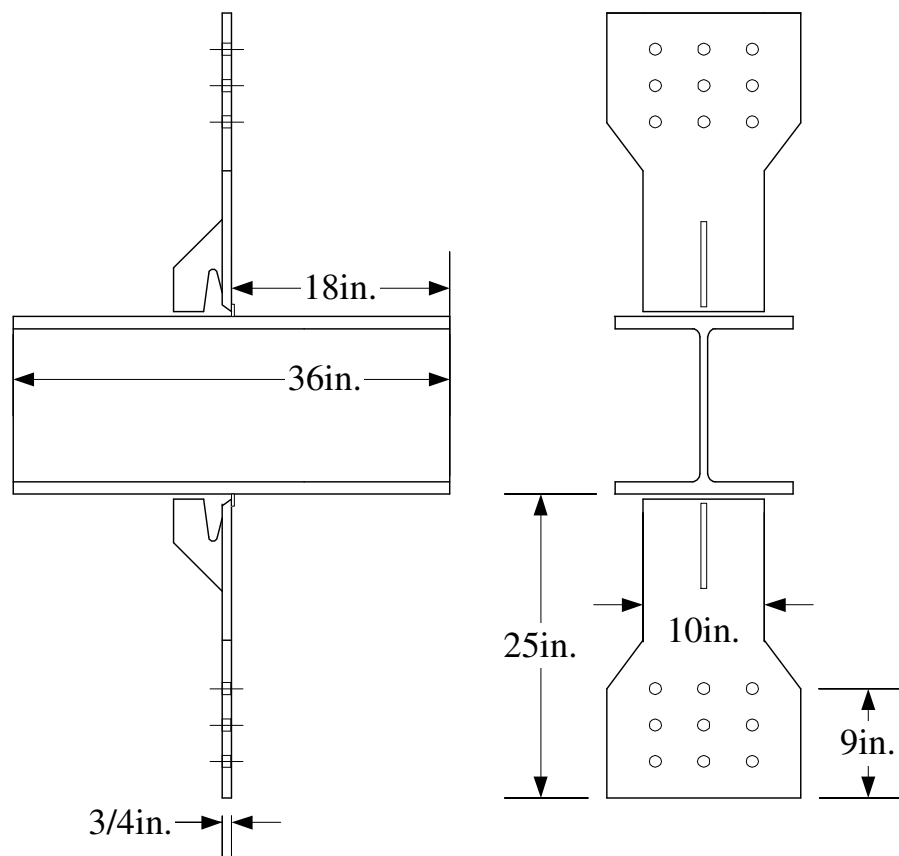


Figure 3.11: Specimens 1-LWY, 2-LWY, and 3-UNST

Stiffened Specimens

Specimens 1-HCP and 1B-HCP were comprised of W14x132 column sections with continuity plates that had half the thickness of the girder flanges (or pull-plates).

Figure 3.12 is a specimen drawing that also includes the half-thickness continuity plate details, including welding specifications and clip size. The design of the continuity plates was checked with the guidelines of the Steel Design Guide Series (AISC, 1999a). The dimensions of the continuity plates met all of the provisions for low-seismic design. However, for high-seismic design, the half-thickness continuity plates failed to meet the thickness requirement, since the guidelines state that they are to be the same thickness as the girder flanges. The double-sided fillet welds just met the minimum required size for connecting the continuity plates to the column flanges for non-seismic design. The fillet welds connecting the continuity plates to the column flanges were standard full length minus the weld size on each end. However, in order to avoid welding in the k-line, the welds connecting the continuity plate to the column web were held back 1.5 in. from the column flange face or $\frac{3}{4}$ in. from the end of the continuity plate clip, in accordance with the AISC k-line Advisory (AISC k-line Advisory, 1997).

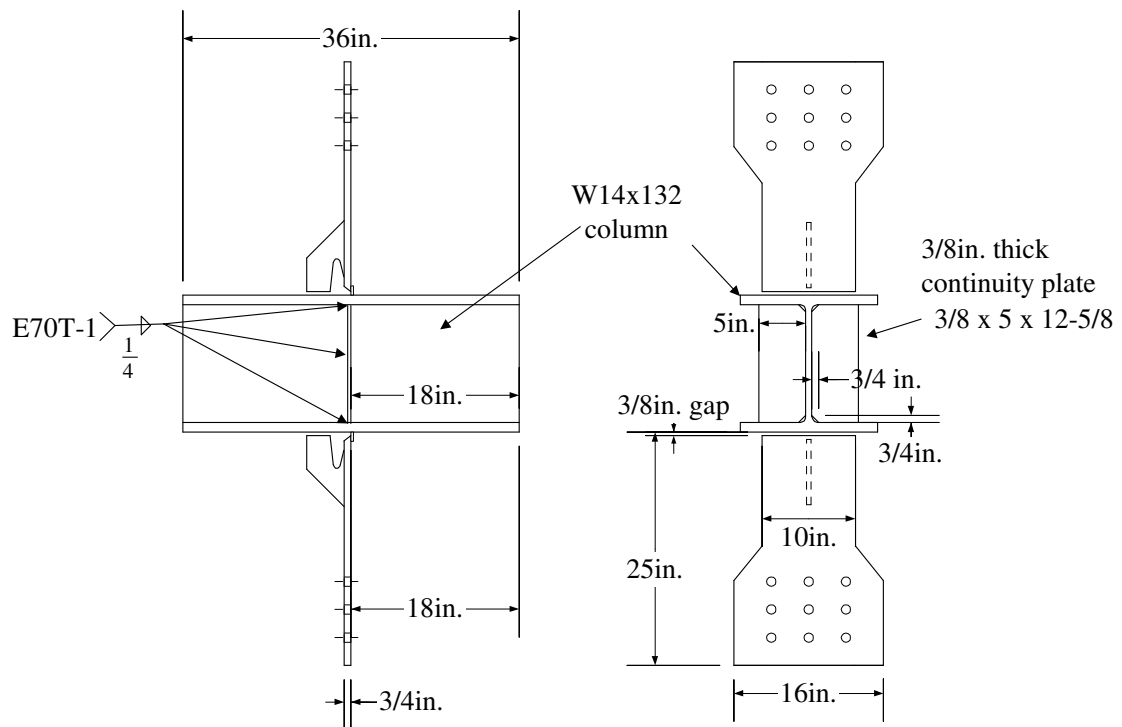


Figure 3.12: Specimens 1-HCP and 1B-HCP

Specimen 1-FCP was fabricated to be the standard continuity plate design for high-seismic zones. It consisted of a W14x132 column with continuity plates that have the same thickness as the girder flanges. The continuity plates were fillet-welded to the column web, but attached to the column flanges with CJP welds. This specimen, shown in Figure 3.13, was tested in order to compare to the behavior of the thinner continuity plates with fillet welds (Specimens 1-HCP and 1B-HCP). Similar to Specimens 1-HCP and 1B-HCP, the fillet welds connecting the continuity plates to the column flanges were held back 1.5 in. from the face of the column flange.

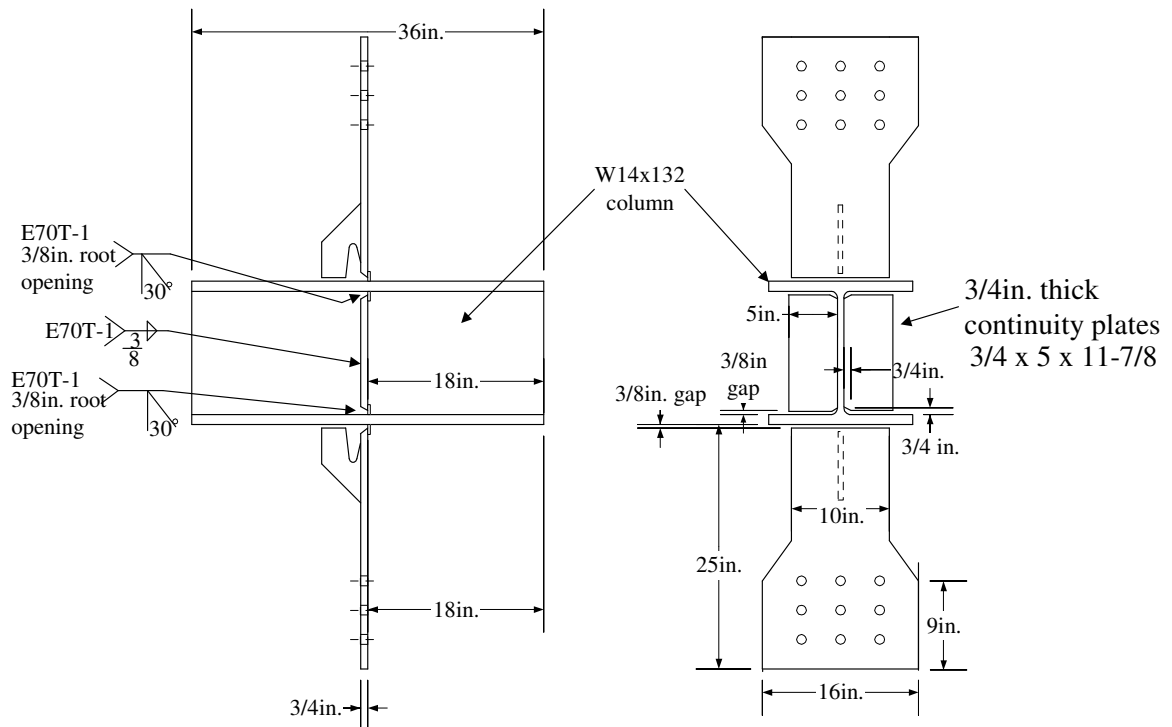


Figure 3.13: Specimen 1-FCP

The final specimen, 1-DP, consisted of a W14x132 column and no continuity plates, but rather two $\frac{3}{4}$ in. thick doubler plates placed out towards the column flange tips, as shown in Figure 3.14. In the box detail, the doubler plates act both as continuity and doubler plates. This detail, first investigated by Bertero et al. (1973), is included in the AISC Seismic Provisions (AISC, 1997) and provides an economical alternative to

connections that require two-sided doubler plates plus four continuity plates. Because Bertero et al. (1973) indicated that the box detail is less effective than a doubler plate flush with the web, the doubler plates in Specimen 1-DP were increased in size to mitigate panel zone shear as per AISC Seismic Provisions (AISC, 1997). Finite element analyses (Ye et al., 2000) found that placing the doubler plates at approximately 2/3 of the girder flange half width from the column web was the optimum distance between the column web and the doubler plates.

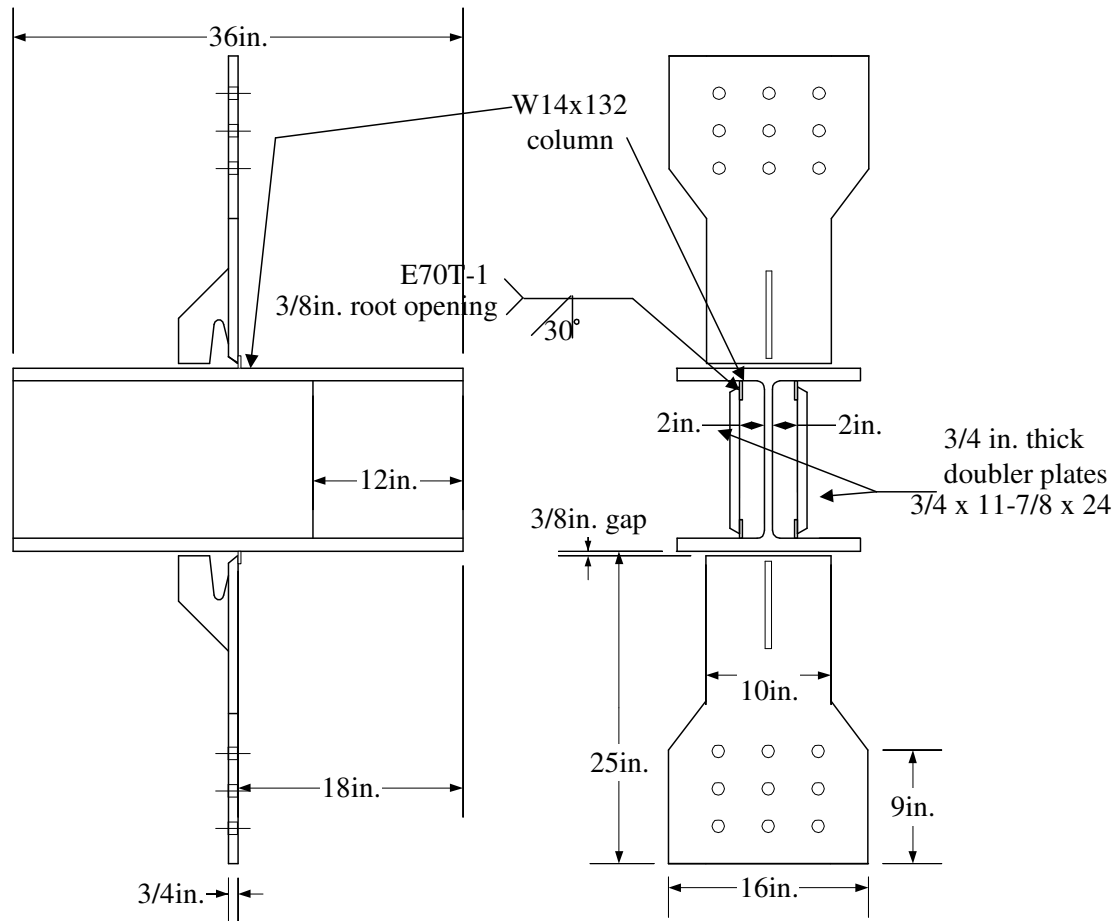


Figure 3.14: Specimen 1-DP

Table 3.4 compares averaged values of the actual specimen dimensions of the column flange and web thicknesses to the nominal dimensions reported in AISC (1995). As shown, all of the actual flange thicknesses are slightly less than the nominal

dimensions, while the actual web thicknesses for the W14x132 and W14x159 sections are either slightly greater or the same as the nominal dimensions. However, the web thickness for the W14x145 section is noticeably less than the nominal thickness, which affects the LWY behavior of this section and is discussed further in Chapter 4.

Table 3.4: Actual and Nominal Flange and Web Thicknesses

Column Section	Actual Flange Thickness, in.	Nominal Flange Thickness, in.	Actual Web Thickness, in.	Nominal Web Thickness, in.
W14x132	1.011	1.030	0.657	0.645
W14x145	1.073	1.090	0.646	0.680
W14x159	1.187	1.190	0.745	0.745

3.3.2 Weld Description

All of the CJP welds joining the pull-plates to the column sections were made using the self-shielded FCAW process and E70T-6 filler metal with a minimum Charpy V-Notch (CVN) energy of 20 ft-lb at 0° F. The E70T-6 wire had a diameter of 0.068 in. Figure 3.15 shows the detail of the pull-plate-to-column flange connection, including the weld type and access hole dimensions. A restrictor plate, representing a portion of the girder web, was tack welded to the girder flange and column flange before making the CJP weld for two reasons. The main reason was to simulate a bottom girder flange-to-column flange weld, in which the welder must stop and start the weld passes around the column web. A secondary reason for the restrictor plate was to keep the pull-plate at a 90 degree angle to the column flange. The column tack weld was removed before testing.

Continuity plates and web doubler plates were fillet-welded using the 100% carbon dioxide gas-shielded FCAW process and E70T-1 filler metal with a 0.0625 in. diameter. In one specimen, CJP welds were used to join the continuity plate to the column flanges and in another specimen CJP welds were used to join the web doubler

plate to the column flanges. These CJP welds were also made with the gas-shielded FCAW process and E70T-6 filler metal.

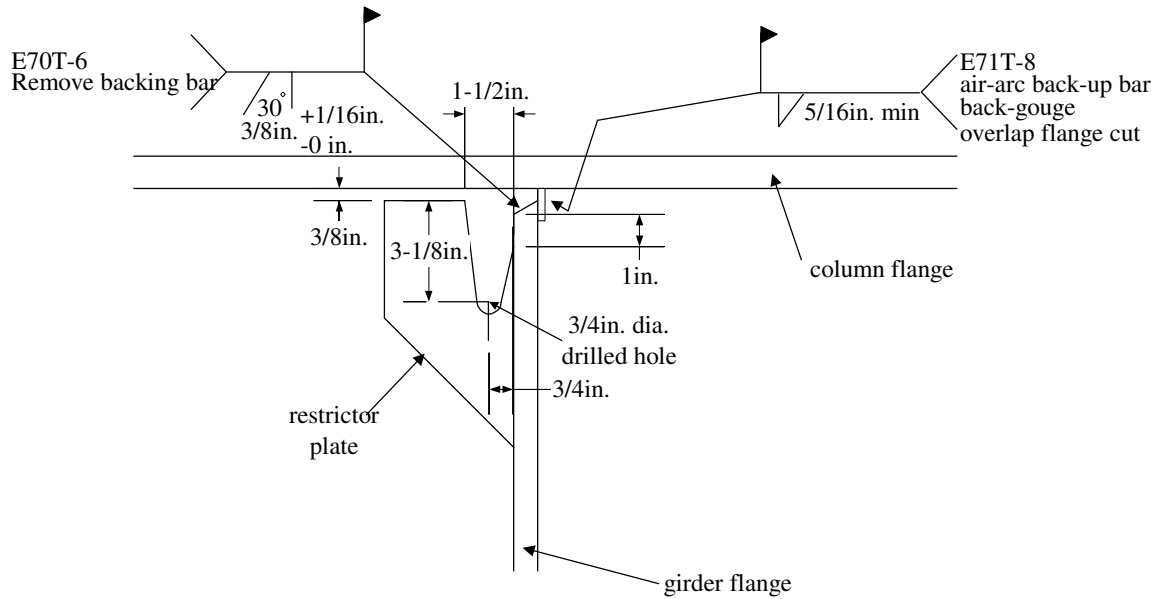


Figure 3.15: CJP Weld Connecting Pull-Plate to Column Flange

3.4 Material Properties

Ancillary tests were performed to measure the stress-strain characteristics, toughness, and hardness of the column sections and the stress-strain characteristics of all plate material, including pull-plates, continuity plates and doubler plates, used in fabricating the specimens. Also, transverse and longitudinal sections of the CJP girder flange-to-column flange weld were polished and etched to characterize the welds.

3.4.1 Steel Material Properties

Tension Testing

Tensile tests were performed on all column sections and plate material in accordance with Structural Stability Research Council (SSRC) Technical Memorandum

No. 7 for tension testing (SSRC, 1998). All plate material of the same thickness and columns with the same sizes were produced from the same heat. Two coupons were milled from the each of the column flanges and column webs, and three coupons from the plate material. For each coupon several different values were obtained, including the static yield strength, “slow strain rate” yield strength (defined as the 0.2% offset), strain hardening modulus, modulus of elasticity, ultimate strength, and total percent elongation. Table 3.5 summarizes the results of the coupon tests and the mill report values. All values given in Table 3.5 are averaged values and are in units of ksi.

As shown in Table 3.5, the measured “slow strain rate” yield stresses were lower than the yield strengths given in the mill reports for all but one of the coupon locations. This was expected since the mill coupon tests are conducted at a high strain rate, which increases the yield stress of the steel. The tensile strength is not as significantly affected, since the coupon test also had an increase in speed during the latter part of the test. The strain hardening modulus (E_{sh}) was calculated using the procedure defined in the SAC Protocol (SAC, 1997). The average E_{sh} of the plate material was 496 ksi, while the average for the column shapes was 333 ksi. Frank (FEMA, 2000d) indicates that his study of wide-flange shapes resulted in an average E_{sh} of 380 ksi. The ASTM specification for A992 steel (ASTM, 1998a) specifies a minimum tensile strength of 65 ksi, a yield strength between 50 and 65 ksi, a minimum elongation of 18%, and a maximum yield-to-tensile (Y/T) ratio of 85%. In comparison, the measured values of the column sections met the requirements for tensile strength, percent elongation, and Y/T ratio, and all but the flange of the W14x132 column section met the yield strength requirements.

Table 3.5: Steel Tension Coupon Test Properties

	Pull-plate	HCP*	FCP*	DP Box*	DP*	W14x132 web	W14x132 flange	W14x145 web	W14x145 flange	W14x159 web	W14x159 flange
Static Yield Stress, ksi	43.4	45.8	42.6	43.2	53.3	50.3	46.7	54.5	53.9	48.7	49.3
0.2% Offset Yield Stress, ksi	48.2	50.0	46.0	46.5	56.2	54.4	49.2	59.4	58.2	55.2	51.1
Mill Yield Stress, ksi	51.2	61.3	51.2	51.2	57.0		53.0		57.0		53.5
Coupon Tensile Stress, ksi	72.5	72.2	72.5	72.5	73.8	70.3	69.4	74.1	75.1	71.5	71.8
Mill Tensile Stress, ksi	72.1	80.4	72.1	72.1	71.0		70.5		73.5		72.0
Modulus of Elasticity, ksi	28200	28000	29100	28800	27000	28600	29800	29300	30200	29800	28700
Strain Hardening Modulus, ksi	576.1	485.6	510.0	539.4	368.9	279.2	348.2	317.0	337.6	356.4	359.3
Strain at Strain Hardening	0.016	0.016	0.010	0.012	0.019	0.018	0.012	0.024	0.009	0.024	0.013
% Elongation	30.0%	24.6%	28.9%	29.0%	23.9%	23.7%	25.7%	28.2%	26.2%	30.5%	30.9%
Measured Y/T	66.4%	69.0%	63.4%	64.1%	76.1%	77.4%	70.9%	80.2%	77.5%	77.2%	71.1%

* HCP = half-thickness continuity plate, FCP = full-thickness continuity plates, DP Box = doubler plate box detail, DP = doubler plate

Toughness

The notch toughnesses of the column sections were measured with CVN specimens milled from the k-line area of the column flanges in the L-T (longitudinal) orientation, as shown in Figure 3.16. This is the specified location for toughness testing of jumbo shapes (AISC, 1999b; AISC, 1997). For jumbo shapes, the AISC Seismic Provision (AISC, 1997) requires a minimum toughness value of 20 ft-lbs at 70°F. Single measurements of each column section were made at room temperature (70°F). Table 3.6 compares the measured CVN values to average CVN values for Group 2 and 3 shapes. (W14x132 is a Group 2 shape, while the W14x145 and W14x159 are Group 3 shapes). The “Typical CVN” values included in Table 3.6 are average values from a study of approximately 250 wide-flange A992 shapes (Dexter et al., 2000). Only the measured CVN value of the W14x145 is less than the average CVN values. However, this value is still considerably higher than the toughness of the weld metal (63.7 ft-lbs at 70°F), and therefore is most likely not the weak-link of the connection.

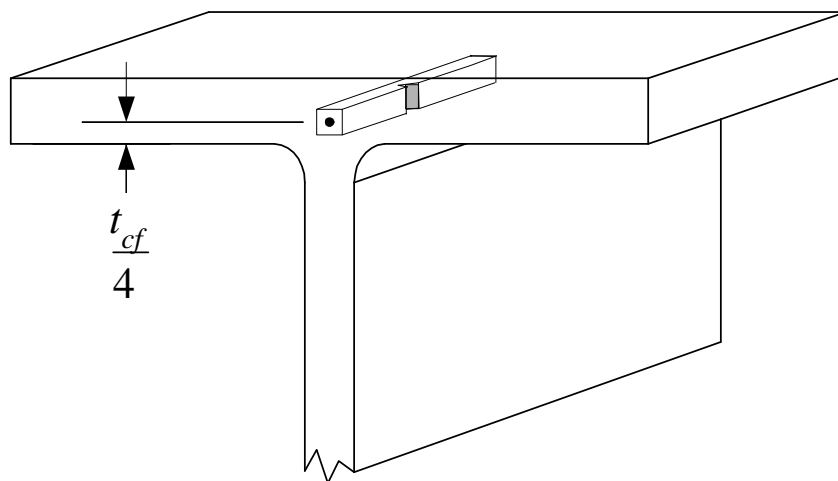


Figure 3.16: Location of CVN Coupons

Table 3.6: CVN Values of Column Sections

	W14x132	W14x145	W14x159
Measured CVN, ft-lbs	166.0	102.0	204.0
Typical CVN, ft-lbs	161.0	137.1	137.1

Hardness

Past research studies (Tide, 1996; FEMA, 2000d) have shown that the wide-flange shapes that are rotary-straightened have a higher yield-to-tensile ratio, lower toughness, and higher hardness in the k-line area than in the rest of the shape. Research confirmed that this higher hardness in the k-line area was a contributing factor to fabrication cracks (Tide, 1996). However, recent (2000) anecdotal evidence indicates that there no longer is a significant problem with fabrication cracking due to higher hardness in the k-line area.

Rockwell hardness values were measured in the test specimens following ASTM procedure E18 (ASTM, 1984). The Rockwell Hardness Testing Machine used was checked using a standardized test block in conformance with the specification. A 5/8 in. thick cross-sectional slice of each of the column sizes was cut to produce a surface with a roughness value of 65. The cross-sectional slices of the column sections were cut into many smaller pieces in order to fit onto the Rockwell Hardness Testing Machine platen. All measurements were taken using a 1/16 in. steel ball penetrator, and the values were read on the Rockwell B-Scale.

According to past research, it was predicted that the k-line areas would have much higher hardness. However, as shown in Figures 3.18 and 3.19, the k-line areas for the W14x145 and W14x159 have hardness values similar to the rest of the flanges and webs. The W14x132 column section has slightly higher values in the flange-web junction, as shown in Figure 3.17

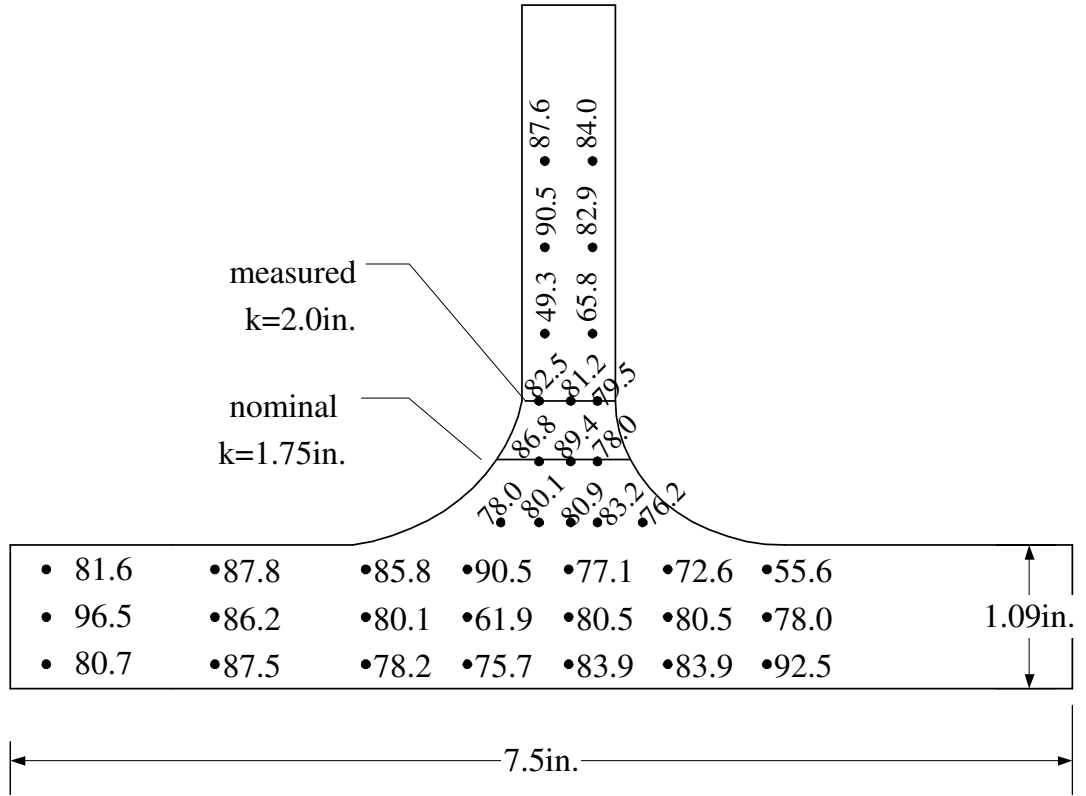


Figure 3.17: Rockwell Hardness Values B-Scale of W14x132

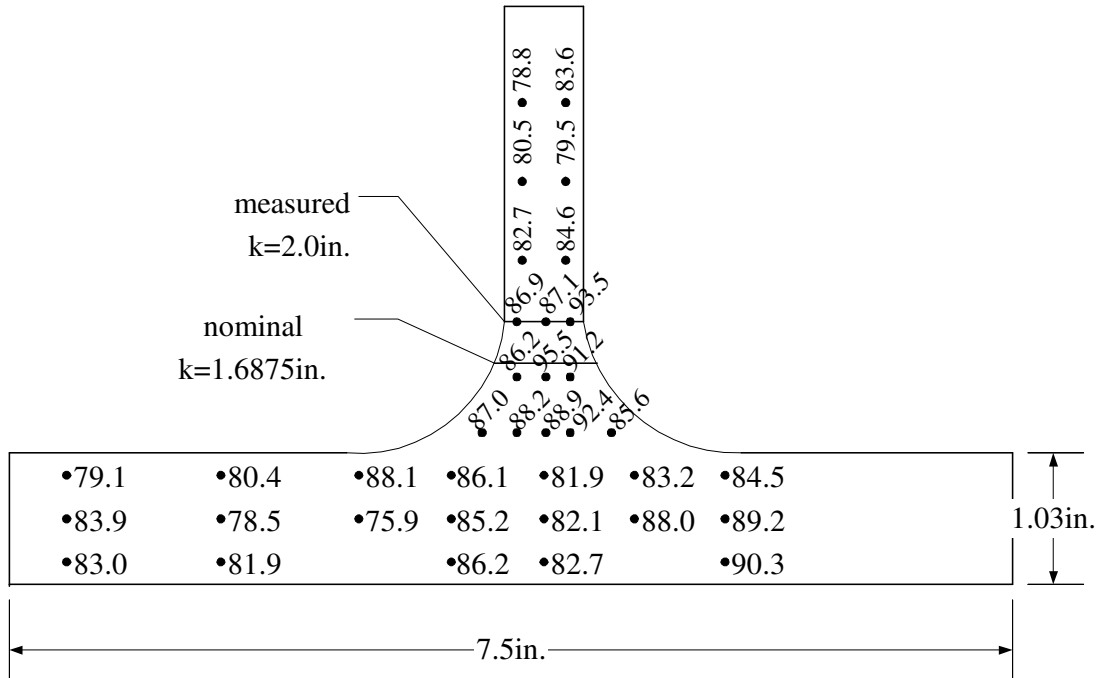


Figure 3.18: Rockwell Hardness Values B-Scale of W14x145

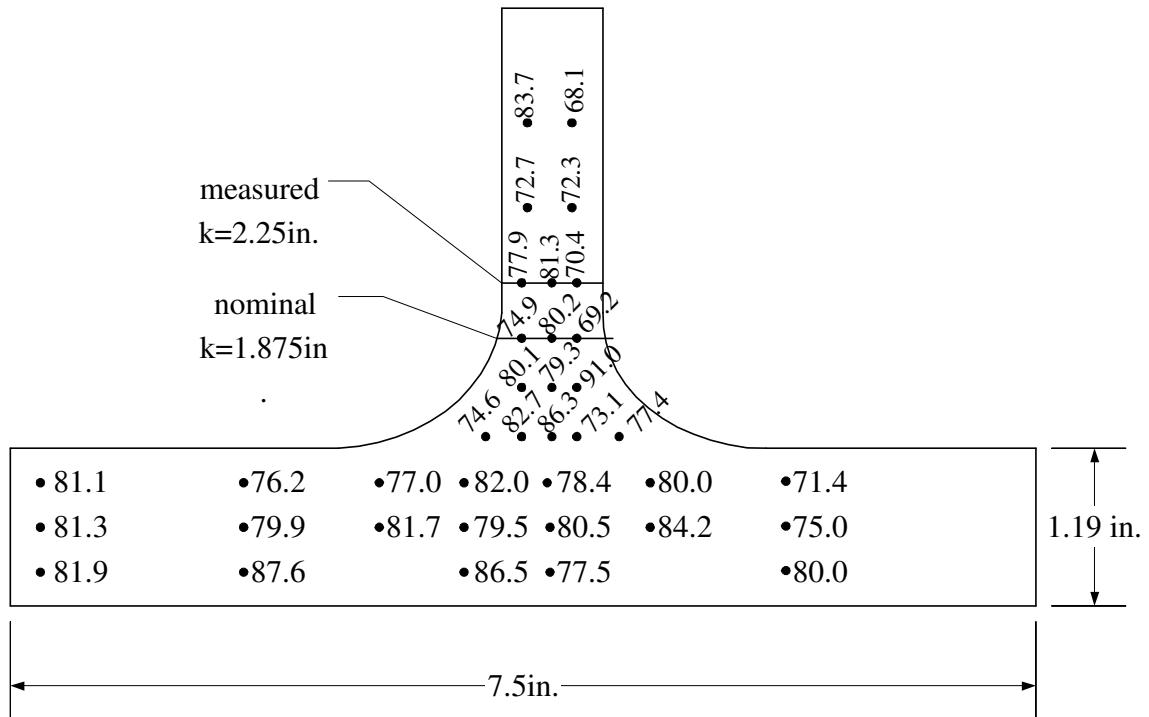


Figure 3.19: Rockwell Hardness Values B-Scale of W14x159

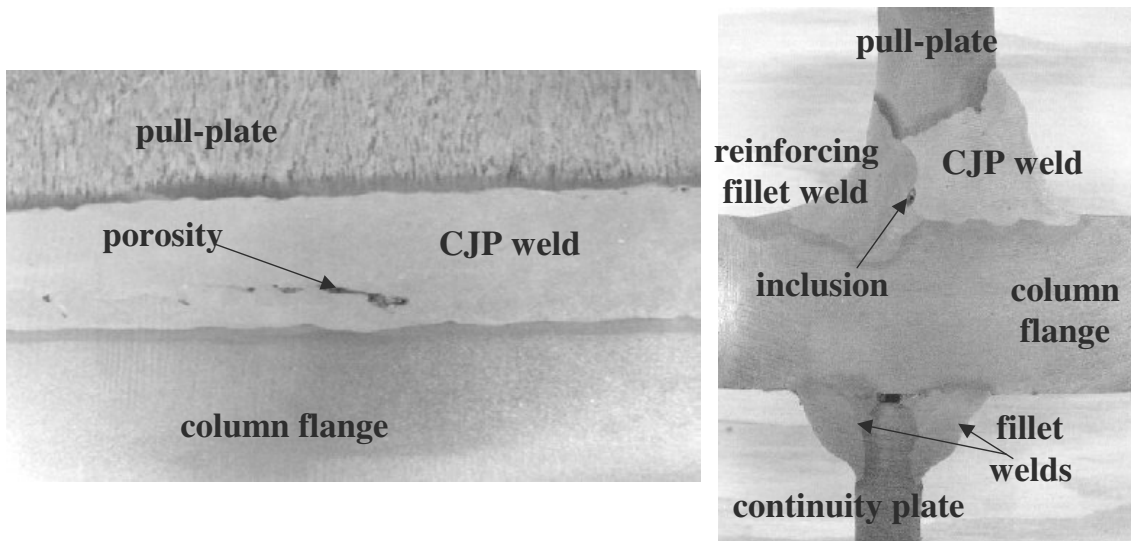
3.4.2 Weld Material Testing

Tension and Toughness Testing

Tensile tests and CVN tests were also performed on the E70T-6 weld metal that was used to join the pull-plates to the column flanges. The tensile tests followed ASTM Specification E8 (ASTM, 1985), while the Charpy Tests was performed in accordance with ASTM Specification E23 (ASTM, 1991). The minimum toughness requirement for notch-tough weld metal is 40 ft-lbs at 70°F and 20 ft-lbs at 0°F (FEMA, 2000c). The weld metal that was used in this research program had a measured ultimate strength of 77 ksi and toughness measurements of 63.7 ft-lbs at 70°F and 19.0 ft-lbs at 0°F. Thus, the weld metal met the minimum ultimate strength requirement but did not meet the lower shelf minimum toughness requirement.

Weld macrosections

In order to examine the welds, particularly the CJP pull-plate-to-column flange welds, transverse and longitudinal cross-sectional slices of three of the welds were polished and etched. The welds from Specimens 1-HCP, 2-LFB, and 3-UNST were chosen for investigation. Figures 3.20a and b are the welds from Specimen 1-HCP. Figure 3.20a shows the characteristics of the weld, including pockets of porosity, as it was placed along the length of the weld passes. Figure 3.20b shows the CJP weld and reinforcing fillet weld and contains an inclusion in the CJP weld. Figure 3.20b also includes the fillet welds joining the half-thickness continuity plates to the column flanges. Figures 3.21a and b are the welds from Specimen 2-LFB. The CJP weld for Specimen 2-LFB has no visible discontinuities in these cross-sections. However, one of the fillet welds of the doubler plates has a root crack, but it did not progress into a weld failure during the test. Figures 3.22a and b are welds of Specimen 3-UNST. Despite the inherent discontinuities in the welds, there were no weld fractures in any of the specimens. It is important to note that the behavior of the specimens was not augmented by having “perfect” welds, but that the welds were typical of standard field welds.



Figures 3.20a and b: Longitudinal and Transverse Cross-Section of CJP and Fillet Welds of Specimen 1-HCP

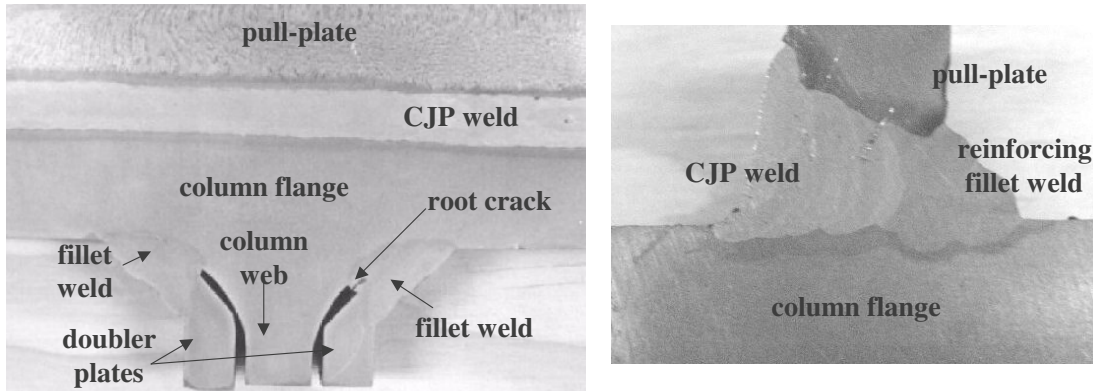


Figure 3.21a and b: Longitudinal and Transverse Cross-Section of CJP and Fillet Welds of Specimen 2-LFB

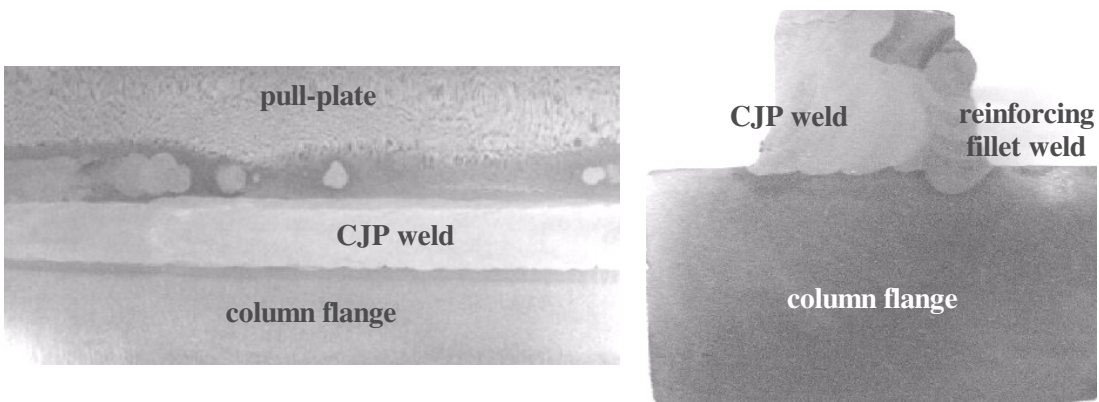


Figure 3.22a and b: Longitudinal and Transverse Cross-Section of CJP and Fillet Welds of Specimen 3-UNST

3.5 Testing Procedure

Testing of the pull-plate specimens followed the SAC protocol (SAC, 1997), where it was applicable. The SAC protocol includes recommendations for test documentation, data processing, and a cyclic loading history. However, the protocol does not specify a loading rate or strain rate for static pull-plate tests. For the pull-plate tests, a high strain was used for two reasons. The first was to increase the yield strength of the specimen, which increases the probability for brittle fracture, thereby putting the specimens under the most severe testing situation (Uang et al., 1998). The second reason

was to approximate a building cycling between tension and compression yield points in an earthquake. The specimens were loaded in a 600-kip capacity MTS hydraulic testing machine. Initially the specimens were loaded to approximately 50 kips, and then unloaded at a slow strain rate to ensure proper gage and data acquisition setup. Then a strain rate of 0.004 in/in/sec, which approximates tension-compression cycling in a building with a 2 second period, was used to test the specimens to failure. A data acquisition system was used that collected 56 channels of data at 100 Hz.

3.6 Instrumentation Plan

The SAC protocol (SAC, 1997) was also followed for minimum instrumentation requirements. However, the given instrumentation specifications are primarily directed towards cyclic cruciform or cantilever tests. The objectives of the instrumentation in the pull-plate tests were to aid in verification of the local flange bending and local web yielding equations and to analyze the difference in the strain distributions of connections with and without stiffeners. The specimens were instrumented using general-purpose and high-elongation strain gages and rosettes and linear variable differential transformers (LVDTs).

The strain gages were placed on the girder flanges (pull-plates), column webs, column flanges, and continuity plates. Figures 3.23 through 3.26 show the locations of the strain gages. Most of the gages used were general-purpose strain gages that have a strain limit of $\pm 3\%$. The other gages used were high-elongation gages capable of strain ranges of $\pm 20\%$. The high-elongation gages were used on the pull-plates, on the column k-line directly under the pull-plates, on the half-thickness continuity plates, and on the column flange directly under the pull-plates.

The instrumentation plans of the nine specimens can be categorized into three groups: a plan that used the majority of the data acquisition channels on instruments to examine the LFB behavior, a plan that focused on investigating LWY, and a plan that spread the data acquisition channels evenly over the column section and stiffening plates.

Complete diagrams of the instrumentation plans, including the instrumentation-naming scheme, can be found in Appendix A. Also included in Appendix A are the data for all nine specimens and description of the instruments that failed to gather data for the entire testing period.

Local Flange Bending Specimens

The instrumentation plan that focused on examining the LFB behavior was used on specimens 1-LFB and 2-LFB and is shown in Figure 3.23. This plan had two general-purpose strain gages, 12 high-elongation strain gages, six general-purpose rosettes, five high-elongation rosettes, and seven LVDTs. The 11 rosettes were used to aid in verification of the LFB criterion. The rosettes were placed on the inside face of the column flanges along yield lines seen in preliminary finite element analyses and along yield lines that are assumed to have been used by Graham to develop the LFB equation (Graham et al., 1960), as discussed in Section 2.1. LVDTs were used to measure the separation of the column flanges. In order to describe the deformation of the column flanges along the length of the column stub, five of the LVDTs were placed between the inside faces of the column flanges, underneath the tip of the pull-plates at third points along the length of the column stub. Another LVDT was placed underneath the pull-plate but very near the column web. The final LVDT was connected to the extreme ends of the pull-plates in order to measure the overall specimen elongation.

Local Web Yielding Specimens

The instrumentation plan for specimens 1-LWY, 2-LWY, and 3-UNST, as shown in Figure 3.24, was altered after the testing of the first two specimens. The first two tests showed some bending in the test set-up. In order to account for the effects of the bending, most of the gages were placed on the specimens symmetrically around the bending of the column web. The instrumentation plan included 14 gages on the column web to compare the column web's behavior to the LWY criterion (AISC, 1999b). The LWY criterion assumes that the force of the girder flange will be distributed into the column web over a region that is $(5k+N)$ wide. However, Graham et al. (1960) stated that

the force could be distributed over a region as large as $(7k+N)$. This plan had 14 gages on the column flanges and no rosettes. The number of column flange gages was reduced compared to the number of gages on the LFB specimens. The column flange gages on the LWY specimens were placed at locations that were most useful during the LFB tests. LVDTs were included as before to measure the column flange separation and specimen elongation.

Stiffened specimens with continuity plates or box detail

For the specimens that included continuity plates, 1-HCP, 1B-HCP, and 1-FCP, 20 gages were located on the continuity plates, 13 gages on the column web, four gages on the column flanges and 10 gages on the pull-plates, as shown in Figure 3.25. Seven LVDTs were used to measure the column flange separation and specimen elongation. The focus of the gages was to characterize the strain behavior of the continuity plates and column web and how this behavior differed from the unstiffened specimens. The objective of the gages on the column web was to examine the local web yielding criterion and to determine the strain contours in the web.

Specimen 1-DP with the doubler plate box detail, shown in Figure 3.26, had 18 strain gages each on the column web and doubler plates. Since there was only a 2 in. clearance between the doubler plates that comprised the box detail and the face of the column web, gages were placed on the column web before the box detail was welded onto the column. Eighteen gages were soldered onto the column web and protected, however only eight gages survived the welding process. The rest of the instrumentation plan included two gages on the column flanges and six LVDTs.

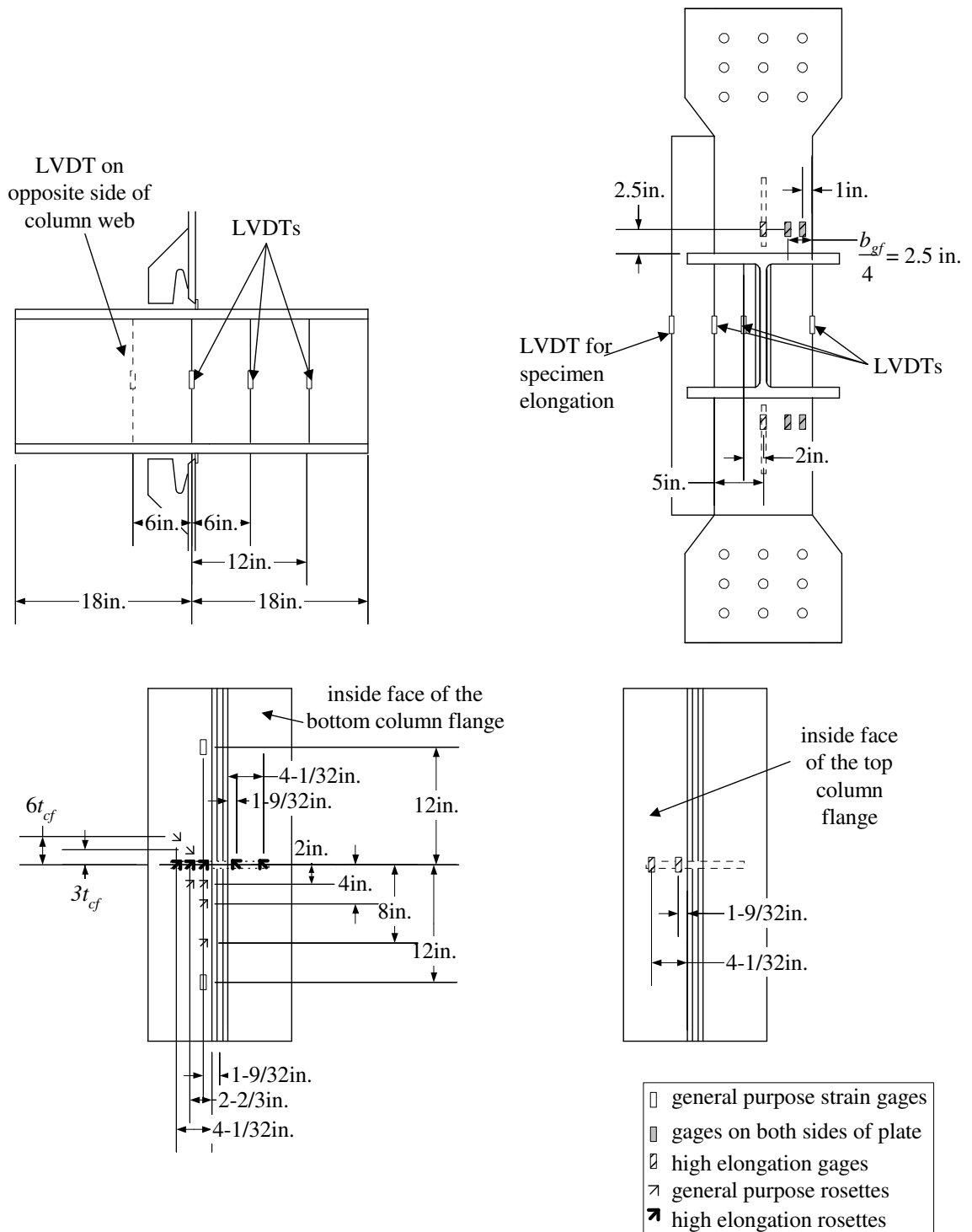


Figure 3.23: Instrumentation Plan of Specimens 1-LFB and 2-LFB

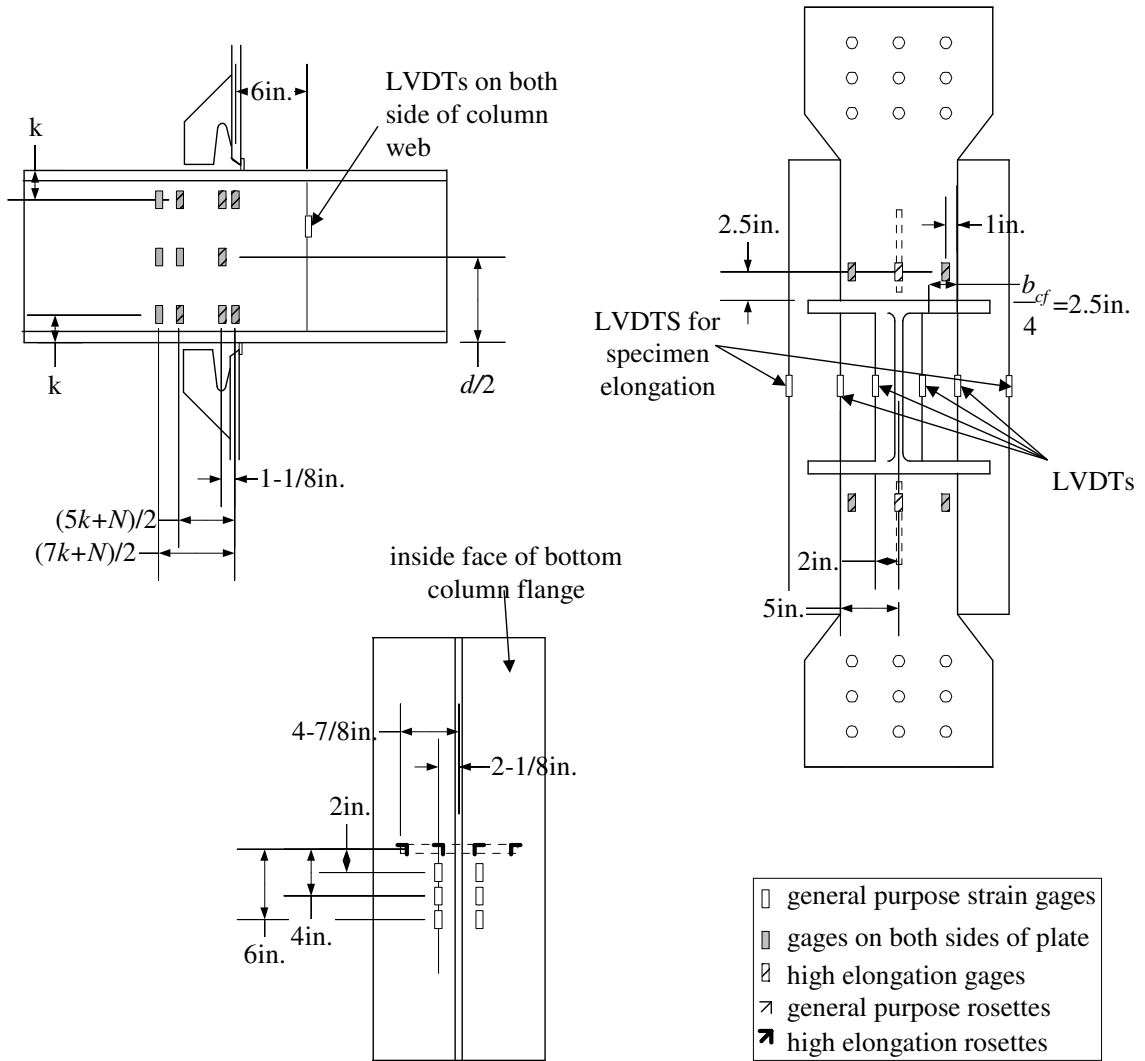


Figure 3.24: Instrumentation Plan for Specimens 1-LWY, 2-LWY, and 3-UNST

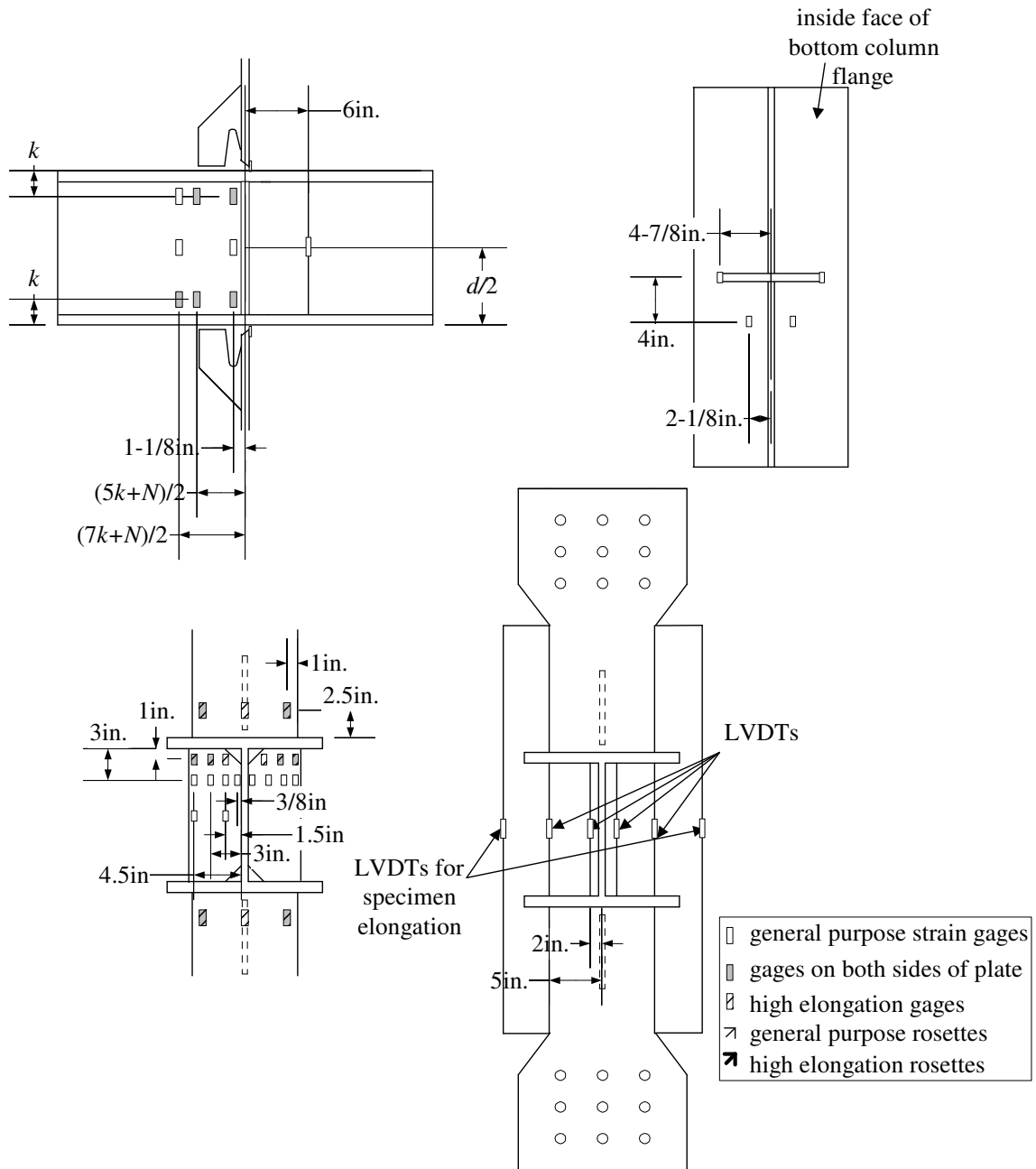


Figure 3.25: Instrumentation Plan of Specimens 1-HCP, 1B-HCP and 1-FCP

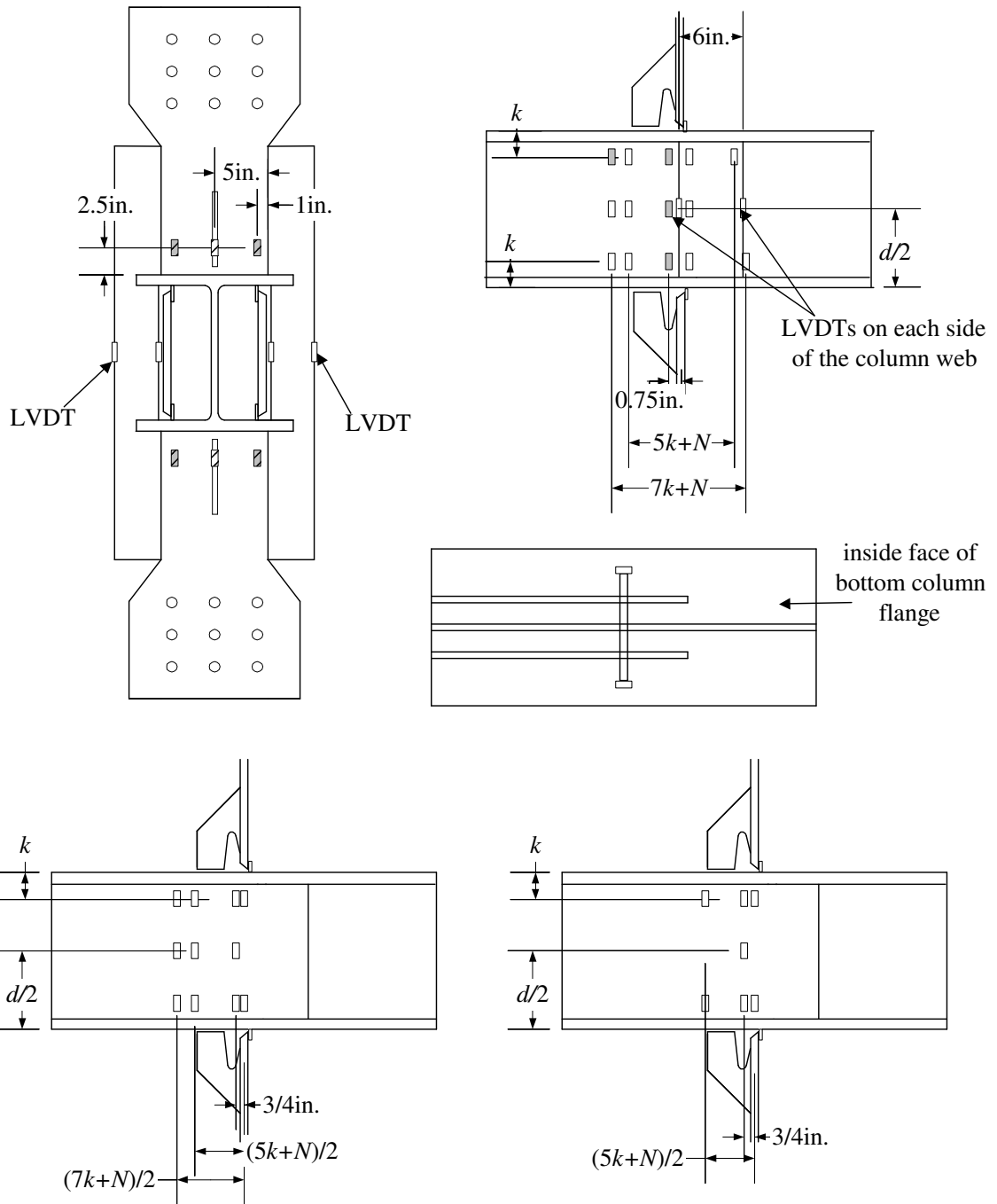


Figure 3.26: Instrumentation Plan of Specimen 1-DP

Chapter 4

Specimen Behavior and Interpretation of Results

This chapter includes the results from the nine pull-plate experiments:

1. Specimen 1-LFB: W14x132 without continuity plates, with doubler plates
2. Specimen 2-LFB: W14x145 without continuity plates, with doubler plates
3. Specimen 1-LWY: W14x132 without any stiffeners
4. Specimen 2-LWY: W14x145 without any stiffeners
5. Specimen 3-UNST: W14x159, without any stiffeners
6. Specimen 1-HCP: W14x132, with half-thickness continuity plates and fillet welds
7. Specimen 1B-HCP: repeat of 1-HCP to verify results
8. Specimen 1-FCP: W14x132, with full-thickness continuity plates and CJP welds
9. Specimen 1-DP: W14x132, with doubler plate box detail

A definition of specimen yield mechanisms and failure modes is presented. Comparisons are made between the measurements from the experiments and the finite element predictions, and between the experimental yield mechanisms and what was predicted from the AISC Provisions (1999). Possible alternatives for the LWY and LFB non-seismic equations are also presented. A discussion is included of the behavior of fillet-welded half-thickness continuity plates versus full-thickness continuity plates attached by CJP welds. The behavior of the doubler plate box detail is discussed for non-seismic applications, and will be further discussed for seismic applications in Cotton et al. (2001). All strain gage and LVDT data for the nine specimens are included in Appendix A.

4.1 Definition of Failure Modes and Yield Mechanisms

The terms “yield mechanism” and “failure mode” are defined in the Connection Performance State of the Art report (Roeder, 2000):

Failure modes cause cracking, fracture, loss of deformation capacity, or significant loss of resistance. Yield mechanisms cause inelastic deformation that lead to plastic rotation, reduction in stiffness and dissipation of energy.

Using these definitions, the potential failure modes of the pull-plate tests were identified as:

- fracture of the pull-plate
- fracture of the column flange-to-girder flange CJP weld
- fracture of the column section
- fracture of stiffeners
- fracture of stiffener welds

Fracture of the pull-plate was predicted as the likely failure mode for all the tests. However, fractures of the welds, column sections, or stiffeners were still possibilities. Brittle weld fracture of the column flange-to-girder flange was considered, because the fracture toughness of the E70T-6 weld metal is only marginally better than the E70T-4 weld metal that was used in the pre-Northridge connections (FEMA, 2000e). Fracture of the stiffener welds was less likely, since the welds were made with the E70T-1 weld electrode, which has a higher toughness. Fracture of the column section was considered, because some cyclically loaded cruciform tests have shown a lack of toughness in the column k-line, which has led to brittle fractures and ductile tears in the k-region (Tide, 1999; Barsom and Pellegrino, 2000).

In order to better understand the behavior of the specimens and to create a basis for comparing the specimens, yield mechanisms were defined that would describe the behavior of the specimens as the tests progressed. The yield mechanisms were based on finite element analyses, AISC provisions for LWY and LFB (AISC, 1999b), and previous research, (e.g. Sherbourne and Jensen, 1957; Graham et al., 1960).

As described in Section 3.1.1, two girder demand load levels, R_u , were calculated in order to examine the specimens for failure modes and yield mechanisms.

- Non-seismic: $R_u = F_{yg} A_{gf}$ (3.1)

- Seismic: $R_u = 1.1R_y F_{yg} A_{gf}$ (3.6)

where $R_y = 1.1$ for grade 50 or 65 rolled shapes (see Chapter 2 for variable definitions). The calculation of the seismic girder demand takes into account strain hardening of the girder and includes an overstrength factor, R_y , of the shapes. Using the nominal yield strength and girder flange (pull-plate) dimensions of $\frac{3}{4}$ in. by 10 in., the girder flange demands were approximately 375 and 450 kips, respectively. Using pull-plate coupon results the girder flange demands were approximately 360 and 435 kips, respectively. These were below nominal values because the coupon tests (Table 3.4) showed the yield stress to be 48.2 ksi. The nominal values of 375 kips and 450 kips will be used for comparison to all results, because these represent values corresponding to design practice. For investigating the specimen behavior relative to the failure modes and yield mechanisms in this work, the pull-plate load of 450 kips (which corresponds to approximately 1.5% specimen elongation) was used as the primary target for demand. This value accounts for strain-hardening and material overstrength relative to the non-seismic demand, and thus yields a more robust assessment of the specimen performance. Note that a demand value of $1.8F_{yg}A_{gf}$ (Equation 3.2) yields a load larger than the actual fracture strength of all of the pull-plates and is not considered further in this work.

For the LWY limit state, a two-part yield mechanism was developed. One part limits the web strain in the highly concentrated area of the k-line, directly under the pull-plate. The second part uses similar failure criterion of Graham et al. (1960), which based LWY failure on yielding of the $5k+N$ region of the k-line.

Justification for the LWY yield mechanism is based on Figure 4.1. This figure shows the finite element strain distribution in the column k-line of the three unstiffened column sections at a load of approximately 450 kips. The reported strain values are in the direction of loading, as shown in Figures 3.4 and 3.5. The finite element models were nearly the same as the preliminary finite element models as defined in Section 3.2.2.1. The only difference was the stress-strain curve. For the finite element models in Chapter 4, mill report values for yield and tensile strengths were used (as reported in Table 3.4).

In Figure 4.1, Specimen 1-LWY had a strain value above the yield strain (approximately 0.18%) for the entire $5k+N$ region. In addition, as discussed in Section 3.2.2.1, Specimen 1-LWY was expected to exceed the LWY yield mechanism, which limits the strain in the k-line at the centerline of the column length. Therefore, the maximum strain of 3.6% for Specimen 1-LWY, as shown in Figure 4.1, was judged excessive, while the maximum strain value of 1.9% for Specimen 2-LWY was considered not excessive. Thus, the following criteria were used to determine if a test specimen exceeded the LWY yield mechanism: at 450 kips load level, the strain in the column k-line directly under the pull-plate is greater than 3.0%, or the strain in the column k-line is greater than the yield strain for the entire $5k+N$ area.

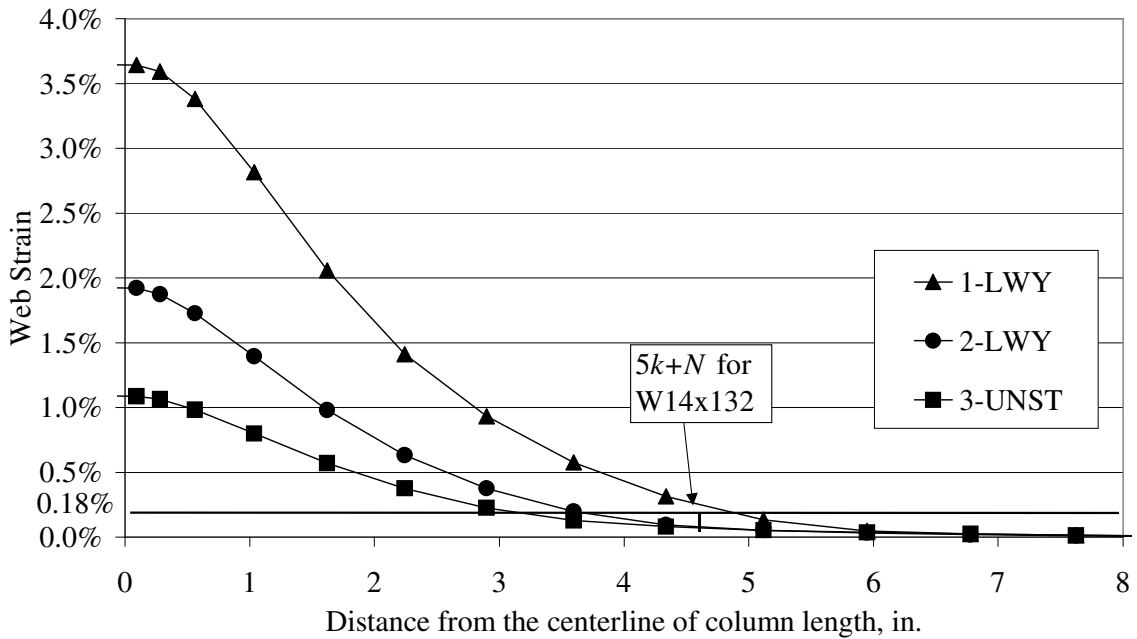


Figure 4.1: Finite Element Strain Distribution along the k-line in the Column Web at 450 kips

The experiments were determined to have exceeded the LFB yield mechanism if at 450 kips the column flange tip separation was greater than $\frac{1}{4}$ in. This LFB yield mechanism was based on the permissible variations in cross section sizes as per ASTM A6 (1998b). The ASTM provisions allow the flanges of a wide-flange section to be $\frac{1}{4}$ in.

out of square from the tips of the two flanges on the same side of the web. Presumably, this amount of flange irregularity is tolerable, and a column section fabricated in this way would be expected to retain sufficient resistance to local flange buckling in spite of this initial imperfection. Therefore, it was assumed that it would also be acceptable to have this much flange deformation caused by local bending of the girder flanges. The probability of an initially out-of-square flange combining in the same direction with additional deformation due to the girder was deemed to be insignificant.

The continuity plates were determined to have exceeded their yield mechanism if the entire full-width region of the continuity plates was above the yield strain. Figure 4.2 describes the full-width and narrow-width regions as discussed relevant to the behavior of the continuity plates. The yield mechanism was defined as yielding the full-width region because even after the narrow-width portion of the continuity plates has yielded the plate and the connection are still able to resist additional girder flange load.

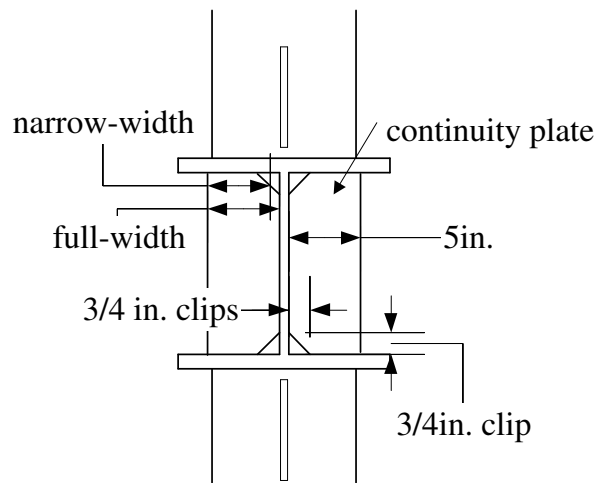


Figure 4.2: Full-Width vs. Narrow-Width Regions of Continuity Plates

4.2 Effect of Eccentric Loading

The first four specimens tested were 1-LFB, 2-LFB, 3-UNST, and 1-HCP. After the data of these tests were analyzed, unintended lateral bending in the plane of the pull

plates was noticed in the specimen results. The eccentric loading was due to a small misalignment of the top loading grip bolt-hole pattern. After the first four tests, the misalignment was corrected, and the bending in the specimens was insignificant.

Although this variation in the boundary conditions was unintentional, localized bending of the beam flange is known to be an important factor in the connection performance. Having the bending in one group of experiments could make the demand slightly greater for that group and allow an assessment the significance of this localized bending to be made.

Figure 4.3 shows a comparison of the data from the LVDTs that measured the overall elongation of the specimens that had no continuity plates or box detail. Figure 4.4 shows the position of these LVDTs. The specimen elongation data for Specimen 1-LFB are from LVDT 9. The data for Specimens 2-LFB and 3-UNST are from LVDT 10. Specimens 1-LWY and 2-LWY had both LVDTs 9 and 10, so the specimen elongation data are the results of the average of the two LVDTs. As seen in Figure 4.4, the LVDT for specimen 1-LFB was on the opposite side of the specimen compared to all the other specimens, and thus the effect of bending was in the opposite direction as the other specimens. When the pull-plate yielded at approximately 385 kips (i.e., just above the actual yield load of the pull-plates), the specimen had straightened itself out. Similar behavior is seen for Specimens 2-LFB and 3-UNST. The subsequent behavior is comparable to the specimens without the eccentric loading (e.g., Specimens 1-LWY and 2-LWY).

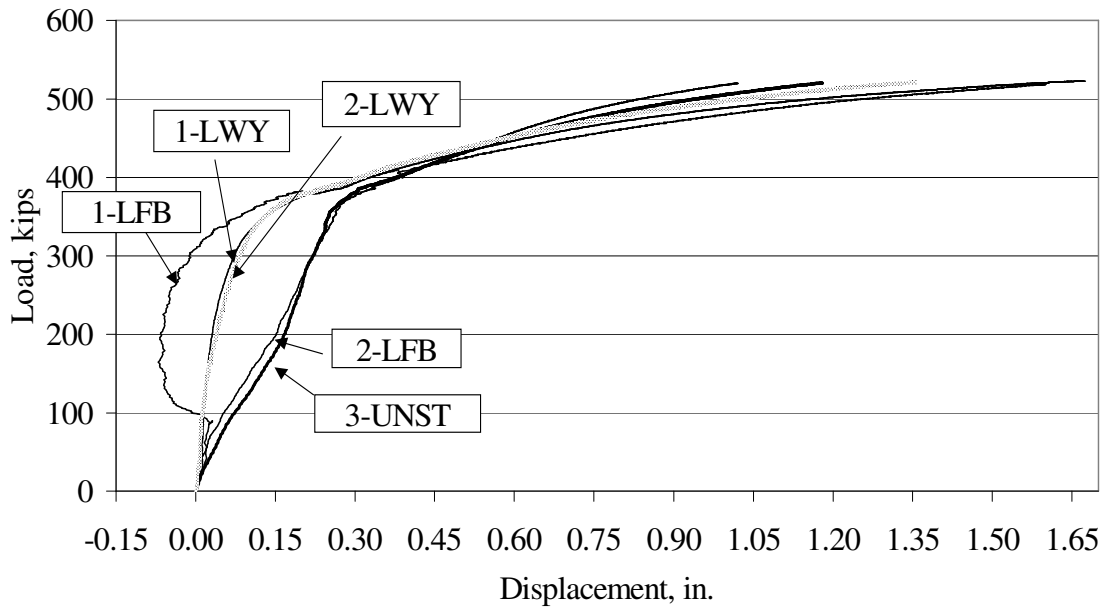


Figure 4.3: Comparing Specimen Elongation with and without Eccentric Loading

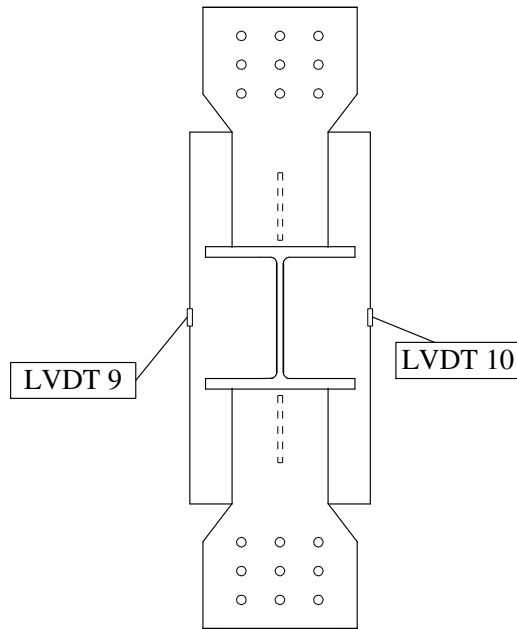


Figure 4.4: Location of Specimen Elongation LVDTs

Figure 4.5 shows the measurements from the LVDTs that were located at the column length centerline underneath the tip of the pull-plates on each side of the column

web for Specimens 1-LFB and 1-LWY (see Figures 3.23 and 3.24). Specimen 1-LFB was tested with the misalignment, while Specimen 1-LWY was tested after the misalignment was corrected. The measurements from the two LVDTs of each specimen should theoretically be identical to each other. The two LVDTs from Specimen 1-LFB have a greater deviation from each other than the two LVDTs of Specimen 1-LWY. While a difference still exists between the LVDTs of Specimen 1-LWY, it is much less. Since the behavior after substantial yielding has occurred is of primary interest, the deviations at the beginning of the loading in Specimens 1-LFB, 2-LFB, 3-UNST, and 1-HCP are not considered to have affected the final conclusions from these tests.

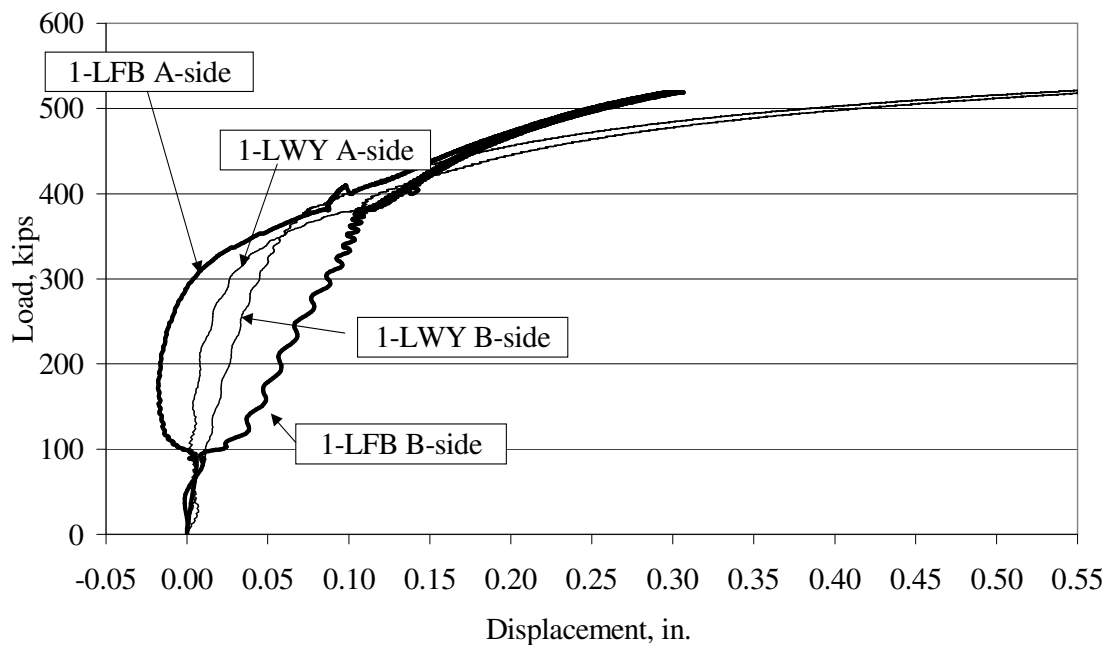


Figure 4.5: Comparison of Flange Separation Measurements Before and After Misalignment Correction

4.3 Comparison of Specimens and Finite Element Analysis

As discussed in Chapter 3, finite element analyses were used to aid in specimen selection justification, yield mechanism definitions, and design of connection stiffening details. In order to justify using the finite element predictions, a reasonable correlation

must exist between the finite element response and the experimental behavior. This section presents this correlation; a more detailed description is included in Ye et al. (2000).

The finite element models of the specimens used the nominal component dimensions rather than the measured dimensions of the actual specimens, which were not available at the time the analyses were performed. As explained later, this can be a source of uncertainty in the predictions of behavior. Similarly, the finite element models used the yield and ultimate tensile strength values from the mill reports of the component materials rather than the results of coupon tests reported in Chapter 3, which were obtained later. Therefore, the results from the finite element models represent an a-priori prediction of the behavior based upon mill report data.

All comparisons are shown at 0.6% and 1.5% specimen elongation, which approximately correspond to load levels of 385 kips (the approximate experimental yield load of the pull-plate) and 450 kips (the approximate experimental $1.1 * R_y * F_{yg} * A_{gf}$ of the pull-plate), respectively. The experimental specimen elongation was calculated by dividing the overall LVDT measurement (as shown in Figure 4.3 and in Appendix A) by the LVDT gage length, which ranged between 35 and 38 inches. The specimen elongation for Specimens 1-LFB, 2-LFB, 3-UNST, and 1-HCP was calculated from a single LVDT, while the specimen elongation for Specimens 1-LWY, 2-LWY, 1B-HCP, 1-FCP, and 1-DP was an averaged result of the two LVDTs. Comparisons of finite element and experimental results of Specimens 2-LWY, 1-HCP, and 1B-HCP are shown in Figures 4.6 through 4.16. These three specimens were chosen as typical examples of the agreement between the finite element and experimental results. The remaining six specimens had similar correlations with their respective finite element results.

Figures 4.6 through 4.10 are comparisons of finite element and experimental results of Specimen 2-LWY. All measurements are average results of gages or LVDTs located on opposite sides of the column web, unless noted. For Specimen 2-LWY, the coupon yield strength results were approximately 3.5 ksi lower than the mill report yield strength used in the finite element model, while the coupon tensile strength was approximately 1.5 ksi higher than the mill report.

Figure 4.6 shows the percent specimen elongation for Specimen 2-LWY. As shown in Figure 4.6, the finite element curve has a more defined strain-hardening plateau. This is a result of the finite element model elongation being more defined by just the behavior of the pull-plate. Figure 4.7 shows the strain in the pull-plate 2.5 in. from the CJP pull-plate-to-column weld measured in the direction of the applied load (see Figure A.6 for gage locations). In this figure, the finite element results are clearly defined by the piece-wise linear stress-strain curve that was used to model the pull-plates. Correlation in both of these figures is good.

Figure 4.8 shows the separation of the column flanges underneath the edge of the pull-plate plotted versus the distance from the centerline of the column length. The finite element results less flexibility in the column flanges than the experiments, although correlation at 1.5% strain is quite good. Figure 4.9 shows the strain in the column k-line and in the mid-depth of the column section plotted versus the distance from the centerline of the column length. The strain was measured in the direction of the applied load. As shown, the areas of high strain gradients, such as the k-line, have the poorest correlation. At 0.6% specimen elongation the finite element results show that the web is stiffer than the experiment. However, at 1.5% specimen elongation, the finite element results show the web to be more flexible. The web strains at the mid-height of the column section, where the strains are less sensitive to the gage location, have a much better agreement with analysis. Figure 4.10 shows the strain in the inside face of the column flange plotted versus the distance from the centerline of the column length. The strain was measured in the longitudinal direction of the column length. The finite element results show the column flange to be stiffer than the experiments. However, the difference is only noticeable at the area of a high-stress concentration at the center of the column length.

Figures 4.11 through 4.16 show that the finite element and experimental results of Specimens 1-HCP and 1B-HCP are very similar. Figure 4.11 shows the results of load versus the percent specimen elongation, while Figure 4.12 shows the results of the strain in the pull-plate at a distance of 2.5 in. from the CJP weld (see Figure A.6). Both of these figures show that the finite element results are clearly defined by the piece-wise linear stress-strain curve used in the model, compared to the experimental results. This

behavior was also seen in Figures 4.6 and 4.7 for Specimen 2-LWY. Figure 4.13 shows the separation of the column flange tips versus the distance from the centerline of the column length. As shown, the experimental and computational results are very similar at both 0.6% and 1.5% specimen elongation. Figure 4.14 shows the column web strain in both the k-line and the mid-depth of the column web versus the distance from the centerline of the column length. The strain was measured in the direction of the applied load. Figure 4.14 shows that the results of the finite element analysis correlate very well with Specimen 1-HCP. However, the results show that Specimen 1B-HCP seems to have a slightly more flexible web. Figure 4.15 shows the strain in the inside face of the column flange versus the distance from the centerline of the column length. The strain is measured in the longitudinal direction of the column length. The experimental column flange strain was only measured at one location in the longitudinal direction, so the comparison between with the finite element results is limited. Figure 4.16 shows the strain in the full-width region of the continuity plates (see Figure 4.2) versus the distance away from face of the column web. The strain was measured in the direction of the applied load. The experimental strain results show the continuity plate to be more flexible than the finite element results. This could be due to the large difference between the mill report and coupon results for the half-thickness continuity plate. The mill report showed yield and tensile strengths of 61.3 ksi and 80.4 ksi, respectively. However, the average of three coupon tests of that plate produced a yield strength of 50.0 ksi and tensile strength of 72.2 ksi.

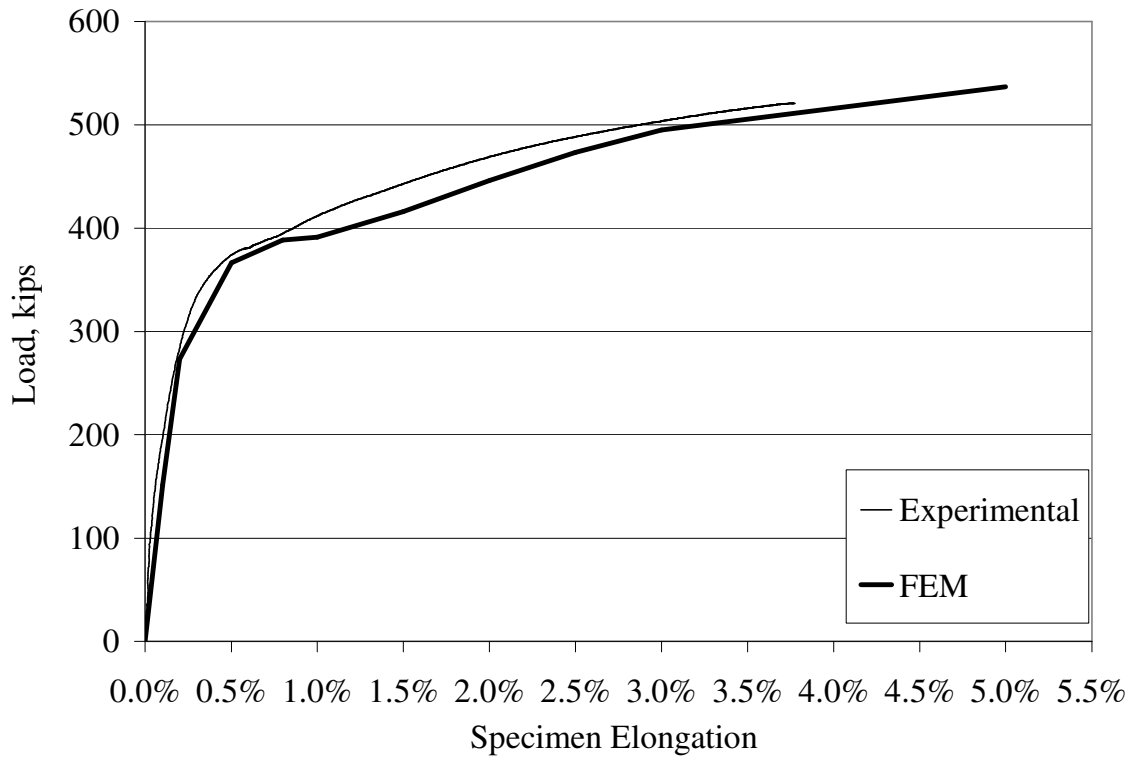


Figure 4.6: Experimental and FEM Results of Specimen 2-LWY Specimen Elongation

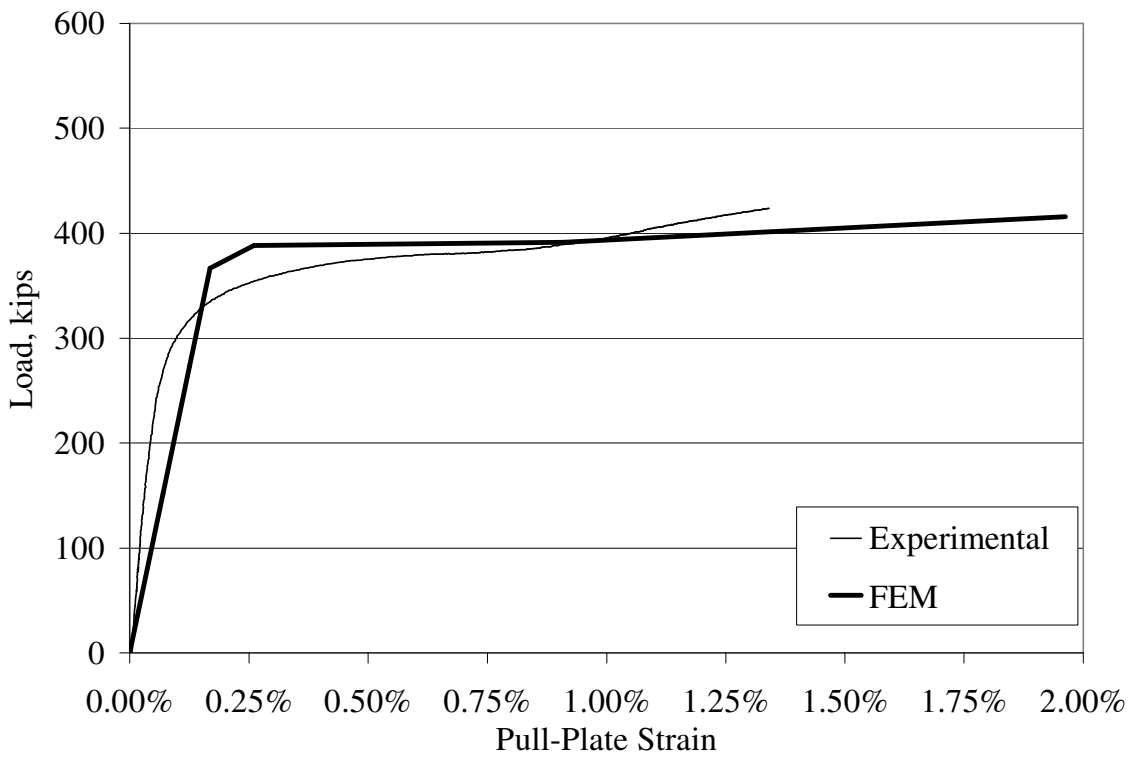


Figure 4.7: Experimental and FEM Results of Specimen 2-LWY Pull-Plate Strain

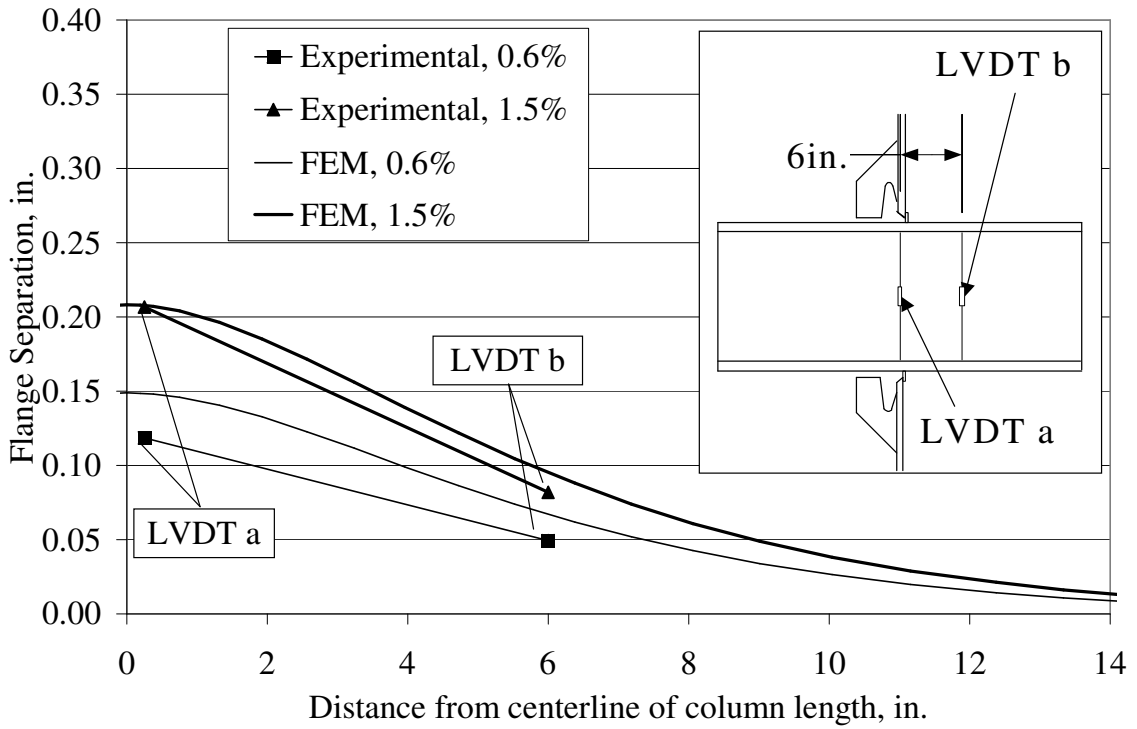


Figure 4.8: Experimental and FEM Results of Specimen 2-LWY Flange Separation

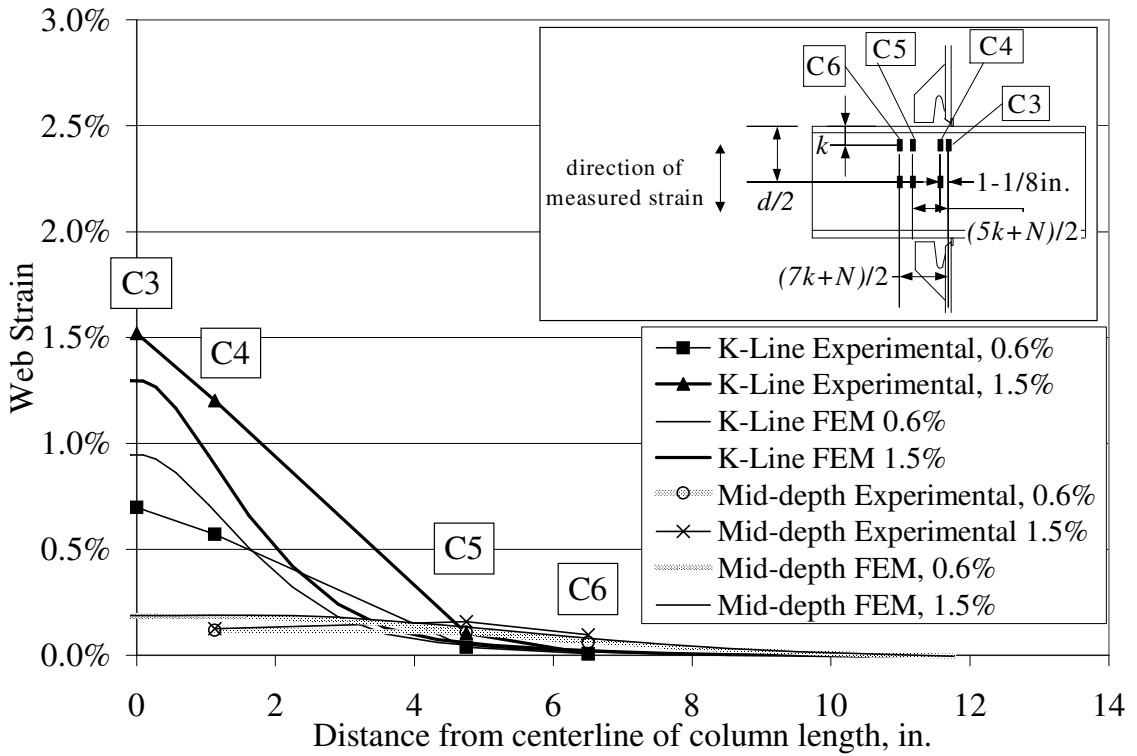


Figure 4.9: Experimental and FEM Results of Specimen 2-LWY Column Web Strain

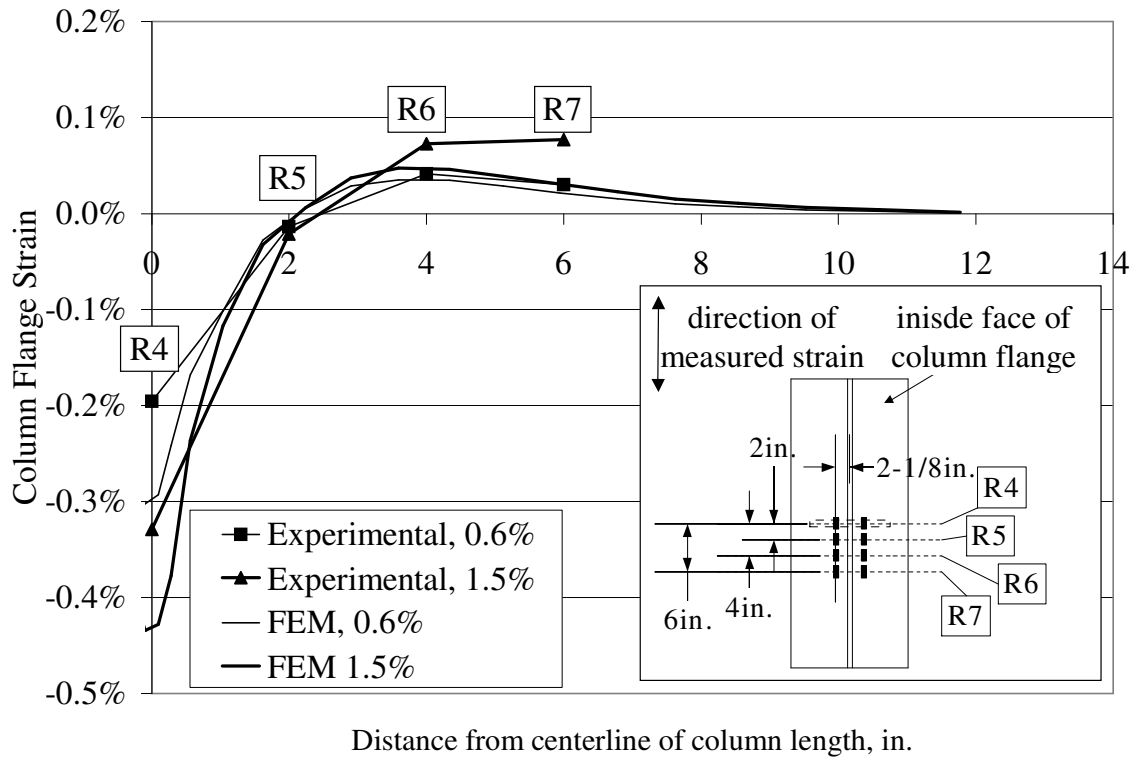


Figure 4.10: Experimental and FEM Results of Specimen 2-LWY Column Flange Strain

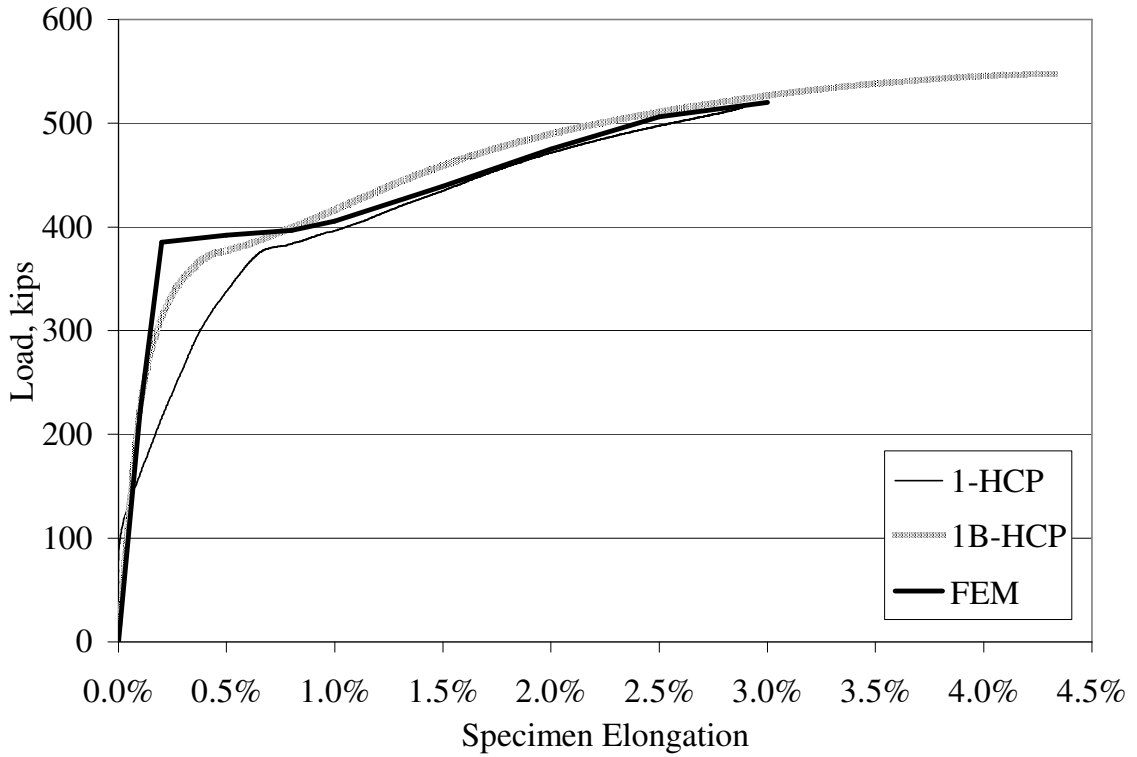


Figure 4.11: Experimental and FEM Results of Specimens 1-HCP and 1B-HCP

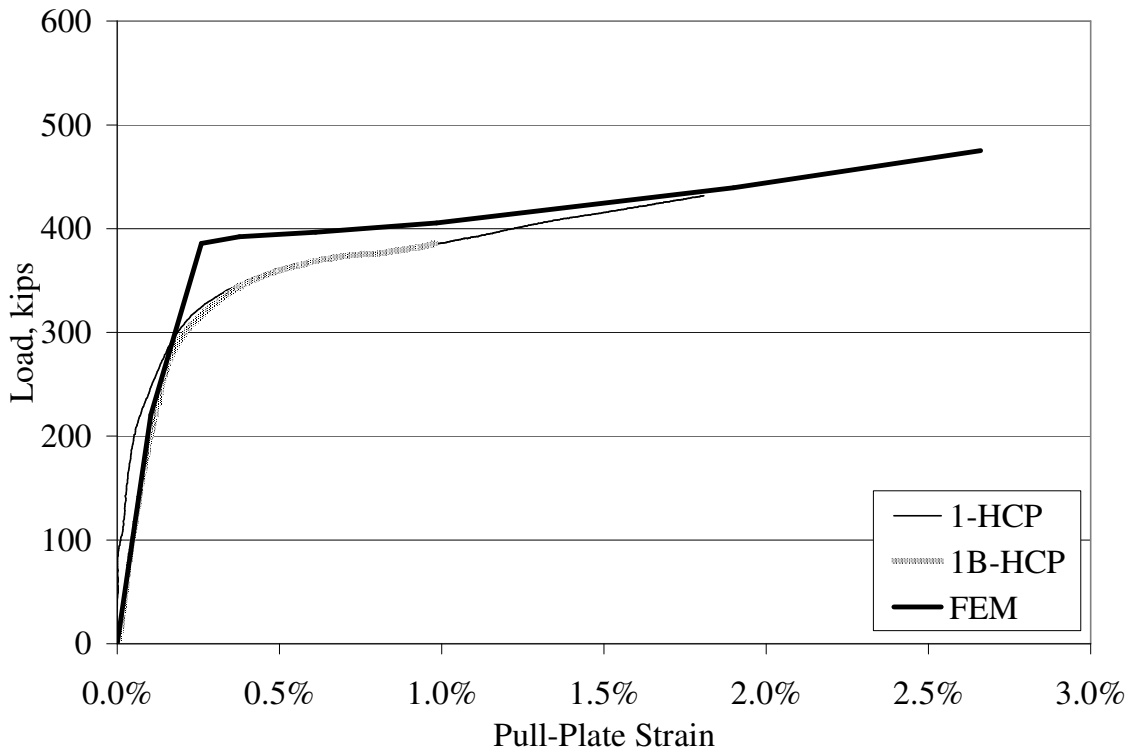


Figure 4.12: Experimental and FEM Results of Specimens 1-HCP and 1B-HCP

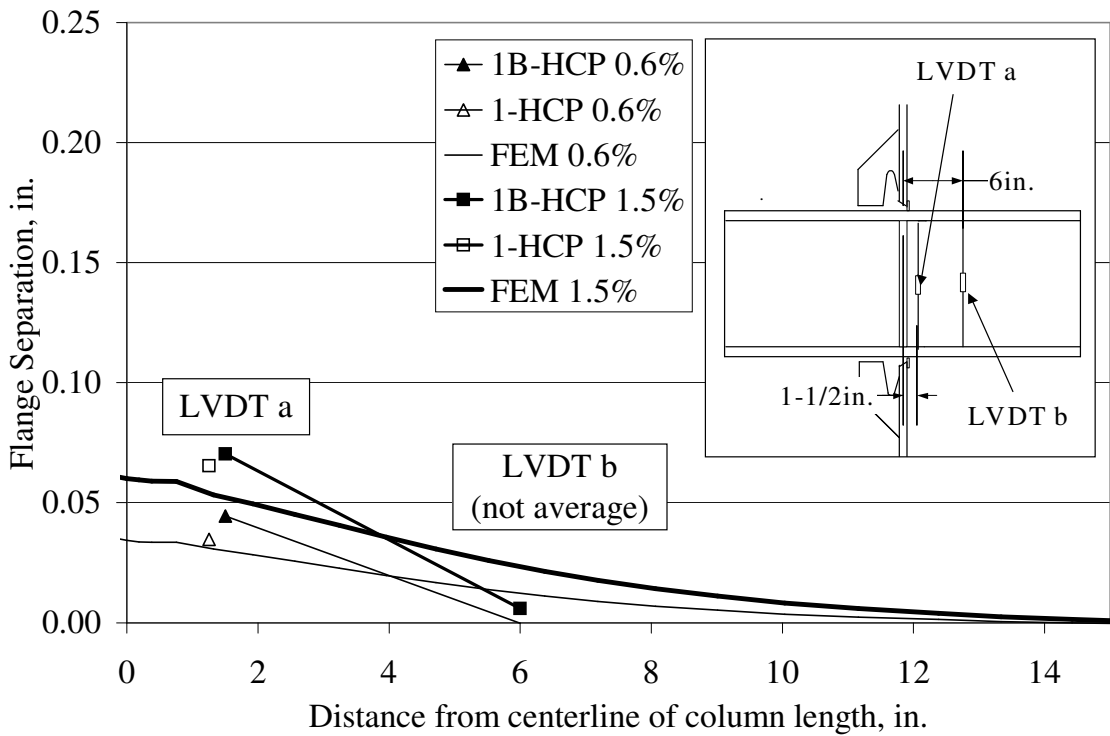


Figure 4.13: Experimental and FEM results of Specimens 1-HCP and 1B-HCP

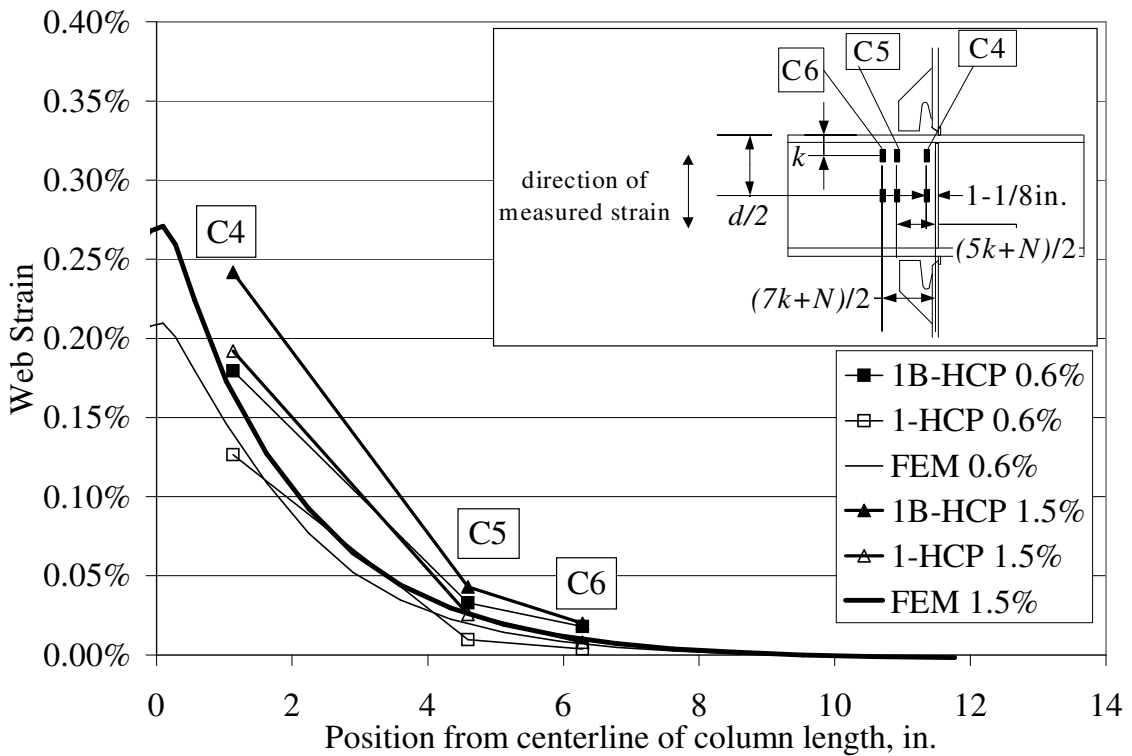


Figure 4.14: Experimental and FEM Results of Specimens 1-HCP and 1B-HCP

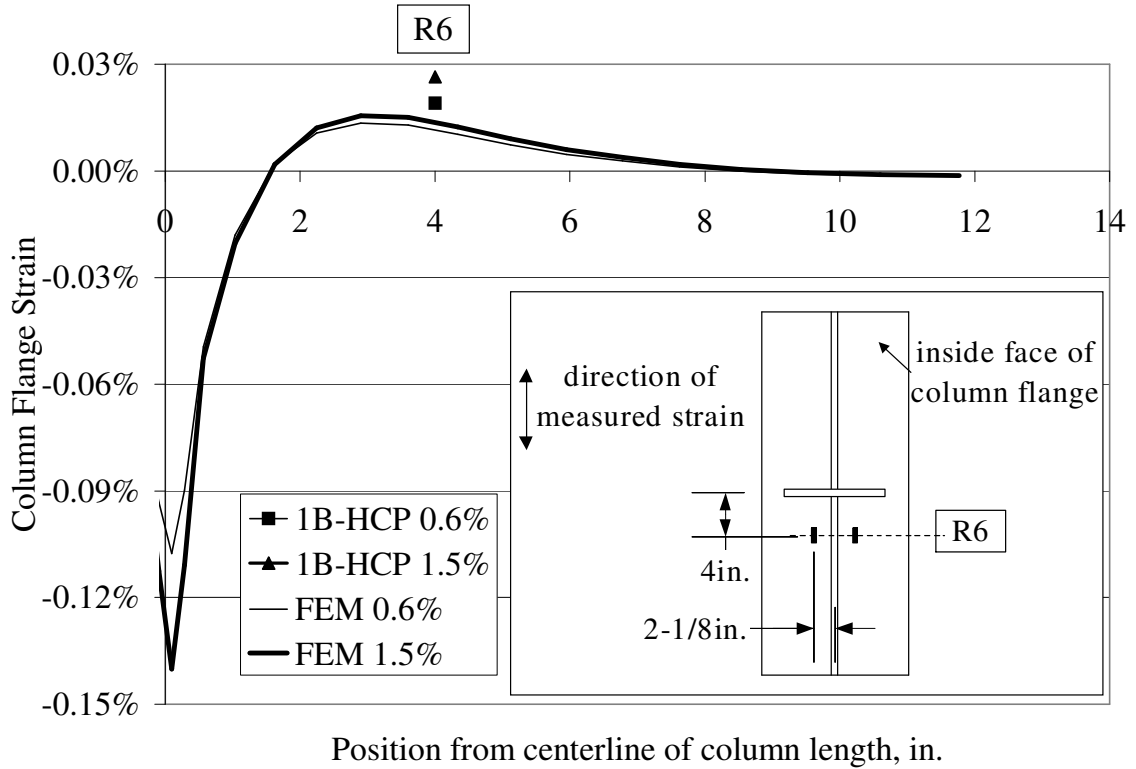


Figure 4.15: Experimental and FEM Results of Specimens 1-HCP and 1B-HCP

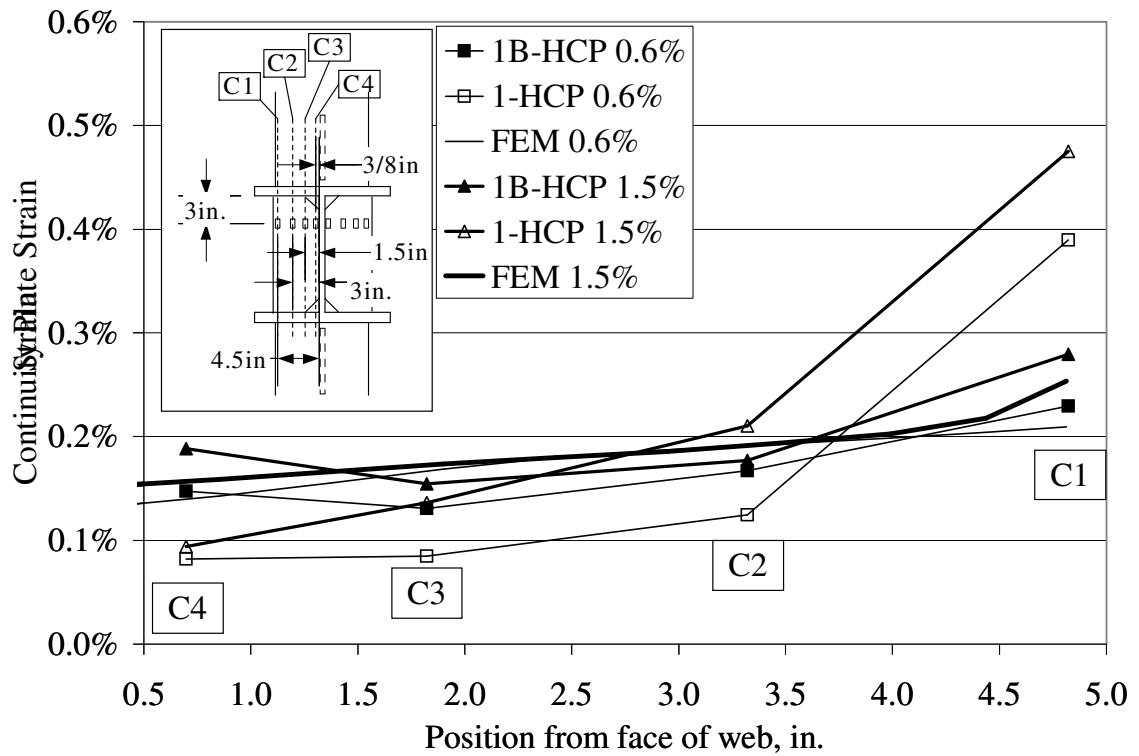


Figure 4.16: Experimental and FEM results of Specimens 1-HCP and 1B-HCP

4.4 Specimen Behavior

The global behavior of the nine specimens were similar since complete failure of the specimen was always due to fracture of the pull-plate. The load-deformation curves of the specimens closely resemble the tensile stress-strain curve of the pull-plate coupons. The difference is due to the amount that the column and connection region elongate, which is small in comparison to the elongation of the pull-plates.

Figure 4.17 shows the load versus specimen elongation curves for five of the specimens and for the pull-plate coupons. Only the specimens without eccentric loading are shown in Figure 4.17. As discussed in Section 4.2, due to the bending of the first four specimens, the specimen elongation curves are not reasonable for comparison purposes at load levels less than the yield load of the pull-plates. Table 4.1 is a summary of the pertinent results of the tests, including loads and specimen elongations at the specimen failure and when the different yield mechanisms (as defined in Section 4.1) were exceeded. The resistance factors ϕ were taken as 1.0 for LWY and 0.9 for LFB. The following sections discuss the results relative to the limit states of LWY and LFB.

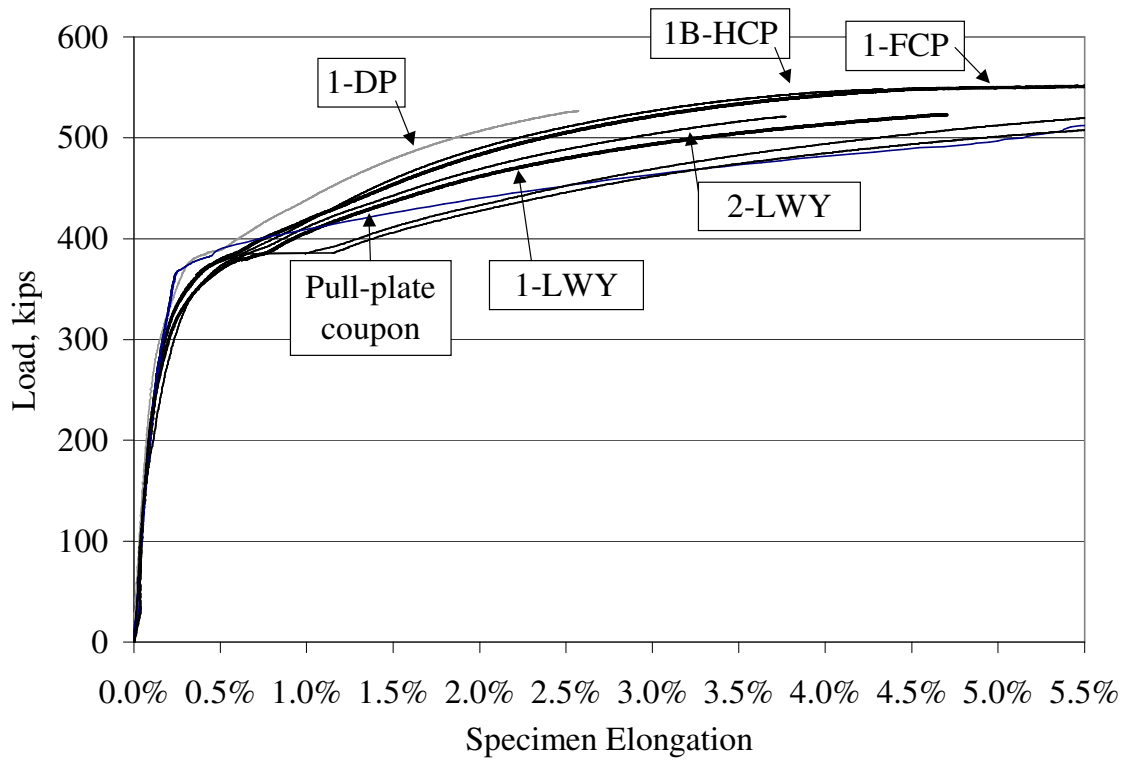


Figure 4.17: Load-Deformation Curves for Five Specimens and Pull-Plate Coupon

Table 4.1: Specimen Results

	1-LWY	1-LFB	2-LWY	2-LFB	3-UNST	1-HCP	1B-HCP	1-FCP	1-DP
Ultimate Load / Specimen Elongation	523 k 4.7%	519 k 4.2%	519 k 3.8%	520 k 3.1%	520 k 3.5%	526 k 3.1%	548 k 4.3%	551 k 5.5%	527 k 2.6%
Load /Specimen Elongation at LWY YM 1*	471 k 2.2%	---	483 k 1.6%	---	514 k 3.2%	---	---	---	---
Load /Specimen Elongation at LWY YM 2*	500 k 3.3%	---	437 k 1.4%	---	496 k 2.7%	---	---	---	---
Nominal ϕR_n for LWY Equation 3.7	296 k		323 k		377 k				
Actual ϕR_n for LWY Equation 3.7 [†]	348 k		404 k		457 k				
Load /Specimen Elongation at LFB YM	412 k 1.1%	410 k 1.2%	463 k 1.9%	---	490 k 2.5%	---	---	---	---
Nominal ϕR_n for LFB Equation 3.8	298 k		334 k		398 k				
Actual ϕR_n for LFB Equation 3.8 [†]	323 k		423 k		468 k				
Load /Specimen Elongation at Continuity Plate YM	---	---	---	---	---	---	---	---	---
Load at 0.6% Specimen Elongation	379 k	382 k	381 k	276 k	274 k	365 k	383 k	387 k	399 k
Load at 1.5% Specimen Elongation	437 k	426 k	443 k	435 k	433 k	435 k	459 k	454 k	479 k

* LWY YM 1 = local web yielding yield mechanism 1 = strain at the column length centerline in the k-line is above 3%

* LWY YM 2 = local web yielding yield mechanism 2 = strain in the entire 5k+N region of the k-line is above the yield strain

- * LFB YM = local flange bending yield mechanism = flange tip separation is over ¼ in.
- * CP YM = continuity plate yield mechanism = strain in the full-width region of the continuity plate is above the yield strain
- † actual ϕR_n values use measured specimen dimensions and coupon yield strength results

4.4.1 Local Web Yielding

Three specimens, 1-LWY, 2-LWY, and 3-UNST, were focused on examining the LWY limit state, although the specimens were also susceptible to LFB. In addition, the four stiffened specimens, 1-HCP, 1B-HCP, 1-FCP, and 1-DP were gaged to compare the column web behavior. Data from all gages and LVDTs are shown in Appendix A. As discussed in Chapter 2, the LWY equation (AISC, 1999b) conservatively assumes that the load is transferred from the girder flange into the k-line at a slope of 2.5:1. In all three unstiffened specimens, the whitewash flaked off the k-line covering a region approximately 9 to 11 in. wide. This corresponds to a slope of approximately 2.8:1. Figure 4.18 shows the whitewash yield patterns of Specimen 1-LWY. The whitewash first flaked off the k-line region then progressed into the column web along lines at approximately 40° angles from the horizontal. These lines can be seen in Specimen 2-LWY, Figure 4.19.

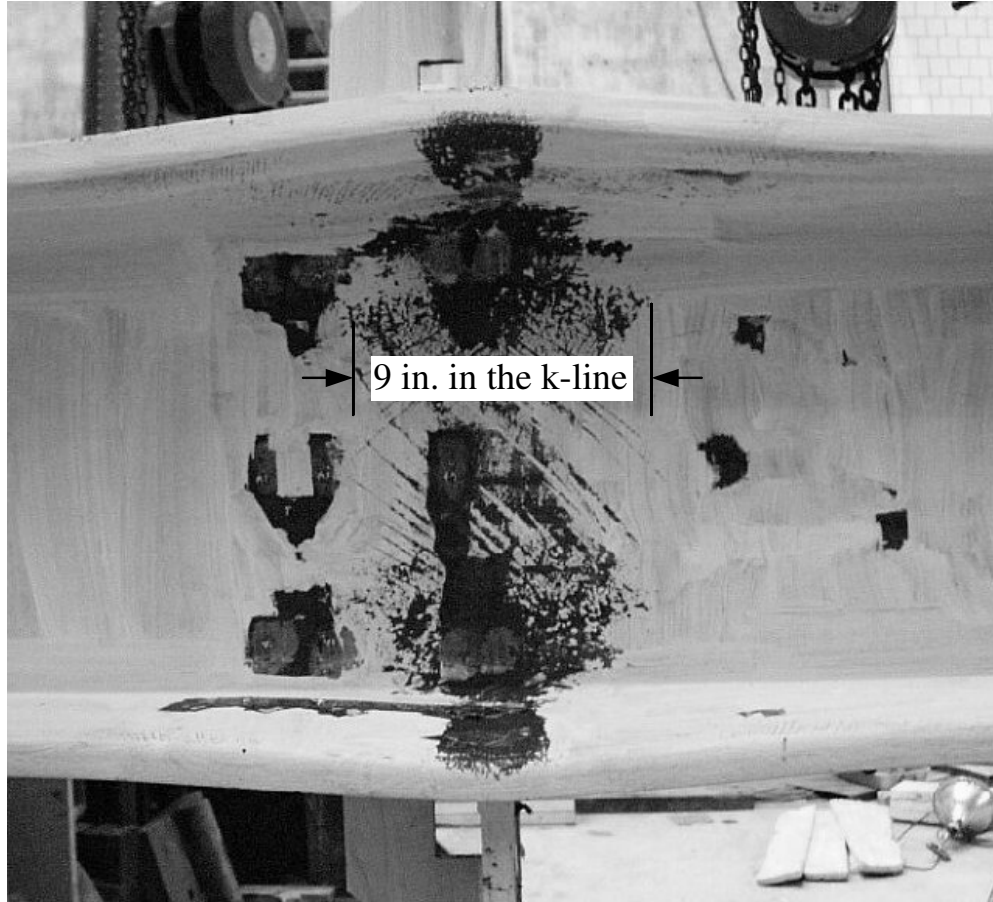


Figure 4.18: Whitewash Yield Patterns of Specimen 1-LWY

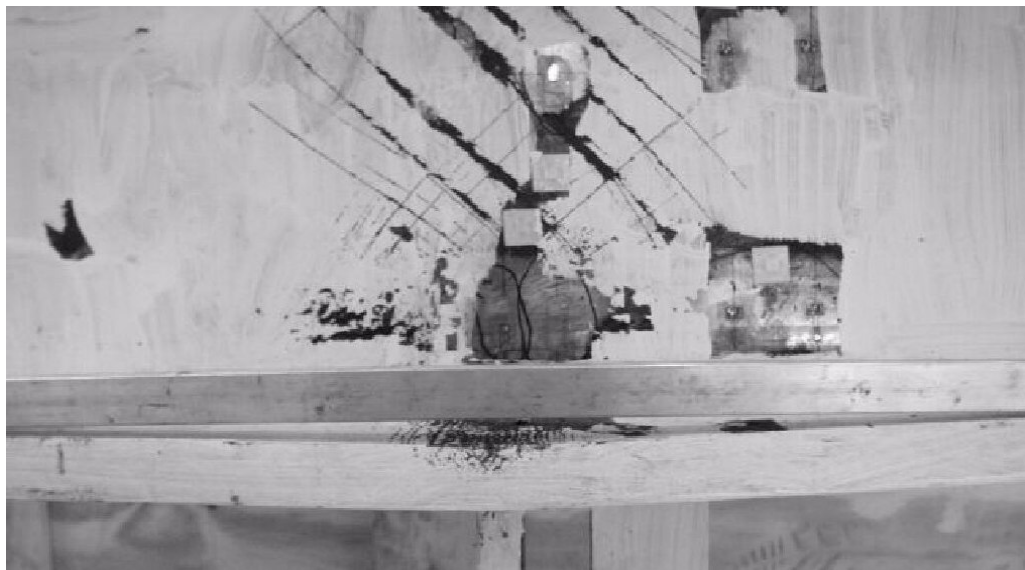


Figure 4.19: Specimen 2-LWY 40° Angle Yield Lines

Table 4.1 shows the load level and specimen elongation when both LWY yield mechanism limits were reached in the nine specimens. Only the three totally unstiffened specimens (1-LWY, 2-LWY, and 3-UNST) exceeded the LWY yield mechanisms prior to fracture of the pull-plate. Only Specimen 2-LWY yielded the entire $5k+N$ region by a load level of 450 kips (corresponding to the nominal seismic R_u value of Equation 3.6), and none of the specimens breached the LWY yield mechanism limits at a load of 375 kips (corresponding to the nominal LWY non-seismic R_u value of Equation 3.1). Only Specimen 2-LWY (W14-145) reached a LWY yield mechanism before the LFB yield mechanism. Specimens 1-LWY (W14x132) and 3-UNST (W14x159) reached the LFB limit first. This was unexpected, because according to the AISC provisions (1999b), the nominal resistance calculated by the LWY equation (Equation 3.7) is less than the nominal resistance calculated by the LFB equation (Equation 3.8), as seen in Table 4.1. However, the actual column sections used in the experiments had web thicknesses that were not the same as the nominal dimensions. The nominal web thickness of Specimen 2-LWY (W14x145) is 0.68 in., but the actual thickness was measured to be 0.646 in. The web thickness of the W14x132 column section is 0.657 in. compared to the nominal value of 0.645 in. (see Table 3.4). As was shown in Figure 4.1, the finite element analyses predicted that the W14x132 should have the greater strains, primarily because of the lesser web thickness. However, because the actual web thickness was greater in the W14x132 than the W14x145, the W14x145 actually had the greater strain. The seemingly small difference in dimensions actually makes a noticeable difference in the finite element and experimental results.

Figure 4.20 shows the experimental strain distribution along the k-line of the column web for all seven specimens at 1.5% specimen elongation. As shown in the figure, at this level of elongation none of the specimens had strain levels exceeding 3% directly under the pull-plate and only the unstiffened W14x145 specimen (2-LWY) had strain values greater than yield for the entire $5k+N$ region. Initially these results seemed implausible, since a W14x145 nominally has a thicker web than a W14x132 section. However, the actual thinner web of the W14x145 section justifies the difference in the

strain distribution between these specimens. There is no tolerance on web thickness in ASTM A6; the tolerance is only on the weight per foot (ASTM, 1998b). The strain distribution also shows a much steeper gradient for the W14x132 (1-LWY) than the other two unstiffened sections. This gradient is likely due to its thinner column flange. The thicker column flanges of the W14x145 and W14x159 act to distribute the load more evenly into the column web.

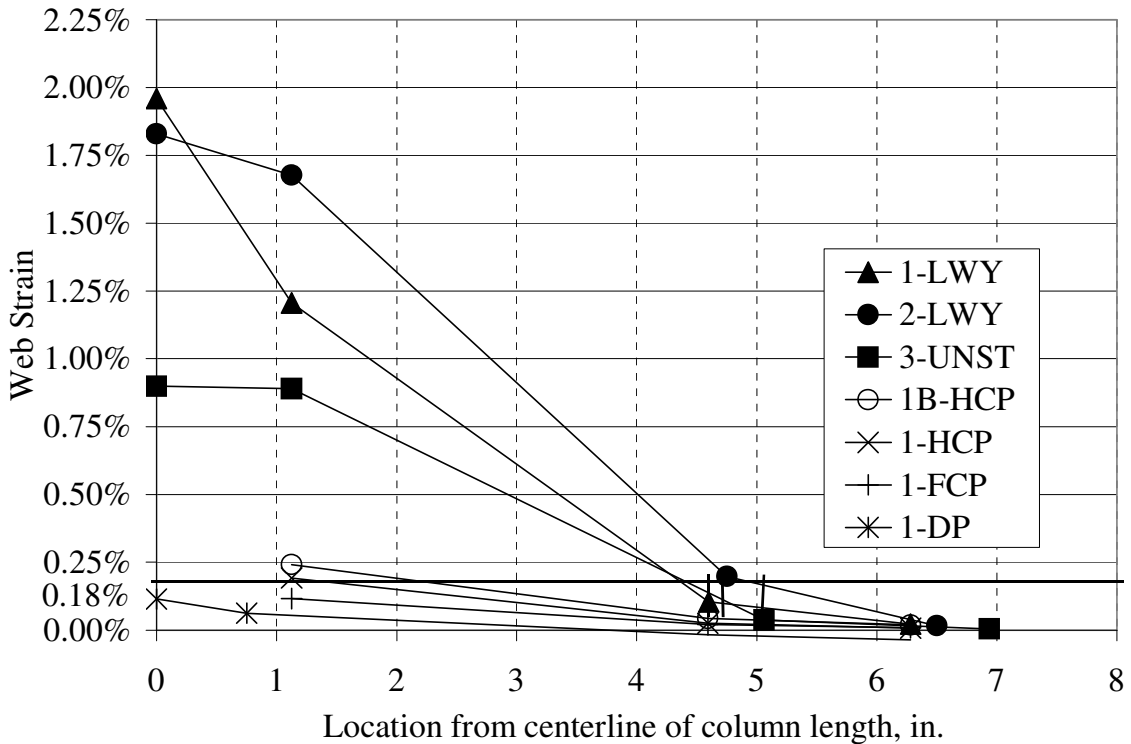


Figure 4.20: Strain Distribution in the Column k-line at 1.5% Specimen Elongation

The results indicate that the strain distribution in the k-line is sensitive to web thickness and distance from the column length centerline. The difference in nominal web thickness between W14x132 and W14x145 sections is only 0.035 in., but the difference in the strain values is considerable. Figure 4.1 shows the finite element distributions for the unstiffened specimens. The strain value for Specimen 1-LWY (W14x132) at the centerline of the column length is almost three times as large as the strain value for

Specimen 2-LWY (W14x145) at a load in the analysis of approximately 450 kips. The high stress concentration can be seen in the comparison of the strain values of all three specimens as they decrease by approximately 30% in only 1 in. from the centerline of the column.

This sensitive web region complicates the development of a robust equation representing LWY behavior. Therefore, an equation to describe this behavior would seemingly have a likelihood of scatter in the data that warrants a low resistance (ϕ) factor. However, the current LWY equation (Equation 3.7) has a ϕ factor of 1.0 (AISC, 1999b). Nevertheless, these results show that the nominal strength (Equation 3.7) is predicted conservatively as compared to the experimental results, as will be discussed more below. In addition, the equation is based upon an estimated stress distribution along the k-line that assumes that the stress distribution within the $5k+N$ region is constant. As seen in Figure 4.20, the strain distribution is highly nonlinear, thus likely resulting in a nonlinear stress distribution. The end of this section discusses the stress distribution inherent in the current LWY equation and possible ways to change the equation to better fit the stress distribution.

Comparisons were made in this work between the three unstiffened pull-plate tests of this research project and the 11 tensile pull-plate tests from the research of Graham et al. (1960). Table 4.2 includes the measured dimensions of the column sections and pull-plates for Specimen 1-LWY, 2-LWY, and 3-UNST, and gives the nominal dimensions of the column sections and pull-plates Specimens F-1 through F-15 [measured dimensions were not reported by Graham et al. (1960)]. All of the yield strengths are averaged results from coupon tests.

Table 4.2: Material Dimensions and Yield Strengths for Specimens Analyzing LWY

	Shape	t_{cw}	t_{cf}	b_{cf}	b_{gf}	t_{gf}	k	F_{vc}	F_{vg}
F-1	8WF31	0.288	0.433	8.000	7.0	0.750	0.8125	37.0	38.9
F-2	8WF31	0.288	0.433	8.000	7.0	0.4375	0.8125	37.0	38.9
F-3	12WF65	0.390	0.606	12.000	8.5	0.625	1.1875	36.0	31.6
F-4	14WF68	0.418	0.718	10.040	8.5	0.625	1.3125	34.2	31.6
F-5	14WF84	0.451	0.778	12.023	11.5	0.875	1.6250	34.2	31.9
F-9	12WF65*	0.390	0.3125	12.000	8.5	0.625	1.1875	36.0	31.6
F-10	14WF84*	0.451	0.375	10.130	11.5	0.875	1.6250	34.2	31.9
F-12	12WF65	0.390	0.606	12.000	8.5	1.500	1.1875	36.0	31.8
F-13	14WF68	0.418	0.718	10.040	8.5	1.500	1.3125	34.2	31.8
F-14	8WF67	0.575	0.933	8.287	7.0	0.750	1.3125	33.5	31.9
F-15	14WF176	0.820	1.313	15.640	11.5	0.875	1.9375	36.0	31.9
1-LWY	W14x132	0.657	0.998	14.725	10.0	0.750	2.0000	49.2	48.2
2-LWY	W14x145	0.646	1.073	15.500	10.0	0.750	2.0000	58.2	48.2
3-UNST	W14x159	0.745	1.187	15.565	10.0	0.750	2.2500	51.1	48.2

*column flange machined to 5/16 in. for test F-9 and 3/8 in. for Test F-10.

Table 4.3 compares the experimental results of the Specimens F-1 through F-15, Specimens 1-LWY, 2-LWY, and 3-UNST, and the predicted results of LWY equations. For Specimens 1-LWY, 2-LWY, and 3-UNST, the experimental load used for LWY comparison purposes is the load level at which the LWY yield mechanism that restricted the strain in the $5k+N$ region was exceeded. The load level that coincided with this yield mechanism was not given for Specimens F-1 through F-15. Instead the failure load was stated when either the column fillet region cracked or the girder-to-column weld fractured. Most likely the loads at which the LWY yield mechanism was exceeded for Specimens F-1 through F-15 were lower load levels, and therefore the test-to-predicted ratios would also be lower. Therefore, to compare the test-to-predicted ratios of the tests of Graham et al. (1960) with the ratio of the tests of this research project is not accurate.

Table 4.3: Comparison of LWY Equations and Experimental Results

Specimen	Shape	Load Predicted by Eq. 3.7	Load Predicted by Eq. 4.1	Load at LWY first YM or Ultimate Load of Test*	Test-to-Predicted Ratios			
					Eq. 3.7 with Nominal Dim.	Eq. 3.7 with Measured Dim.	Eqn. 4.1 with Nominal Dim.	Eqn. 4.1 with Measured Dim.
F-1	8WF31	51	69	100	2.00		1.50	
F-2	8WF31	48	65	95	2.04		1.50	
F-3	12WF65	92	125	149	1.62		1.19	
F-4	14WF68	103	140	167	1.54		1.13	
F-5	14WF84	139	189	212	1.45		1.07	
F-9	12WF65*	92	125	82	0.89		0.65	
F-10	14WF84*	139	189	125	0.86		0.63	
F-12	12WF65	104	138	189	1.81		1.37	
F-13	14WF68	115	153	199	1.64		1.24	
F-14	8WF67	141	191	256	1.69		1.24	
F-15	14WF176	312	426	444	1.42		1.04	
1-LWY	W14x132	347	477	500	1.59	1.36	1.16	0.99
2-LWY	W14x145	404	555	437	1.35	1.08	1.07	0.79
3-UNST	W14x159	457	628	496	1.32	1.09	0.96	0.79

*The load given for Specimens F-1 through F-15 is the ultimate load of the test as reported by Graham et al., 1960. The load given for Specimens 1-LWY, 2-LWY, and 3-UNST is the load level when the strain in the entire $5k+N$ region was above the yield strain.

The predicted loads in Table 4.3 were calculated using two equations for LWY and nominal dimensions and yield strengths. The two LWY equations are the current AISC (1999b) equation, Equation 3.7, and Equation 4.1.

$$R_n = (5k + N)t_{cw}F_{yc} \quad (3.7)$$

The only test-to-predicted ratios that are less than 1.0 are for Specimens F-9 and F-10, which had considerably thinner column flanges than any other specimens. However, the column flanges were machined to be thinner, so the k-line dimensions that were used to calculate the predicted loads were for sections with thicker flanges. Wide-flange sections with similar column flanges thicknesses (approximately 0.35 in. thick)

and web-thicknesses (approximately 0.4 in. thick) have a k-line dimension of approximately $\frac{3}{4}$ in. Using this dimension increases the test-to-predicted ratios above 1.0. It is unclear from Graham's research how the flanges of the two specimens were machined and how the k-line dimension was changed. Therefore, the test-to-predicted ratios for Specimens F-9 and F-10 may be misleading.

For Specimens 1-LWY, 2-LWY, and 3-UNST, the test-to-predicted ratios using Equation 3.7, which is derived from a stress gradient of 2.5:1, are all above 1.0, and therefore the equation is reasonably conservative. Graham concluded that the strain gradient of 2.5:1 was conservative, and that a gradient of 3.5:1 was more accurate but still conservative. Table 4.3 shows the test-to-predicted ratios using the 3.5:1 stress gradient, which results in an augmented LWY equation:

$$R_y = (7k + N)t_{cw}F_{yc} \quad (4.1)$$

These ratios for Specimens 2-LWY and 3-UNST are below 1.0, and thus Equation 4.1 is not always conservative. In addition, as stated earlier, the whitewash yield lines on the specimens showed that the yielded extended a distance of approximately $5k+N$ across the column k-lines (Figure 4.18). Therefore, the specimens of this research project do not reaffirm the conclusion that a 3.5:1 stress gradient in the column web is a more reasonable distribution of the girder flange load.

Comparing the test-to-predicted ratios using the $5k+N$ and the $7k+N$ equations shows that the 2.5:1 stress gradient is a better fit with the experimental data. Figure 4.21 shows both the experimental and finite element stress distributions in the column web in the direction of loading of Specimens 1-LWY, 2-LWY, and 3-UNST. The stress distributions shown are at the load levels at which the entire $5k+N$ region was above the yield strain of each column section. The experimental stress distributions were calculated by using the strain gage data along the k-line and the stress-strain behavior of the coupon results for the column webs. If the strain gage value was below the yield strain of the column web, the stress was calculated by multiplying by the modulus of elasticity of the web. For strain values between the yield strain and the strain at the onset of strain hardening for the web, the stress was equal to the 0.2% offset yield stress. After the onset of strain hardening, the stress was calculated by multiplying the strain beyond the

initiation of strain hardening by the strain hardening modulus and adding the result to the 0.2% offset yield stress. The values for the 0.2% offset yield stress, modulus of elasticity, strain at strain hardening, and strain hardening modulus were determined from the coupon tensile tests, and can be found in Table 3.4.

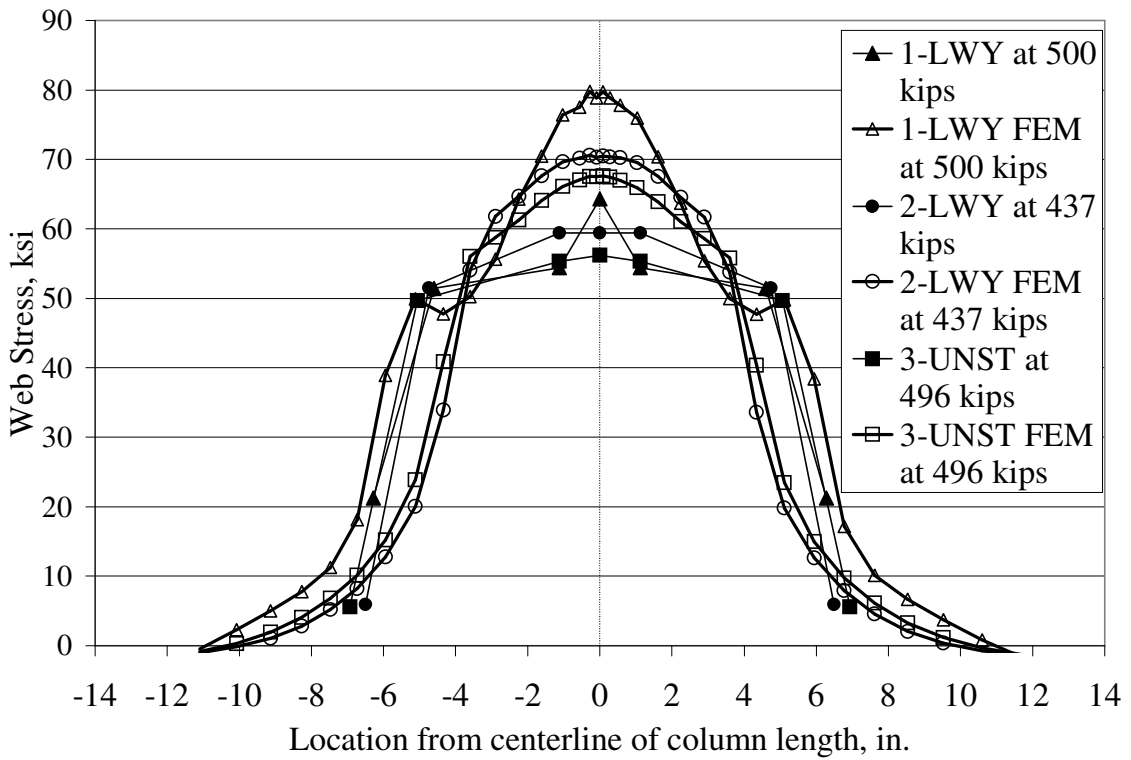


Figure 4.21: Stress Distributions in the Column k-line

As shown in Figure 4.21, a rectangular stress block that is inherent in the LWY equation would not closely describe the actual stress distribution in the column k-line, while a stress distribution with a quadratic equation would more closely fit the data. Thus, a quadratic curve was determined that had the highest R^2 value while maintaining a test-to-predicted ratio above 1.0 for all three of the column sections. The quadratic curve shown in Figures 4.22 through 4.24 has the equation:

$$\sigma = F_{yc} (-0.0352x^2 - 0.0008x + 1.454) \quad (4.2)$$

where:

x = the distance from the centerline of the column length, in inches.

$F_{yc} = 50$ ksi, which is the nominal yield strength of the column

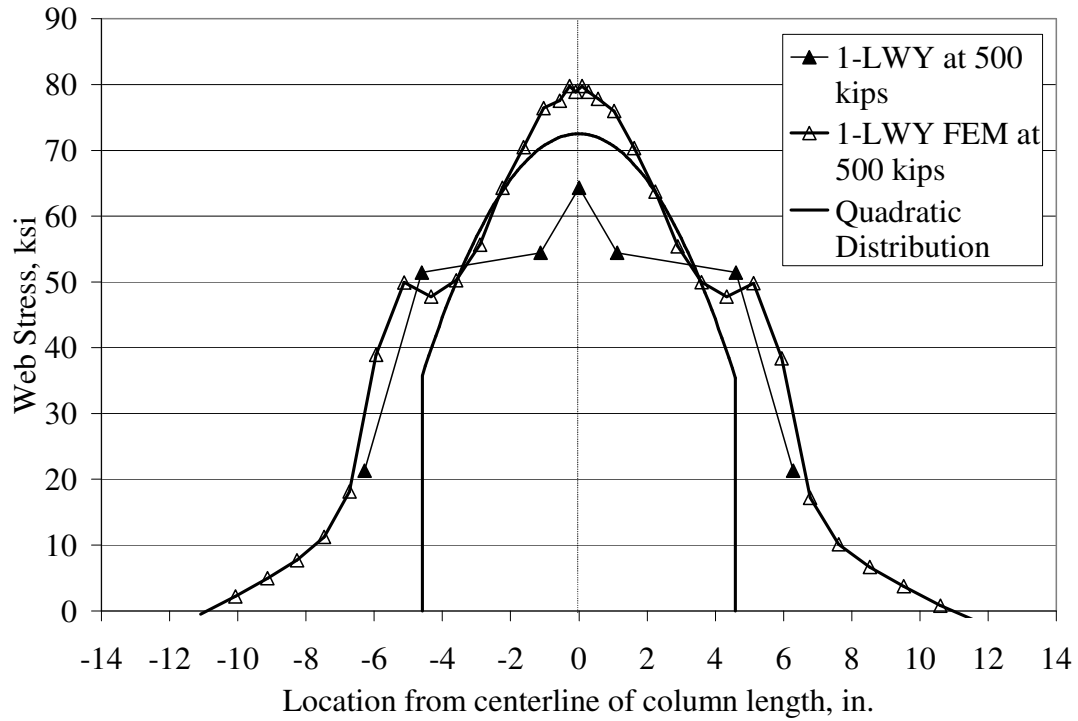


Figure 4.22: Comparing k-line Stress Distributions of Specimen 1-LWY

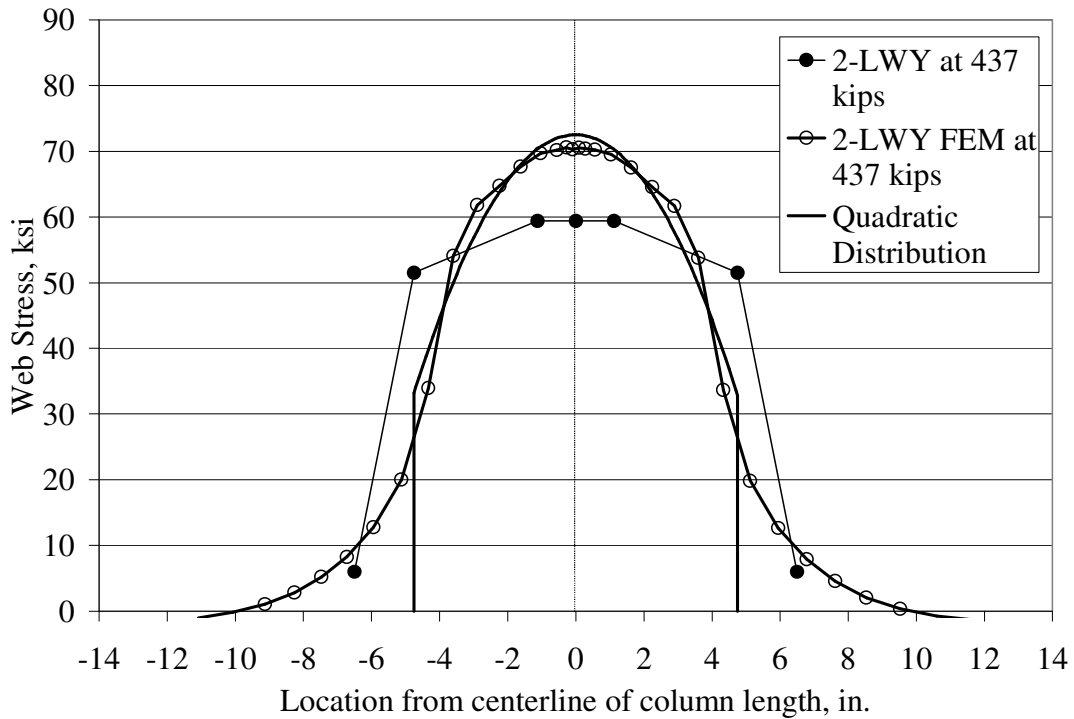


Figure 4.23: Comparing k-line Stress Distributions of Specimen 2-LWY

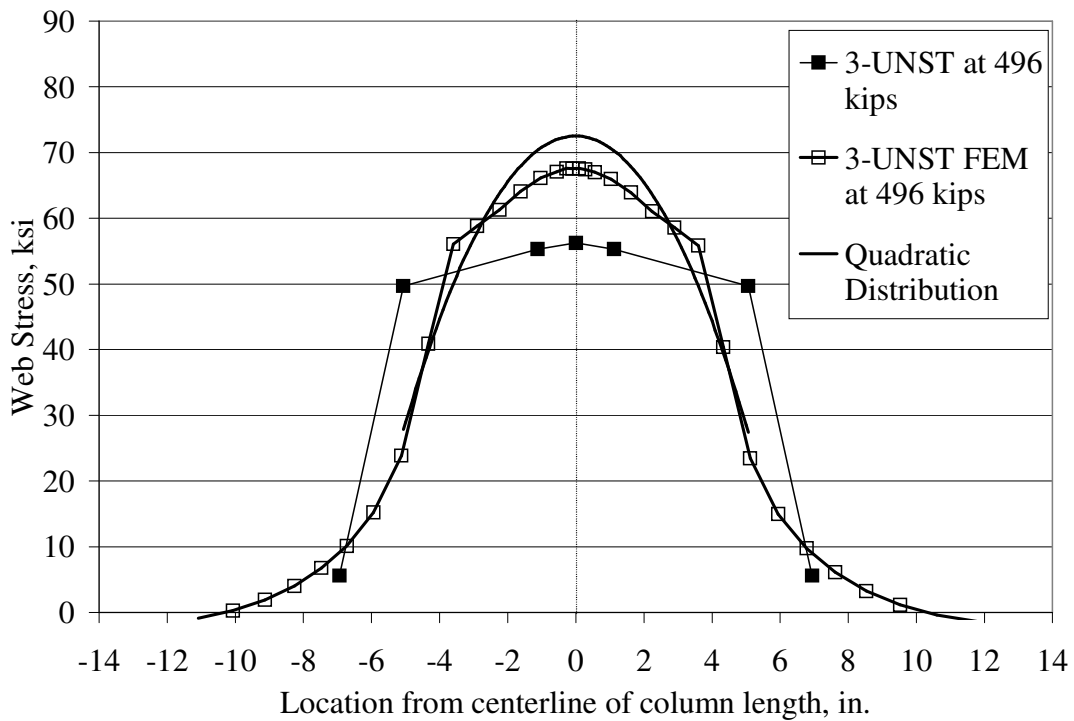


Figure 4.24: Comparing k-line Stress Distributions of Specimen 3-UNST

The resistance of the column web can be calculated by integrating Equation 4.2 from $-\frac{5k+N}{2}$ to $\frac{5k+N}{2}$ and multiplying by the column web thickness, which yields the following equation:

$$R_n = (-0.023x^3 + 0.0007x^2 + 2.9x)t_{cw}F_{yc} \quad (4.3)$$

$$\text{where } x = \frac{5k+N}{2}.$$

This equation was compared to the experimental yield mechanism load, and the test-to-predicted ratios were all greater than 1.0. Table 4.4 shows the ratios for each specimen. The mean and standard deviation for the test-to-predicted ratios for Equation 4.3 are lower than for Equation 3.7. Unfortunately there is insufficient data in the literature reporting the load at which the $5k+N$ region yielded to provide adequate justification for use of Equation 4.3. Nevertheless, this equation more accurately reflects the stress distribution inherent in the LWY limit state.

Table 4.4: Test-to-Predicted Ratios for LWY Equations

		1-LWY	2-LWY	3-UNST	Mean	Standard Deviation
Predicted Loads, kips	Current LWY Eq 3.7	296	323	377		
	Quadratic Eq 4.3	357	384	435		
Yield Mechanism Load, kips		500	437	496		
Test-to-Predicted Ratio	Current LWY Eq 3.7	1.69	1.35	1.32	1.45	0.21
	Quadratic Eq 4.3	1.40	1.14	1.14	1.23	0.15

For non-seismic design, the current AISC provisions (AISC, 1999b) require the column web yielding behavior to be stiffened if it cannot resist a girder demand equal to the yield strength of the girder flange times its area (in this case 375 kips). The current LWY equation (Equation 3.7) predicts column resistances (see Table 4.4) that are

approximately the same or less than the non-seismic girder flange demand of 375 kips. However, the three unstiffened column sections, a W14x132, W14x145, and W14x159, yielded across the $5k+N$ region at loads of 500 kips, 437 kips, and 496 kips, respectively, which are well above 375 kips, and almost exceeded the seismic girder demand of 450 kips.

4.4.2 Local Flange Bending

Five specimens, 1-LWY, 2-LWY, 3-UNST, 1-LFB, and 2-LFB were tested to examine the LFB behavior. Specimens 1-LFB and 2-LFB had ½ in. thick doubler plates fillet-welded flush to both sides of the column web (see Figures 3.9 and 3.10) in order to eliminate web yielding and isolate the flange bending behavior. The same 11 tensile pull-plate tests done by Graham et al. (1960) will also be used for LFB comparison purposes. The dimensions of the specimens were given in Table 4.2. Specimens 1-LFB and 2-LFB have the same dimensions as 1-LWY and 2-LWY respectively, except for the addition of the ½ in. thick A572 Gr. 50 doubler plates. Data from all strain gages and LVDTs are presented in Appendix A.

The doubler plates had 45° beveled edges in order to fit the filleted regions of the columns. However, the radii of the actual fillets were much larger than the nominal dimensions. The k-line dimensions of the W14x132, W14x145, and W14x159 sections were measured to be 2 in., 2 in., and 2.25 in. respectively, while the nominal dimensions are 1.6875 in., 1.75 in. and 1.875 in. (AISC, 1995). This divergence from the nominal dimensions is substantial, as was the thin web in the W14x145 column.

In order to fit the doubler plates in the column, there were three choices: increase the angle of the bevel in order fit the plates flush against the web, do not bevel the edges and cut the plates in order to just fit within the column flanges (not flush against the web), or keep the 45° beveled edges and cut the plates narrower until they fit flush against the web.

There are problems with all three choices that reflect on issues that may arise in practice with fillet-welded doubler plates. By increasing the angle of the bevel, the fillet

welds would need to be increased to keep the same effective throat thickness. If the bevel is increased too much, the plate becomes very thin at the tip and the weld metal would burn-through the plate. Cutting the doubler plates narrower leaves a gap between the plates and the column web, which does not allow welding of the top and bottom of the plates to the column web. This is a possible problem in weak-axis connections since the plates will be more flexible without the welds. Trimming back the plates and keeping the same beveled edges creates a gap between the plates and the column flanges, which would need to be filled in with weld metal. Fillet welds are not prequalified for gaps over 1/16 in.

For Specimens 1-LFB and 2-LFB the doubler plates were made as ordered and a small gap existed between the plates and the column web and the plates and column flanges. Figure 4.25 shows the approximately 1/8 in. gap between the plates and web and also shows the 3/4 in. fillet welds that connect the plates to the column flanges. While the fillet welds were not prequalified due to the size of this gap, the detail behaved satisfactorily since it sufficiently restrained the web from yielding and no weld failures occurred. However Figure 4.25 does show a root crack in the fillet weld, but it did not progress into a fracture of the weld.

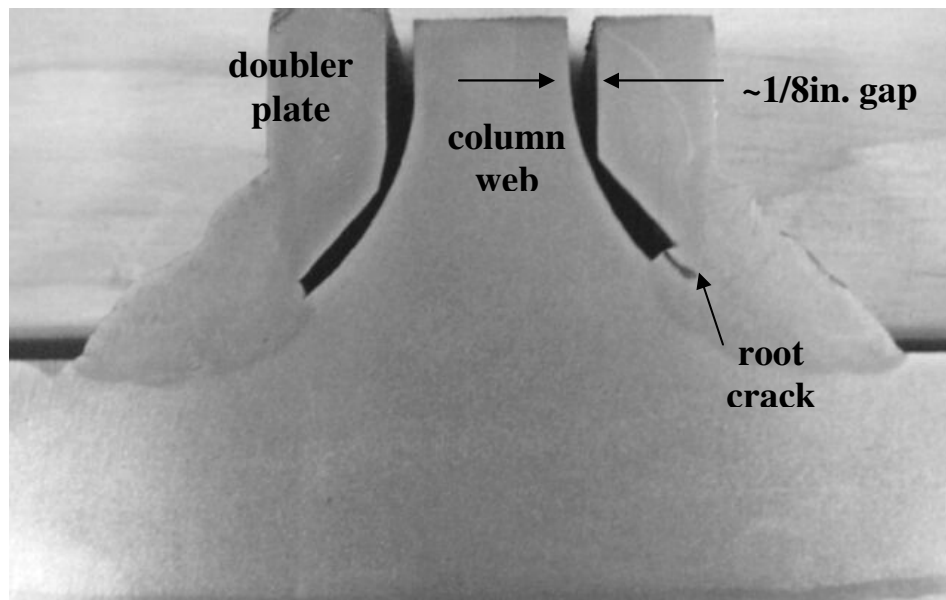


Figure 4.25: Gap between Column Web and Doubler Plates of Specimen 2-LFB

The behavior of Specimens 1-LFB and 2-LFB was very similar. Both specimens had whitewash first flake off from the inside face of the column flanges directly beneath the pull-plates and the yielding continued in diagonal lines radiating out from the center of the column flange-girder flange juncture. Figures 4.26 and 4.27 show these yield patterns. These same yield patterns were noted in the results of the pull-plate tests of Graham et al. (1960), and were used in deriving the LFB equation (AISC, 1999b), as discussed in Chapter 2.



Figure 4.26: Yield Lines on Inside Face of Column Flange under Pull-Plate of Specimen 2-LFB

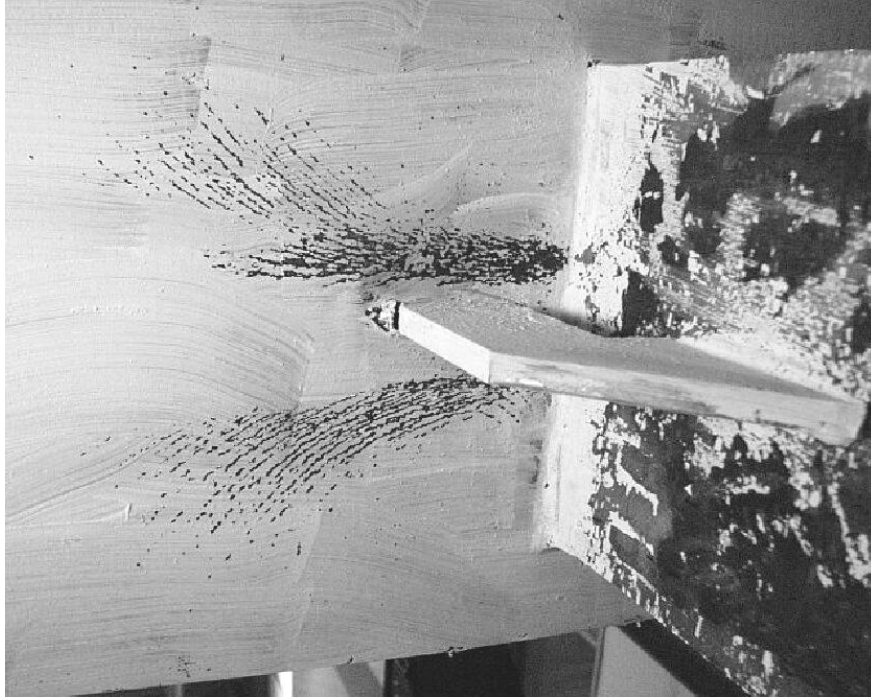
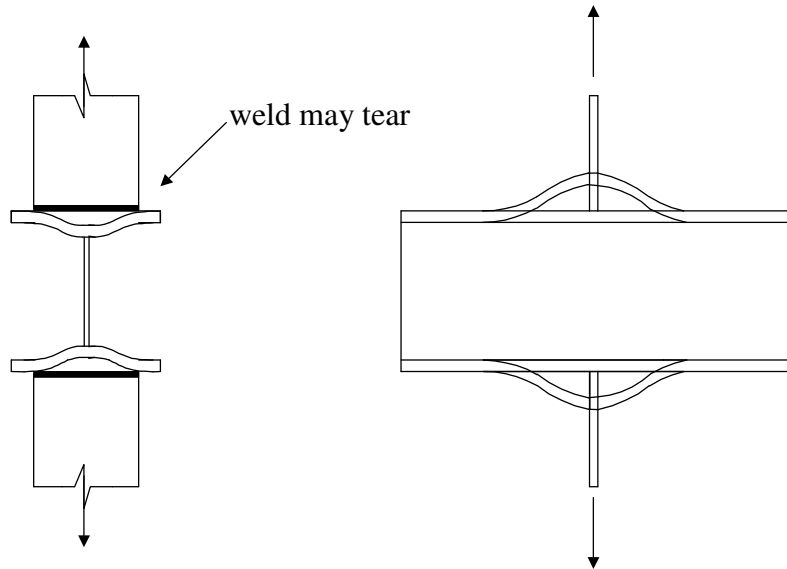


Figure 4.27: Yield Lines on Outside Face of Column Flange Radiating Out from Center of Specimen 1-LFB

The behavior of the column flanges is not that of one-way bending as shown in Figure 4.28a. While this is the direction of bending that would put the most stress on the girder-to-column weld, the primary direction of bending in unstiffened sections is along the length of the column, as in Figure 4.28b. The actual column shape is a combination of both bending shapes.



Figures 4.28a and b: Illustrations of Local Flange Bending

Figures 4.29 and 4.30 show the strain distribution on the inside face of the column flange at 1.5% specimen elongation (approximately 450 kips = $1.1R_yF_{yg}A_{gf}$) for the LFB specimens and the three unstiffened specimens (see Figure A.3 for gage locations). Figure 4.30 does not show the results of Specimen 1-LFB due to malfunction of the strain gages at the plotted locations. The strain values measuring the longitudinal strain of the column flanges in Figure 4.29 are much greater than the transverse strain in Figure 4.30. The longitudinal strain in the column flanges is not due just to the bending of the column flanges, but is also considerably affected by the stretching of the column web. The largest longitudinal column flange strain values are for specimens with unstiffened column webs. For example, in Specimen 2-LWY, the column web stretches considerably at the centerline of the column length (shown in Figure 4.20), which also affects the bending of the column flange. Therefore, the compressive strains in the longitudinal direction at the centerline of the column length of Specimen 2-LWY were larger than for Specimen 2-LFB, which had the stiffened column web. If the column web elongation is controlled, the strain in the transverse direction becomes more prominent. Figure 4.30 shows that for these same two specimens, the transverse direction strain values are larger for Specimen 2-LFB, which has minimal web elongation.

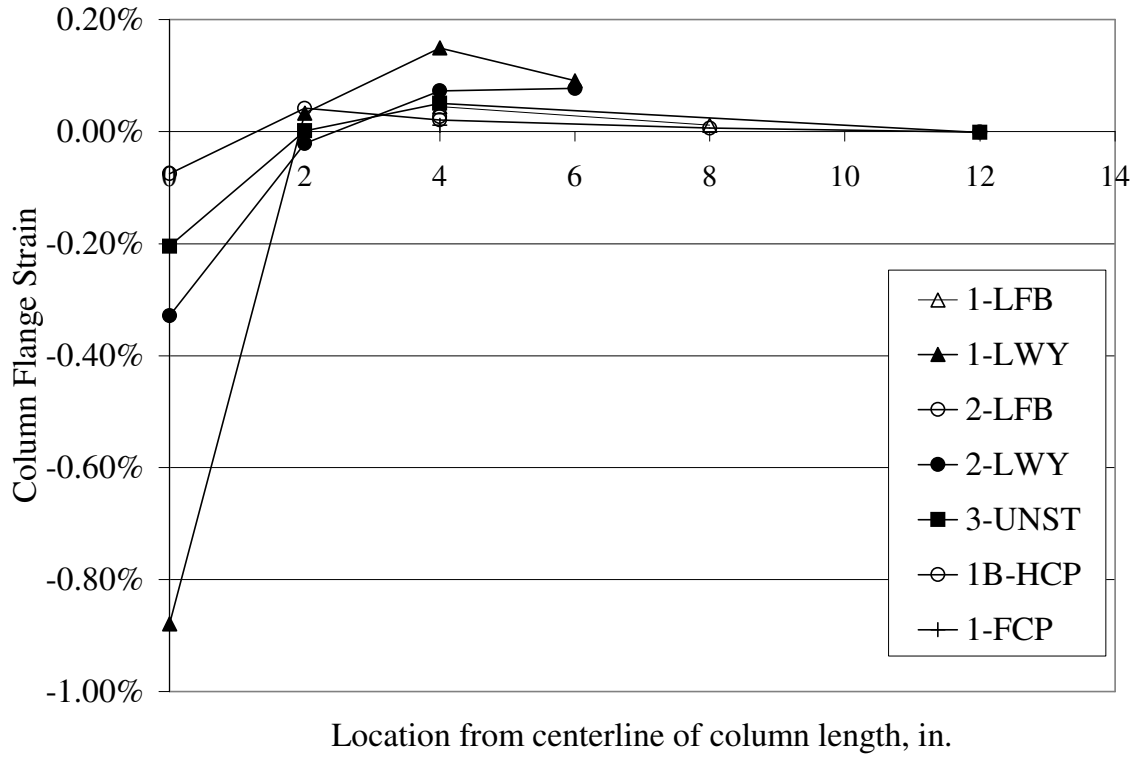


Figure 4.29: Longitudinal Strain on the Inside Face of Column Flanges at 1.5% Specimen Elongation

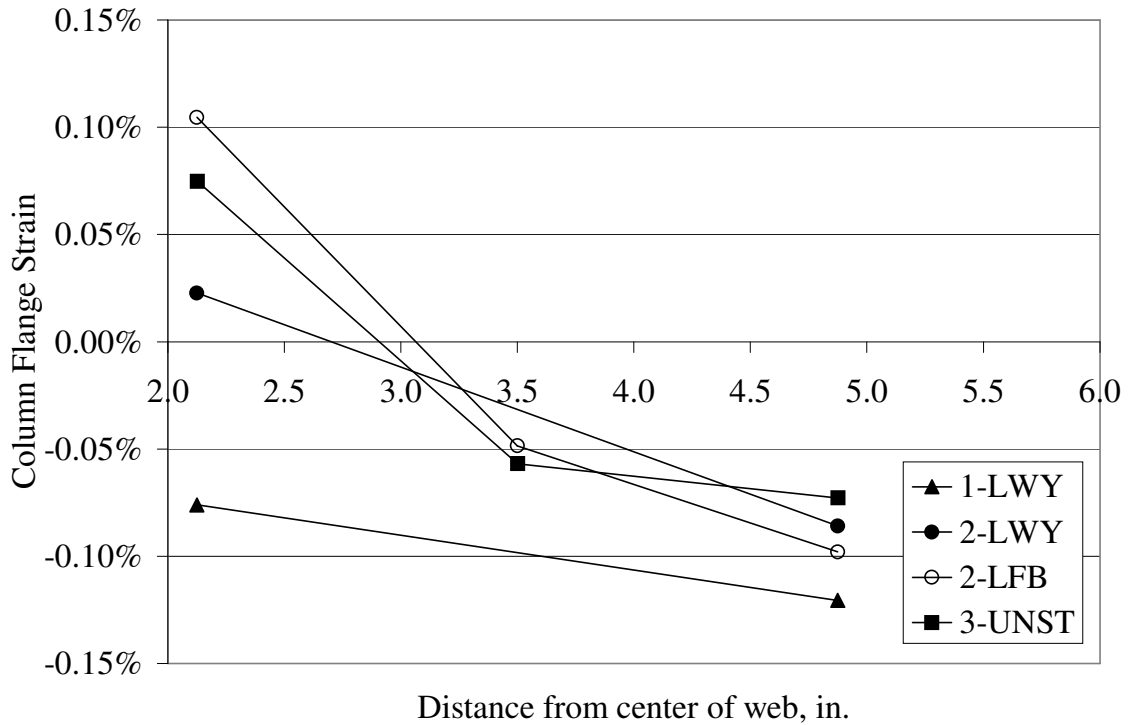


Figure 4.30: Transverse Strain on the Inside Face of the Column Flanges at 1.5% Specimen Elongation

As shown in Figures 4.29 and 4.30, most of the strain values not only are small but they vary greatly in a short distance. This makes it difficult to use strain behavior as a predictor of a column flange yield mechanism. Only the longitudinal strains directly under the pull-plate for the unstiffened specimens are above yield, and these high strains are primarily due the elongation of the web. The longitudinal strain then decrease sharply with distance away from the column length centerline. At distances greater than 2 in. from the centerline, the strains are small, which then means that Poisson’s effect has a significant influence on the strain values. The strains are even smaller in the transverse direction, shown in Figure 4.30. Also, the values change from tensile near the column web to compressive near the edge, in a distance of less than 5 in.

Since the two-way bending of the column flanges creates a strain behavior that is not easily modeled or predicted, the separation of the column flanges was used as a yield mechanism to define the LFB limit state. As stated earlier, the yield mechanism for LFB

is defined as occurring if the separation of the column flanges directly under the pull-plates is greater than $\frac{1}{4}$ in. Figure 4.31 shows the separation of the flanges near the tips of the flanges along the column length for all nine specimens. The W14x132 unstiffened specimen (1-LWY) and the W14x132 specimen with doubler plates on the web (1-LFB) both had flange separation measurements over $\frac{1}{4}$ in., and therefore exceed the LFB yield mechanism.

Figure 4.32 shows the flange separation transverse to the column length. The LVDTs were placed at the column length centerline, near the web and near the edge of the column flange. By comparing the specimens without continuity plates but with web-doubler plates (1-LFB and 2-LFB) to those with no stiffeners at all (1-LWY and 2-LWY), it can be seen that a significant portion of the flange separation is due to web deformation, as stated earlier. In the case of the W14x145 specimens (2-LWY and 2-LFB), which has a stiffer flange and, as it turns out, a thinner web than the W14x132 specimens, half of the flange separation is due to web deformation.

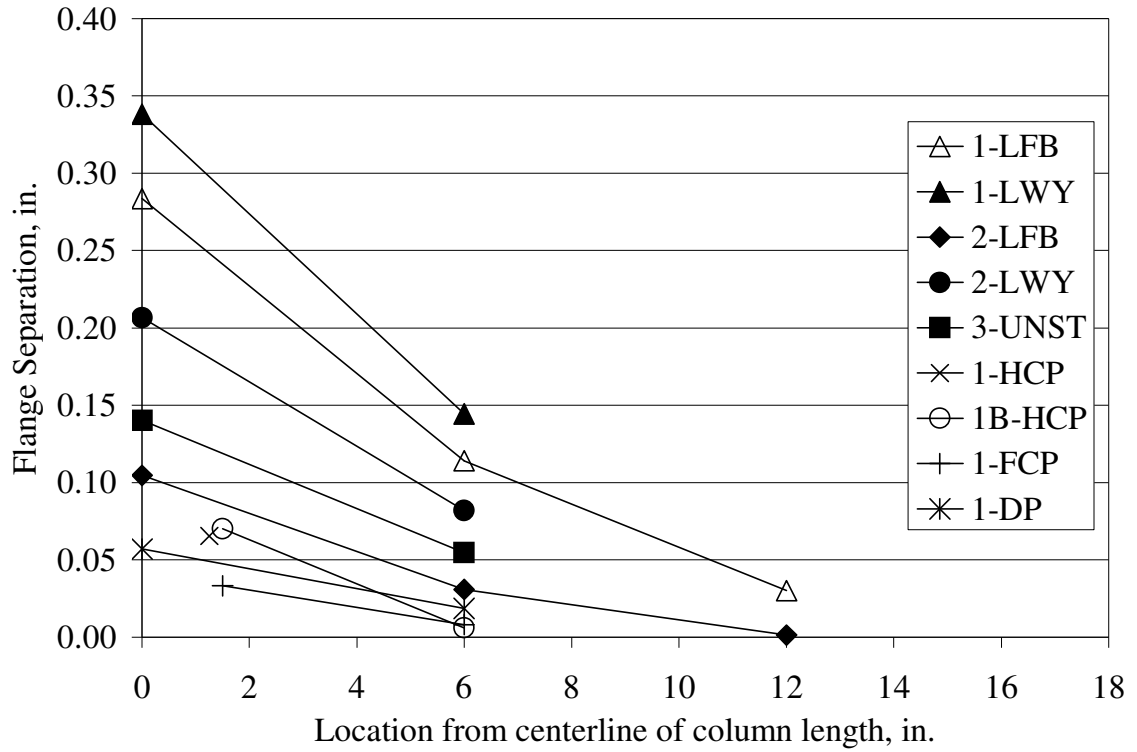


Figure 4.31: Column Flange Separation along Column Length at 1.5% Specimen Elongation

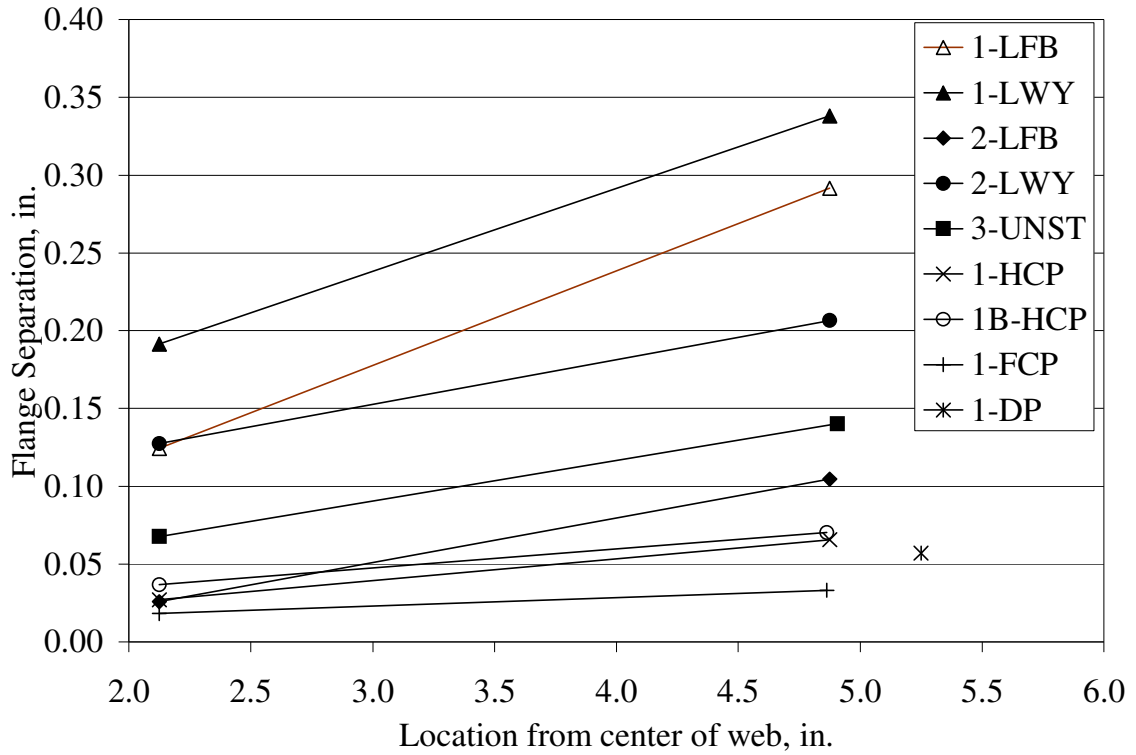


Figure 4.32: Separation of Column Flanges Transverse to Column Length at 1.5% Specimen Elongation

Figures 4.33 and 4.34 are photographs of Specimen 1-LWY after testing. Figure 4.33 clearly shows the column flange separation in the longitudinal direction. At the ultimate load of the test, the flange separation was nearly 1.2 in. at the centerline of the column length. Figure 4.34 is photograph of the top column flange and pull-plate showing the bending in the transverse direction.



Figure 4.33: Specimen 1-LWY Flange Separation in Longitudinal Direction



Figure 4.34: Specimen 1-LWY Flange Separation in Transverse Direction

Two calculations of test-to-predicted ratios were calculated for the five pull-plate tests without continuity plates or doubler plate box details and the 11 tensile pull-plate tests of Graham et al. (1960). The two predicted loads (Equations 3.8 and 2.11) were based on the research by Graham et al. (1960). As discussed in Section 2.1, Equation 2.11 is the LFB equation determined by Graham et al. (1960) that contains no approximations, but uses the nominal dimensions of the columns and pull-plates. Equation 3.8 was derived using approximations for several variables and a 20% conservative reduction in strength:

$$F_{yg} A_{gf} = F_{yc} t_{gf} m + 2c_1 F_{yc} t_{cf}^2 \quad (2.11)$$

where (all variables are defined in Chapter 3):

$m = t_{cw} + 2(k - t_{cf}) \approx k_1$ [k_1 was not used at the time, because the dimension was not yet tabulated in the AISC Manual (AISC, 1950)]

$$c_1 = \frac{\left(\frac{4}{\beta} + \frac{\beta}{\eta}\right)}{\left(2 - \frac{\eta}{\lambda}\right)}$$

$$\eta = \frac{\beta}{4} \left(\left(\sqrt{\beta^2 + 8\lambda} \right) - \beta \right).$$

$$\beta = \frac{p}{q}$$

$$\lambda = \frac{h}{q}$$

$$p = 12t_{cf}$$

$$q = \frac{b_{cf}}{2} - \frac{m}{2}$$

$$h = \frac{b_{gf}}{2} - \frac{m}{2}$$

and:

$$R_n = 6.25t_{cf}^2 F_{yc} \quad (3.8)$$

For the test-to-predicted ratios, the test loads for Specimens F-1 through F-15 [tests from Graham et al. (1960)] were determined when either the pull-plate-to-column weld fractured or a fracture in the column occurred. For the five pull-plate tests of this research program, the test load was taken as the load when the flanges separated by $\frac{1}{4}$ in.

As seen in Table 4.5, the test-to-predicted ratio using Equation 2.11 is considerably less than 1.0 for most of the column section sizes that were tested. Thus, Equation 2.11 is not suitable for design. The test-to-predicted ratio using Equation 3.8 shows that all of the test-to-predicted ratios were above 1.0. This shows that the LFB equation currently in the AISC Specification is conservative. However, for smaller column sections the equation is extremely conservative, while for the W14 column sections the equation is only slightly conservative. Thus, both Equations 2.11 and 3.8 exhibit extensive scatter for failure loads or yield mechanisms as defined previously.

The only possible issue of concern is the derivation of the LFB equation. Possible reasons for the scatter of the local flange bending equation stem from two areas: oversimplifying the original equation (Equation 2.11) and basing the assessment of the accuracy of the equation on the test-to-predicted ratio of specimens [from Graham et al. (1960)] with weld metal that has considerably less toughness than what is being used today.

Table 4.5: Comparison of LFB Equations and Experimental Results

	Column Shape	Pull-.Plate Size		Load Predicted by Equation 2.11	Load Predicted by Equation 3.8	LFB Failure or Yield Mechanism Load, kips	Test-to-Predicted Ratio (Equation 2.11)	Test-to-Predicted Ratio (Equation 3.8)
		b_{gf}	t_{gf}					
F-1	8WF31	7	0.75	84.1	43.4	100	1.19	2.31
F-2	8WF31	7	0.4375	72.0	43.4	95	1.31	2.19
F-3	12WF65	8.5	0.625	154.2	82.6	149	0.97	1.80
F-4	14WF68	8.5	0.625	183.5	110.2	167	0.91	1.52
F-5	14WF84	11.5	0.875	222.3	129.4	212	1.15	1.64
F-9*	12WF65	8.5	0.625	83.8	22.0	82	0.98	3.73
F-10*	14WF84	11.5	0.875	122.2	30.1	125	1.02	4.16
F-12	12WF65	8.5	1.5	203.1	82.6	189	0.93	2.29
F-13	14WF68	8.5	1.5	231.6	110.2	199	0.86	1.81
F-14	8WF67	7	0.75	332.1	182.3	256	0.78	1.40
F-15	14WF176	11.5	0.875	675.0	387.9	444	0.66	1.14
1-LWY	W14x132	10	0.75	580.3	322.5	412	0.71	1.28
2-LWY	W14x145	10	0.75	778.8	423.1	463	0.59	1.09
3-UNST	W14x159	10	0.75	876.7	467.6	490	0.56	1.05
1-LFB [#]	W14x132	10	0.75	693.2	322.5	410	0.59	1.27
2-LFB [#]	W14x145	10	0.75	937.1	423.1	Never reached ¼ in. disp	N.A.	N.A.

*column flange machined to 5/16 in. for test F-9 and 3/8 in. for Test F-10.

[#]two ½ in. thick doubler plates added to column web

There can be a large difference between the predicted LFB failure loads of the simplified Equation 3.8 and Equation 2.11. A parametric study using common girder-to-column combinations was conducted to examine Equation 3.8. The section sizes in the study were column section sizes W14 and smaller and girder section sizes W16 and

larger, and only combinations in which the column flange width was larger than the girder flange width were considered. The average ratio of the load calculated by Equation 3.8 to the load calculated by Equation 2.11 is 43%, but the values range between 3% and 72%. The simplified design Equation 3.8 deviates most from the unsimplified Equation 2.11 when the combination is a larger column with a small girder. The difference between Equations 2.11 and 3.8 clearly shows the great variance in the variables used to approximate Equation 3.8. For example the variable c_1 was defined by Graham et al. (1960) to conservatively be 3.5. However, for common combinations the range of c_1 is from 3.8 to 53.8.

The current LFB equation does not appear to assume that the column and girder yield strengths are the same. However, it must be assumed in part of the equation if an approximated value of the variable m/b_{gf} is used. The following calculations show the steps used to convert Equation 2.11 to Equation 3.8.

$$F_{yg} A_{gf} = F_{yc} t_{gf} m + 2c_1 F_{yc} t_{cf}^2 \quad (2.11)$$

$$F_{yg} t_{gf} b_{gf} = F_{yc} t_{gf} m + 2c_1 F_{yc} t_{cf}^2$$

Solving for t_{cf}^2 :

$$t_{cf}^2 = \frac{F_{yg} t_{gf} b_{gf}}{2c_1 F_{yc}} - \frac{F_{yc} t_{gf} m}{2c_1 F_{yc}}$$

$$t_{cf}^2 = \frac{F_{yg} t_{gf} b_{gf}}{2c_1 F_{yc}} \left(1 - \frac{F_{yc} t_{gf} m}{F_{yg} t_{gf} b_{gf}} \right) = \frac{F_{yg} A_{gf}}{2c_1 F_{yc}} \left(1 - \left(\frac{F_{yc}}{F_{yg}} \right) \left(\frac{m}{b_{gf}} \right) \right)$$

Assuming that $F_{yc} = F_{yg}$:

$$t_{cf}^2 = \frac{F_{yg} A_{gf}}{2c_1 F_{yc}} \left(1 - \frac{m}{b_{gf}} \right)$$

Using the variable approximations and 20% conservatism:

$$c_1 = 80\%(3.5) = 2.8$$

$$\frac{m}{b_{gf}} = 80\%(0.15) = 0.12$$

$$t_{cf} \geq \sqrt{\frac{F_{yg} A_{gf}}{2 * 2.8 F_{yc}} (1 - 0.12)} \cong 0.4 \sqrt{\frac{F_{yg} A_{gf}}{F_{yc}}} = 0.4 \sqrt{\frac{R_n}{F_{yc}}}$$

Solving for R_n :

$$R_n = 6.25 t_{cf}^2 F_{yc} \quad (3.8)$$

As shown in Table 4.5, the predicted loads of Equation 3.8 were compared to the experimental failure loads of the 11 pull-plate tests of various column and girder flange sizes to judge the effectiveness of the equation. As previously stated, failure by LFB in these 11 tests was defined as occurring when brittle fracture of the weld occurred or when a crack in the column section initiated. The welds were made with a 3/16 in. diameter E6020 electrode, but the weld properties were not given. Two possible problems with this definition of failure are that the weld material used in the late 1950's is likely not as tough as weld metal used today and that weld failure or column crack initiation may have occurred well after there was excessive column flange deformation. Measurements of the separation of the column flanges were not reported. In the five pull-plate specimens of this research project that examined LFB, excessive deformations, not brittle weld fracture, were the indications of LFB yield mechanisms. The behavior of these five tests may be a better comparison, since they were constructed of current column and girder sections and current weld metal.

In order to determine the failure load of a plate using plastic yield line analysis, many different yield line patterns must be tried in order to determine the smallest load that causes failure. The whitewash yield line patterns on the experimental pull-plate specimens were examined in order to define several possible yield line patterns (the yield line pattern of Specimen 1-LWY is shown in Figure 4.34). Using the yield line pattern in Figure 4.35, Equation 4.4 was derived.

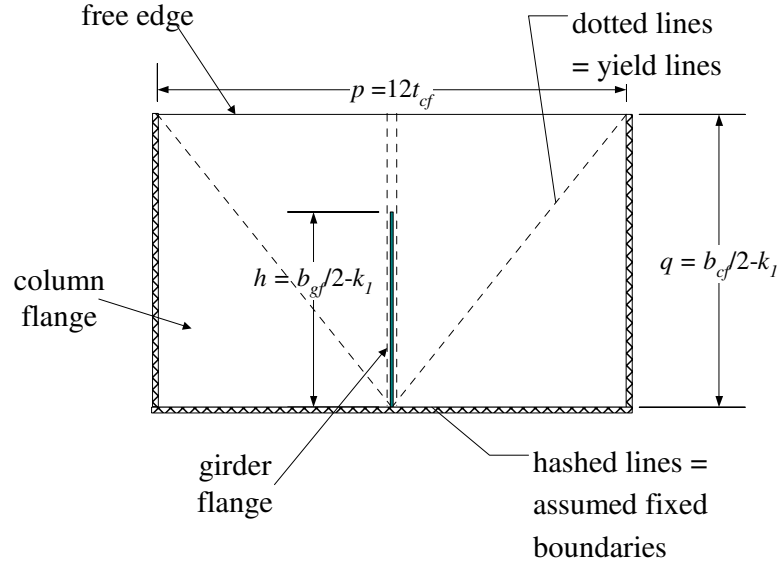


Figure 4.35: Assumed Yield Line Pattern of Column Flange Due to LFB

$$\text{Load to fail by LFB} = F_{yc} t_{gf} 2k_{1c} + 2[F_{yc} t_{cf}^2 S_1] \quad (4.4)$$

where:

$k_{1c} = k_1$ of column section

$$S_1 = \frac{4/\beta + \beta/2}{\lambda}$$

$$\beta = \frac{p}{q}$$

$$p = 12t_{cf}$$

$$q = \frac{b_{cf}}{2} - k_{1c}$$

In a parametric study similar to the one used to assess the reasons for scatter in Equations 3.8 and 2.11, Equation 2.11 was compared to Equation 4.4 for all common column-girder combinations. On average, the proposed unsimplified Equation 4.4 predicts a load that is 23% lower than the predicted load of Equation 2.11. This means that the yield line pattern of the proposed equation calculates a lower LFB failure load. However, in 13.5% of the column-girder combinations, the predicted load by Equation 2.11 was actually larger than the load predicted by Equation 2.11.

Similar to the simplifications made by Graham et al. (1960), common column-girder combinations were used to statistically describe several different variables of Equation 4.4, including $\frac{2k_1}{b_{gf}}$, k_1t_{gf} , and S_I . Table 4.6 summarizes the variables and the values used in the proposed LFB equation. The average minus one standard deviation was used as a conservative approximation for the variables. The average minus two standard deviations was not used because the value would then be less than the minimum value for each variable.

Table 4.6: Statistical Description of Equation 4.4 Variables

Variable	Minimum	Average	Standard Deviation	Average – Standard Deviation
S_I	2.84	5.12	2.14	2.97
k_1t_{gf}	0.22	1.39	0.98	0.40
$2k_1/b_{gf}$	0.11	0.23	0.07	0.15

Using the average minus one standard deviation values for $\frac{2k_1}{b_{gf}}$, k_1t_{gf} , and S_I , the LFB

Equation 4.4 simplifies to:

$$R_n = F_{yc} (0.8 + 5.9t_{cf}^2) \quad (4.5)$$

Table 4.7 compares the predicted loads of Equation 3.8, Equation 4.5 and the experimental LFB loads. The mean and standard deviation of the test-to-predicted ratios using Equations 3.8 and 4.5 were also calculated. As shown, the mean and standard deviation were less for Equation 4.5 than for Equation 3.8. This shows that Equation 4.5 is slightly less conservative than Equation 3.8. However, since the ratios were still greater than 1.0 for all the tests, the equation is still conservative when compared to the experimental LFB loads. The proposed equation is particularly less conservative for the smaller column sections, which were tested by Graham et al. (1960).

Table 4.7: Comparison of LFB Failure Loads

	Column Shape	Load Predicted by Equation 3.8	Load Predicted by Equation 4.5	LFB Failure or Yield Mechanism Load, kips	Test-to-Predicted Ratio (Eq. 3.8)	Test-to-Predicted Ratio (Eq. 4.5)
F-1	8WF31	43.4	70.5	100	2.31	1.42
F-2	8WF31	43.4	70.5	95	2.19	1.35
F-3	12WF65	82.6	106.8	149	1.80	1.40
F-4	14WF68	110.2	131.4	167	1.52	1.27
F-5	14WF84	129.4	149.5	212	1.64	1.42
F-9*	12WF65	22.0	49.5	82	3.73	1.66
F-10*	14WF84	30.1	55.7	125	4.16	2.24
F-12	12WF65	82.6	106.8	189	2.29	1.77
F-13	14WF68	110.2	131.4	199	1.81	1.51
F-14	8WF67	182.3	198.9	256	1.40	1.29
F-15	14WF176	387.9	395.0	444	1.14	1.12
1-LWY	W14x132	322.5	345.8	412	1.28	1.19
2-LWY	W14x145	423.1	446.5	463	1.09	1.04
3-UNST	W14x159	467.6	483.9	490	1.05	1.01
1-LFB [#]	W14x132	322.5	345.8	410	1.27	1.19
2-LFB [#]	W14x145	423.1	446.5	Never reached ¼ in. disp	N.A.	N.A.
Mean					1.91	1.39
Standard Deviation					0.93	0.32

*column flange machined to 5/16 in. for test F-9 and 3/8 in. for Test F-10.

[#]two ½ in. thick doubler plates added to column web

The current non-seismic AISC provisions (AISC, 1999b) require that column flange must be able to resist the non-seismic girder demand (375 kips for these specimens) or else stiffening must be used. For the W14x132, W14x145, and W14x159 column

sections, the current LFB equation (Equation 3.8) predicts column resistances of 322.5 kips, 423.1 kips, and 467.6 kips, respectively (see Table 4.7), which bracket the non-seismic girder (pull-plate) demand of 375 kips. However, these same specimens breached the LFB yield mechanism of $\frac{1}{4}$ in. flange separation at loads of 412 kips, 463 kips, and 490 kips, respectively, which are well above 375 kips, and almost exceed the seismic girder demand of 450 kips.

4.4.3 Column Stiffener Behavior

4.4.3.1 Continuity Plates

Specimens 1-HCP and 1B-HCP were W14x132 column sections with half-thickness continuity plates fillet-welded to the columns. The continuity plate dimensions met all of the provisions for wind or low-seismic design (AISC, 1999a; AISC, 1999b). However, for high-seismic design, the half-thickness continuity plates failed to meet the thickness requirement, since the guidelines state that they are to be the same thickness as the girder flanges. Specimen 1-FCP was a W14x132 column section with full-thickness continuity plate attached to the column flanges with CJP welds, which met all seismic as well as non-seismic provisions (AISC, 1997; FEMA, 2000b).

The results of the specimens with continuity plates (1-HCP, 1B-HCP, and 1-FCP) showed that, at least for monotonically loaded connections, a fillet-welded half-thickness continuity plate was adequate to avoid web yielding and flange bending. Figures 4.20 and 4.31, which show the key experimental data for the LWY and LFB yield mechanisms, respectively, indicate a significant difference that exists between the unstiffened and stiffened specimens and that the half-thickness continuity plates (1-HCP and 1B-HCP) are well below the LWY and LFB yield mechanism limits established in this work.

Whitewash flaked off the half-thickness continuity plates across the entire narrow-width region of the plates and somewhat into the full-width region, as shown in Figure 4.36. As discussed in Section 4.1, the yield mechanism for the continuity plates was complete yielding across the full-width section of the plates at 1.5% specimen elongation. The full-width portion of the continuity plates, as shown in Figure 4.2, was

defined as the area just outside of the $\frac{3}{4}$ in. clips. Figures 4.37 and 4.38 show comparisons of the results of the strain distribution in the full-width and narrow-width regions of the continuity plates of Specimen 1-HCP, 1B-HCP and 1-FCP specimens. The values for Specimen 1B-HCP and 1-FCP are average strain values of gages located on both continuity plates at the same relative location from the column web. The values for Specimen 1-HCP are from strain gages on only one continuity plate. Also, Specimen 1-HCP was tested in the first group of specimens, which had the misalignment in the load frame. The different continuity plate strain distributions are due in part to these differences. Appendix A presents data from all the gages and LVDTs.

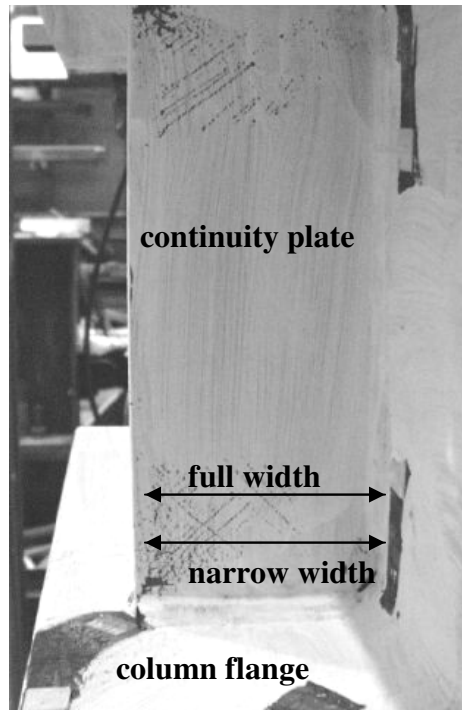


Figure 4.36: Yield Line Patterns on Half-Thickness Continuity Plates

Shown in Figure 4.38, the narrow-width region has exceeded the continuity plate yield strain (approximately 0.18%) in all specimens by 1.5% specimen elongation. However, as shown in Figure 4.37, none of the specimens fully yielded across the width of the continuity plates, and therefore all were still capable of resisting load and had not failed. It is noted that Specimen 1-FCP does have lower, more uniform strains, but even

it yielded in the narrow-width region. In addition, the lack of strain uniformity in Specimens 1-HCP and 1B-HCP (half-thickness continuity plates) did not trigger weld failures.

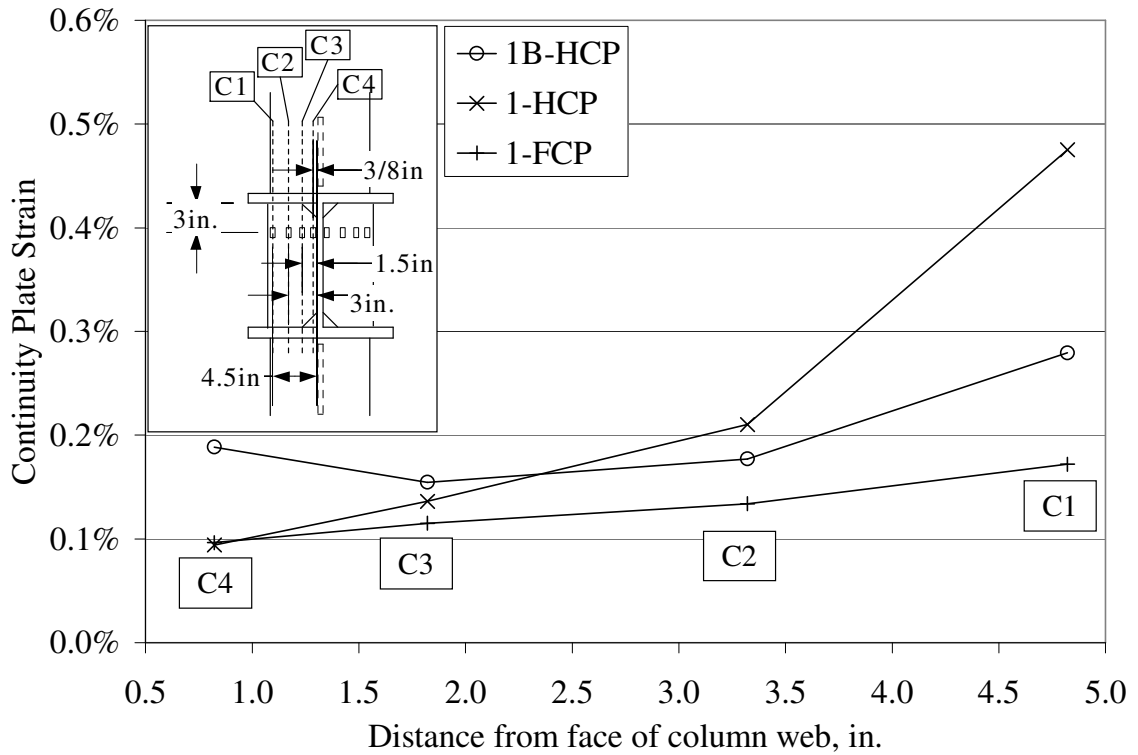


Figure 4.37: Continuity Plate Strain Distribution along Full-Width of Plate at 1.5% Specimen Elongation

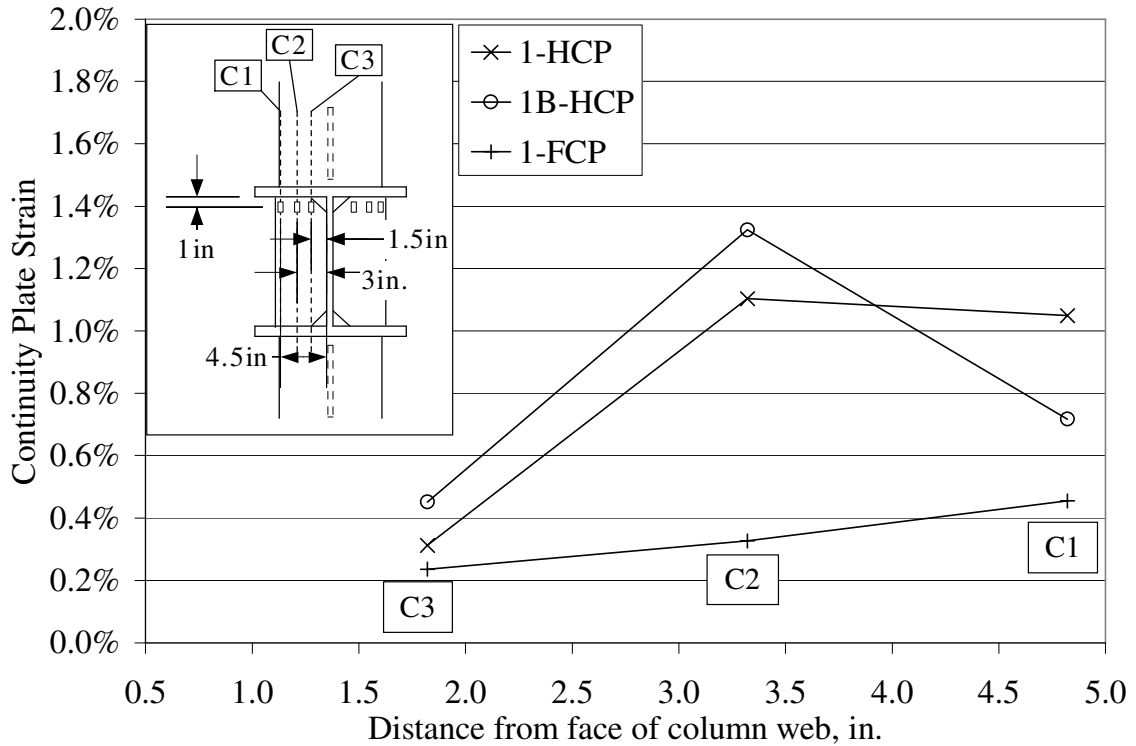


Figure 4.38: Continuity Plate Strain Distribution along Narrow-Width of Plate at 1.5% Specimen Elongation

The fillet welds of the half-thickness continuity plates were examined before and after testing for cracks in the welds. Before testing, a crack was noticed at the end of one of the fillet welds in the clipped region of Specimen 1-HCP. The crack was at the feathered, shallow end of the weld, and appeared to be from the affects of the thin weld cooling. The crack was again examined again after testing, and it had not propagated further into the weld or into the connection. None of the half-thickness continuity plate fillet welds fractured during the tests. The CJP welds attaching the continuity plates to the column flanges of Specimen 1-FCP were examined for cracks during fabrication or testing. However, no cracks or weld fractures were present in the specimen.

4.4.3.2 Doubler Plate Box Detail

The doubler plate box detail as described in Section 3.3.1 consisted of two $\frac{3}{4}$ in. thick plates placed near the tips of the column flanges. The plates were joined to the

column flanges by CJP welds. The strain distribution in the column web and flanges of Specimen 1-DP are similar to those of Specimen 1-FCP. As shown in Figures 4.20 and 4.31 and Table 4.1, Specimen 1-DP did not exceed the yield mechanisms of the LWY or LFB limit states.

The only whitewash that flaked off the column flange was on the inside faces of the flanges directly under the pull-plate. There was no noticeable whitewash that flaked off the outside faces of the doubler plates (the inside faces were not visible).

Figure 4.39 is a comparison of the strain distributions of the k-line region of the column web of Specimen 1-DP and the region in one of the doubler plates at the same location (both doubler plates had similar response) at 0.6% and 1.5% specimen elongation, which corresponds to approximately the non-seismic and seismic girder demands, respectively. As shown, the strain distributions are similar in shape. However, the magnitude of the strain values were over two times greater in the doubler plates than in the column web. At 1.5% specimen elongation, the doubler plate strain values did not exceed 3% strain at the centerline of the column length and did not exceed the yield strength of the plate for the entire $5k+N$ region. Also, the detail provided the needed stiffness to the connection in order to avoid exceeding the LWY or LFB yield mechanisms in the web (see Figures 4.20 and 4.31). Therefore, the box detail performed satisfactorily.

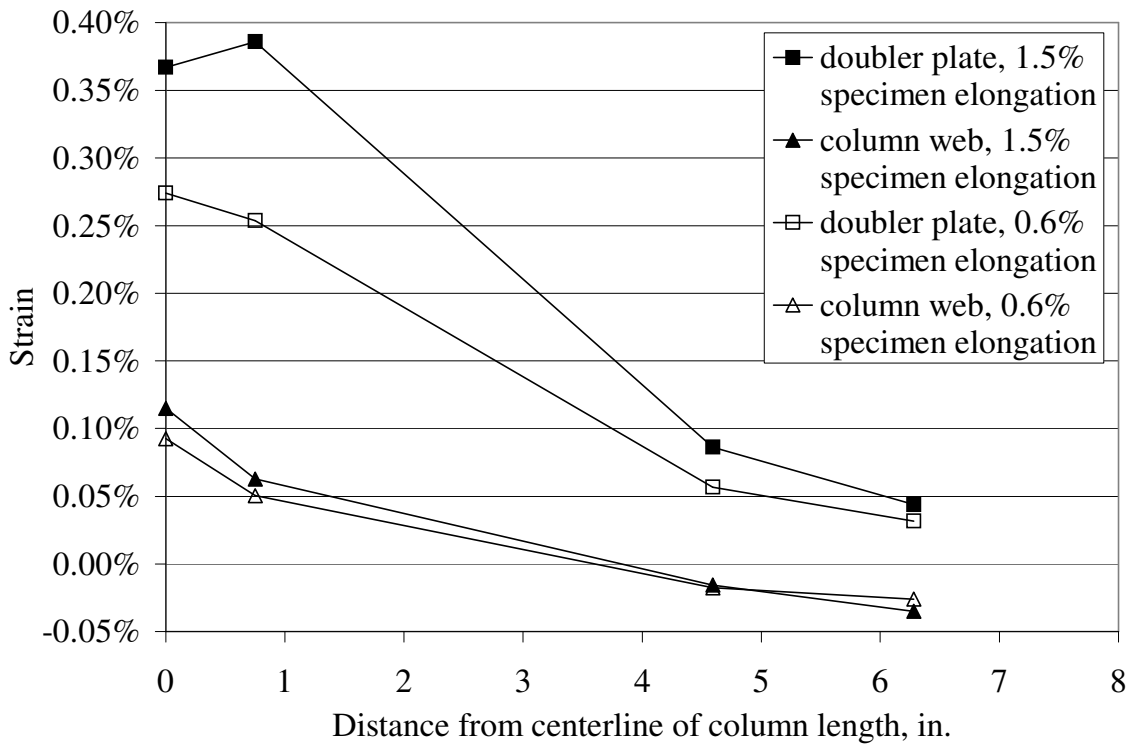


Figure 4.39: Strain Distributions in the Column k-line and Doubler Plate of Specimen 1-DP at 0.6% and 1.5% Specimen Elongation

A finite element parametric study was conducted regarding the optimal position of the doubler plates in the box detail on both monotonically loaded pull-plate specimens and cyclically loaded cruciform connections [Ye et al. (2000) reports details of the study)]. The results of the study showed that locating the doubler plate at a distance of 2/3 of the pull-plate half-width away from the column web provides optimal support to mitigate both LFB and LWY.

To develop guidelines for the design of the doubler plate box detail, it is necessary to assess the effectiveness of the detail relative to using continuity plates coupled with doubler plates near the column web. In this research program, the box detail was designed using AISC Seismic Provisions (AISC, 1997) for standard doubler plates placed flush against the column web, and then the thickness of the plates was increased by 50% to account for possible reduced effectiveness of the doubler plates when they are placed away from the column web. Bertero et al. (1973) first reported this

possible need to increase the size of the doubler plate when they investigated the box detail in cyclically loaded cruciform specimens. The results of their tests showed that the effectiveness of the box detail at reducing panel zone shear was decreased as the doubler plates were placed further away from the column web.

However for non-seismic applications, the effectiveness of the box detail has not been assessed in past work. In non-seismic regions, the doubler plates in the box detail should be designed to mitigate both LWY and LFB. The doubler plate thickness could then be sized using Equation 3.7 for LWY (AISC, 1999b) by increasing the combined doubler plate and column web thickness until the column resistance exceeded the non-seismic girder demand (equal to 375 kips in this work). For the W14x132 column section, two 3/32 in. doubler plates would be needed. To mitigate LFB, it is necessary to assume an effective height of each doubler plate along the column length that is effective in stiffening the column flange against LFB. If it were assumed, as it is for LWY, that the girder flange force is distributed over a region of the doubler plate that has a width of $5k+N$, then, using Equation 3.8 to determine the nominal resistance for LFB, two 3/32 in. doubler plates would be required to mitigate LFB for the W14x132 column section.

Thus, the required doubler plate thicknesses for the non-seismic limit states of LFB and LWY are well below the 3/4 in. doubler plates used in Specimen 1-DP. In order to characterize for non-seismic design the effectiveness of the doubler plates relative to the distance from the column web, it is necessary to identify the smallest doubler plate, located a distance that is 2/3 of the pull-plate half-width from the column web, that does not breach the LWY or LFB yield mechanisms at a load level of 375 kips. For LWY, the yield mechanism is yielding in the doubler plate at a distance k from the outside face of the column flange for a width of $5k+N$. For LFB, the yield mechanism would be separation of the column flanges by 1/4 in. It is unlikely that the LFB yield mechanism would be breached in a stiffened member (as an example, Figure 4.31 shows the small flange separation displacements in Specimen 1-DP). Thus, the effectiveness of the box detail will be assessed for the LWY limit state.

The amount of the girder flange (pull-plate) force that each of the 3/4 in. doubler plates resisted is equal to the integral of the stress in the plate times the thickness of the

plate. Finite element results (Ye et al., 2000) showed that each $\frac{3}{4}$ in. doubler plate resisted approximately 175 kips out of a total of 375 kips. If a smaller doubler plate were used, then the column web may absorb more of the pull-plate load, but also the strain in the doubler plate may increase due to more extensive local flange bending. If one assumes for simplicity that the amount of force absorbed by the column web remains the same as seen in the results of Specimen 1-DP, then it is possible to estimate what size doubler plate would be required to resist 175 kips if that doubler plate were yielded across the length of $5k + N$. This calculation results in two $\frac{3}{8}$ in. thick doubler plates. Compared to the $\frac{3}{32}$ in. thick doubler plates required by the non-seismic LWY and LFB equations, the $\frac{3}{8}$ in. thick doubler plates are 4 times larger.

This approximate analysis thus indicates that, for non-seismic design of the doubler plates in a box detail, the doubler plates should be increased by a factor of 4 over the size determined from the limit states of LFB and LWY (calculated as described above). Of course, this conclusion is based upon an assumed load in the doubler plate resulting from using two $\frac{3}{4}$ in. doubler plate and a W14x32 column, all having a nominal yield strength of 50 ksi. Further research is required to determine the most appropriate factor by which the thickness of a doubler plate in the box detail should be augmented to account for the need to mitigate both LFB and LWY for non-seismic design. This factor will be affected by the distance from the column web to the doubler plates, and by the relative size of the doubler plates and the column web. In addition, Cotton et al. (2001) investigate the effectiveness of the box detail for seismic design, including mitigation of panel zone yielding.

Chapter 5

Summary and Conclusions

5.1 Summary

The objectives of the research project were to examine the limit states of local flange bending (LFB) and local web yielding (LWY) in steel moment frame connections and to assess the need for column stiffening. The nine pull-plate tests and corresponding finite element analyses were one part of a project sponsored by AISC to reassess the design provisions for column stiffeners for non-seismic and seismic conditions and to investigate innovative doubler plate and continuity plate details. The project includes three components: monotonically-loaded pull-plate experiments to investigate the need for and behavior of transverse stiffeners particularly in non-seismic zones; cyclically-loaded cruciform girder-to-column joint experiments to investigate panel zone behavior and local flange bending particularly in seismic zones (Cotton et al., 2001); and parametric finite element analyses to corroborate the experiments and assess the performance of various transverse stiffener and doubler plate details (Ye et al., 2000).

A literature review was conducted, which resulted in the compilation of the histories and background of the design provisions and limit states related to continuity plate design. Opinions regarding the design and behavior of continuity plates were also summarized. As part of the specimen selection process, a parametric study was conducted that examined the need for continuity plates for a comprehensive range of girder-to-column combinations, with varying yield strengths, column axial stresses, and girder demands. The final specimen sizes were selected using factors related to common girder-to-column combinations, testing equipment capacity, girder-to-column

combinations that had recently been tested by researchers, and finite element analyses. The same analyses were also used to define yield mechanisms for the limit states of LWY and LFB.

The pull-plate specimens were grouped into three categories. Two of the specimens, 1-LFB and 2-LFB, used beveled doubler plates fillet welded to the column flanges in order to avoid welding in the k-line. These specimens were focused on examining the LFB limit state. Three of the specimens, 1-LWY, 2-LWY and 3-UNST, were unstiffened column sections that were instrumented to investigate the limit state of LWY and the interaction between LWY and LFB. The final four specimens, 1-HCP, 1B-HCP, 1-FCP, and 1-DP, examined different stiffening details. Specimens 1-HCP and 1B-HCP had continuity plates with thicknesses equal to half of the girder flange (i.e., the pull-plate) thickness and were attached with fillet welds to the column flanges. Specimen 1-FCP had continuity plates with thicknesses equal to the full thickness of the girder flange and were joined to the column flanges with CJP welds. Finally, Specimen 1-DP examined the doubler plate box detail, which had two $\frac{3}{4}$ in. thick doubler plates attached by CJP welds near the tips of the column flanges.

Material tests were performed on the column sections, plate material and weld metal. The results of the tensile, Rockwell hardness, and toughness tests were compared to the current typical values. Macrosections were also taken of several CJP pull-plate-to-column flange welds to examine and discuss any discontinuities in the welds and the effect on connection behavior.

The results of the tests increased the knowledge regarding the behavior of steel moment connections, the limit states of LWY and LFB, and the need for and design of continuity plates and the corresponding welds. Equations were developed to better describe the behavior in the column web k-line and column flange. These equations are presented as potential alternatives to, but not necessarily replacements for, the current equations.

5.2 Conclusions

The conclusions from these tests may be limited to monotonic loading applications. In the near future, cyclic loading experiments will be conducted that will determine if the conclusions from this research can be more widely applied (Cotton et al., 2001). Results of the cyclically tested cruciform specimens will be combined with the pull-plate test results and corroborating finite element analyses (Ye et al., 2000) to evaluate the local web yielding and local flange bending criteria and new stiffener details for seismic applications. The conclusions from the reported research include:

- All nine of the pull-plate tests failed by fracture of the pull-plate at a load approximately corresponding to the tensile strength of the pull-plate coupons (525 kips). The elongation of the pull-plates controlled the deformation of the specimens. The presence of continuity plates had only a slight effect on the elongation results. The unstiffened specimens deformed approximately 8% more than the stiffened specimens.
- None of the E70T-6 CJP welds connecting the pull-plates to the column flanges fractured despite plastic deformation, even when the flange tip separation was over $\frac{1}{4}$ in. This indicates that column stiffener details may have little influence on the potential for brittle weld fracture of the girder flange weld provided the weld is specified with minimum CVN requirements and backing bars are removed. The E70T-6 electrode used had average measured toughness values of 63.7 ft-lbs at 70°F and 19.0 ft-lbs at 0°F, which is slightly lower than the minimum lower shelf requirement recommended by SAC of 20 ft-lbs at 0°F (FEMA, 2000d). The macrosections of the welds showed some discontinuities in the welds, such as inclusions and areas of porosity. Therefore these welds represent a lower bound to the expected toughness and quality of the welds that meet the SAC guidelines (FEMA, 2000d), and the performance was nonetheless satisfactory.
- The AISC provisions for LWY and LFB are reasonable and slightly conservative in calculating the need for column stiffening. The three unstiffened column

sections (W14x132, W14x145, and W14x159) exceeded the LWY yield criterion of yielding across the full $5k+N$ region of the column web at load levels of 500 kips, 437 kips, and 496 kips, respectively, and exceeded the LFB yield criterion of having the flanges separate by more than $\frac{1}{4}$ in. at load levels of 412 kips, 463 kips, and 490 kips, respectively. These values are all considerably greater than the non-seismic girder demand (taken as $R_u = F_{yg}A_{gf}$) of 375 kips and nearly all greater than the seismic girder demand (taken as $R_u = 1.1R_yF_{yg}A_{gf}$) of 450 kips. To better describe the nonlinear behavior in the column web k-line, an LWY equation was determined based upon a quadratic stress distribution in the column web. The LFB bending equation was also examined and augmented to better fit the yield lines seen in the specimens. These equations were presented as alternative methods to better describe the behavior of the column web or flange, which define the limits of LWY and LFB and thus the need for continuity plates. However, the equations do not substantially change the calculated resistance load for either limit state, and so are not proposed as replacements to the current equations (AISC, 1999b).

- Continuity plates that are only half as thick as the beam flange and are fillet-welded to both the column web and flanges performed satisfactorily. The half-thickness continuity plates did not yield across the entire full-width region of the plates, and the plates effectively restrained the column section from excessive web yielding or flange bending. The fillet welds made with an E70T-1 electrode did not fracture.
- The beveled doubler plates of Specimens 1-LFB and 2-LFB, which eliminated welding along the column k-line, performed adequately despite the root crack noted in one of the fillet welds and the approximately $\frac{1}{8}$ in. gap between the column web face and doubler plate. The root crack did not progress throughout the testing, nor did it lead to a fracture of the fillet weld. This doubler plate detail eliminated the column web yielding but did not reduce the flange bending, as expected. The ability of the detail to eliminate excessive panel zone deformation will be tested in future cyclically loaded cruciform tests (Cotton et al., 2001).

- The doubler plate box detail that was CJP welded near the tips of the column flanges performed satisfactorily and provided sufficient stiffness to avoid both LWY and LFB. Further research is required to identify appropriate design guidelines for determining the most efficient plate thickness for mitigating LWY and LFB for non-seismic design. The detail would be most cost effective when needed to act as both a doubler plate (to eliminate excessive panel zone deformation) and a continuity plate (to restrain from exceeding the LWY and LFB limit states). This detail will also be examined for use in seismic applications in the five cruciform connections of Cotton et al. (2001).

Appendix

Displacement and Strain Data of Pull-Plate Specimens

The Appendix contains the data from all the strain gages and LVDTs used in the nine pull-plate specimens of this research. Figures A.1 through A.6 show the names and locations of the possible instruments. Figures A.7 through A.95 contain the data from all the instruments. The figures have been sorted first by specimen and then by location on the specimen. The scales of the graphs are consistent for all specimens for each location on the specimen. For example, the scale for the graphs that contain the pull-plate gages data is the same for all the specimens.

The following section describes the instrument-naming scheme. The first four or five characters of the instrument name identify the specimen, using the following naming scheme:

LWY1 = Specimen 1-LWY, W14x132 unstiffened

LWY2 = Specimen 2-LWY, W14x145 unstiffened

UNST3 = Specimen 3-UNST, W14x159 unstiffened

LFB1 = Specimen 1-LFB, W14x132 with doubler plates flush against web

LFB2 = Specimen 2-LFB, W14x145 with doubler plates flush against web

HCP1 = Specimen 1-HCP, W14x132 with half-thickness continuity plates

HCPB1 = Specimen 1B-HCP, repeat of 1-HCP

FCP1 = Specimen 1-FCP, W14x132 with full-thickness continuity plates

DP1 = Specimen 1-DP, W14x132 with doubler plate box detail

The rest of the instrument name varies depending on if it is a strain gage or an LVDT. The LVDTs were sequentially numbered as follows, and are shown in Figure A.1:

- 1 = near column web at column centerline, a-side
- 2 = at flange tip at column centerline, a-side
- 3 = at flange tip, 6 in. from column centerline, a-side
- 4 = at flange tip, 12 in. from column centerline, a-side
- 5 = near column web at column centerline, b-side
- 6 = at flange tip at column centerline, b-side
- 7 = at flange tip, 6 in. from column centerline, b-side
- 8 = at flange tip, 12 in. from column centerline, b-side
- 9 = overall, a-side
- 10 = overall, b-side

For the strain gages, the two letters after the specimen designation describe where on the specimen the gages are located.

- cw = column web
- cf = inside face of column flange
- gf = girder flange (pull-plate)
- cp = continuity plate
- dp = doubler plate box detail

To measure bending in the specimens, gages were placed on the opposite sides of components of the specimens – the sides were differentiated by “a” and “b” at the end of the name. For example, gages with the names LWY1cwa and LWY1cwb are on opposites of the web from each other. Gages were also placed on both the top and bottom girder flanges, which were designated “T” for top and “B” for bottom.

The last four characters of the strain gage names distinguish the location on the specimen components, except the girder flange gages. For the column web, column flange, continuity plates, and doubler plates, the four characters represent the row and

column number of the gage location. Figures A.2 through A.5 show the locations of these gages. All of the column web, continuity plate and doubler plate gages measured strain in the direction of the applied load. However, the column flange gages have one final character that describes the direction in which the strain was measured, since rosettes were often used. The “y” direction identifies the longitudinal strain or the strain parallel to the column length. The “x” direction designates the transverse strain or the strain perpendicular to the column length. The “z” direction is not actually the third-dimension, but represents the xy strain. The girder flange gages are numbered in sequence 1 through 3, as shown in Figure A.6.

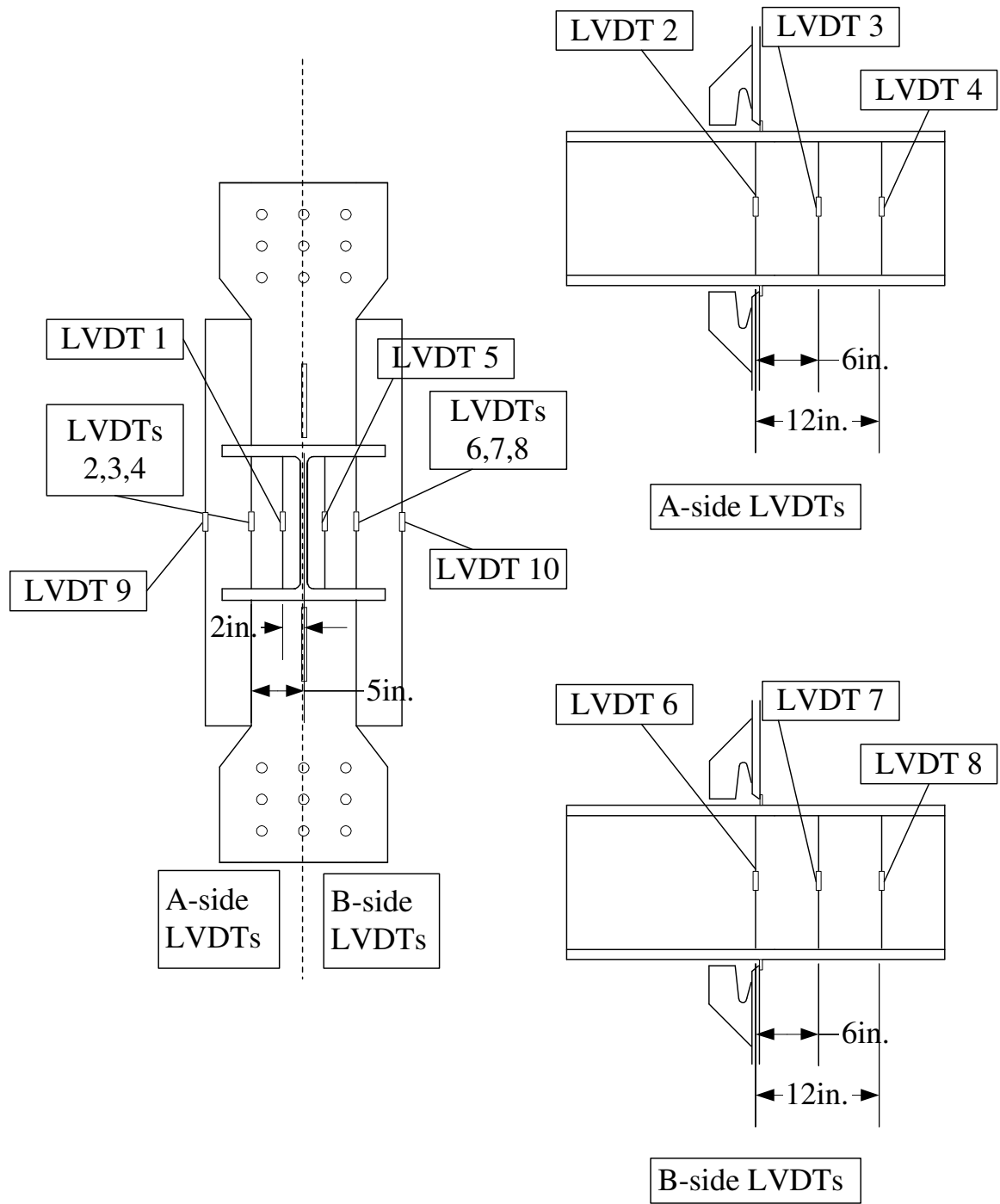
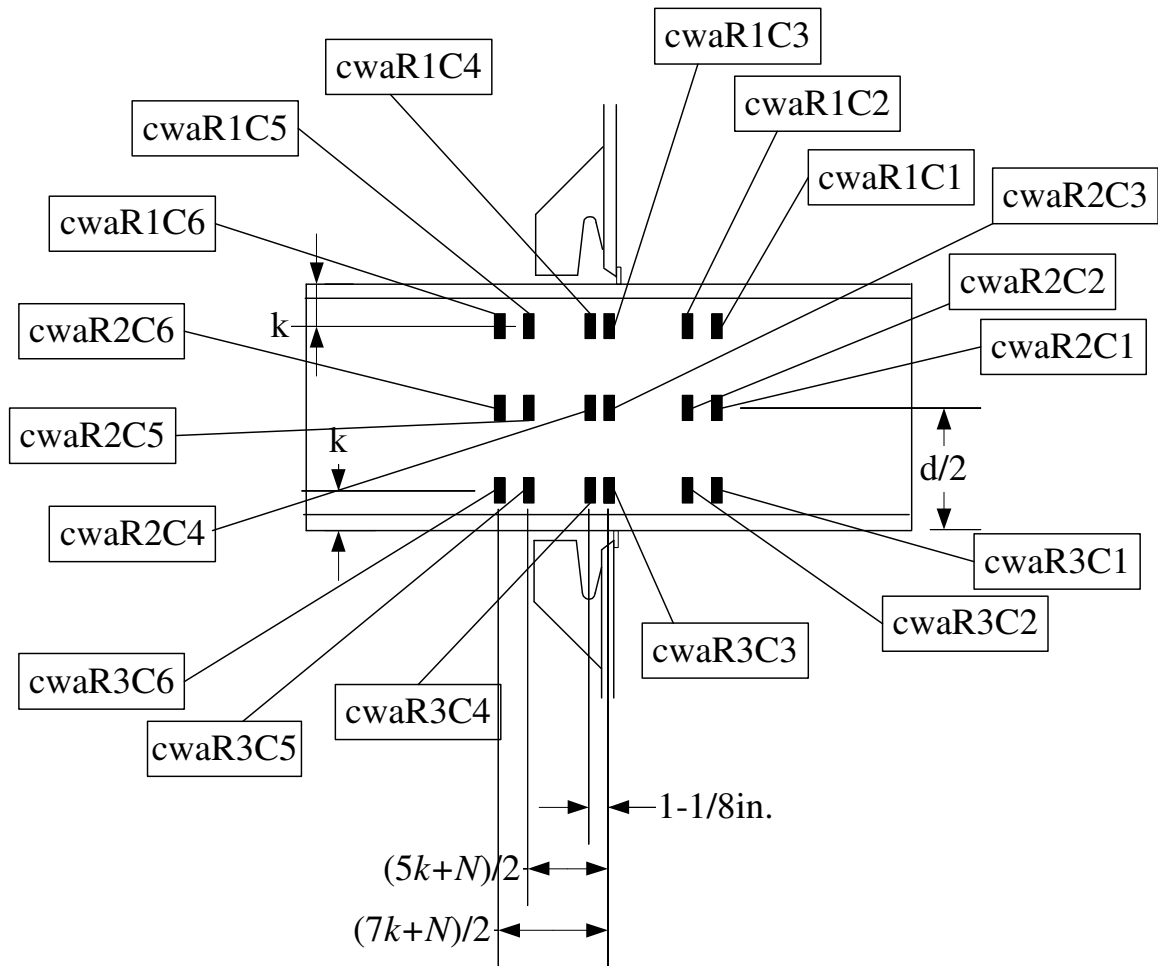


Figure A.1: LVDT Names and Locations



Gages shown are on the A-side of the column web. Gages directly on the opposite side of the web are named "cwb" instead of "cwa". The rest of the gage name is the same.

Figure A.2: Column Web Strain Gage Names and Locations

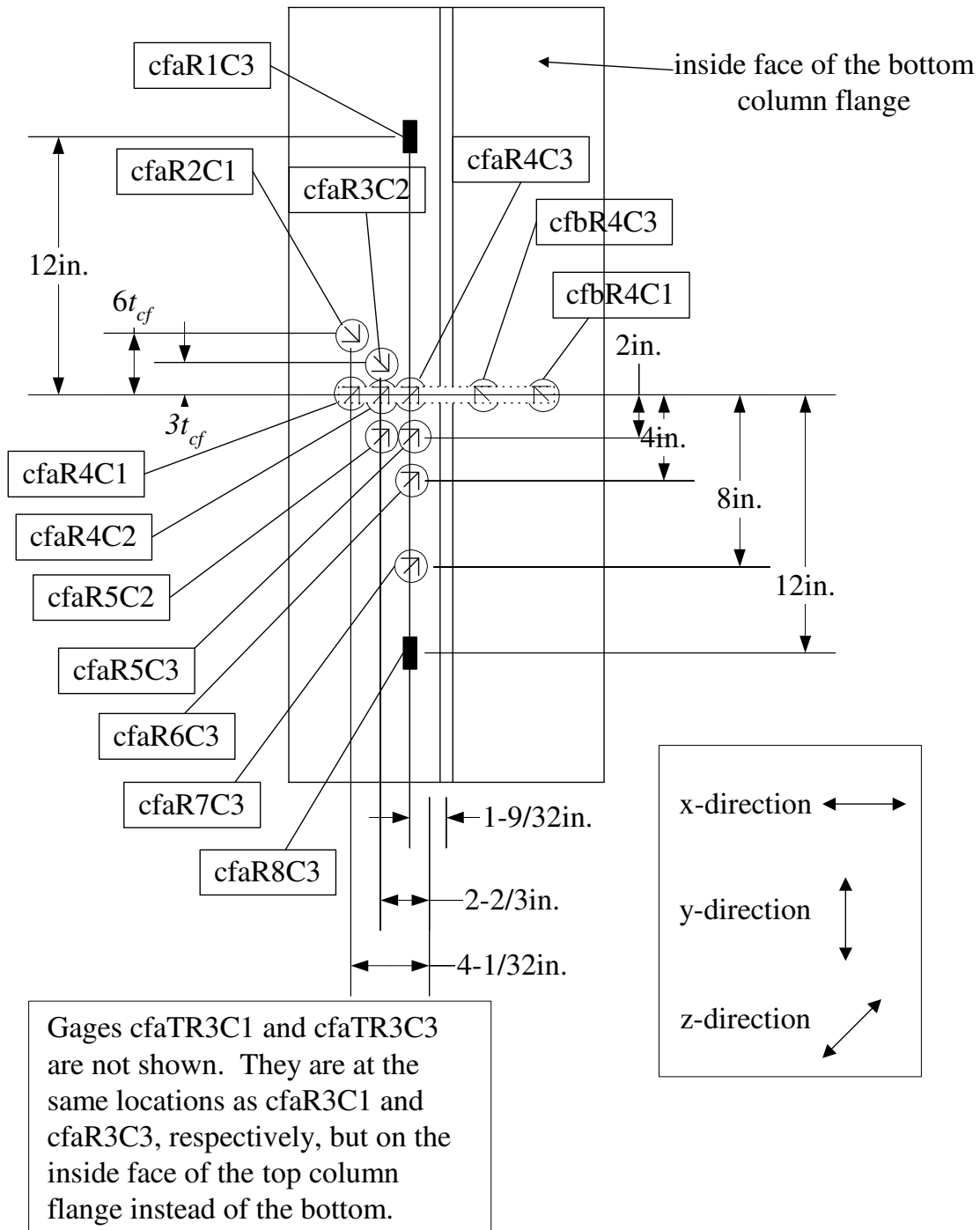
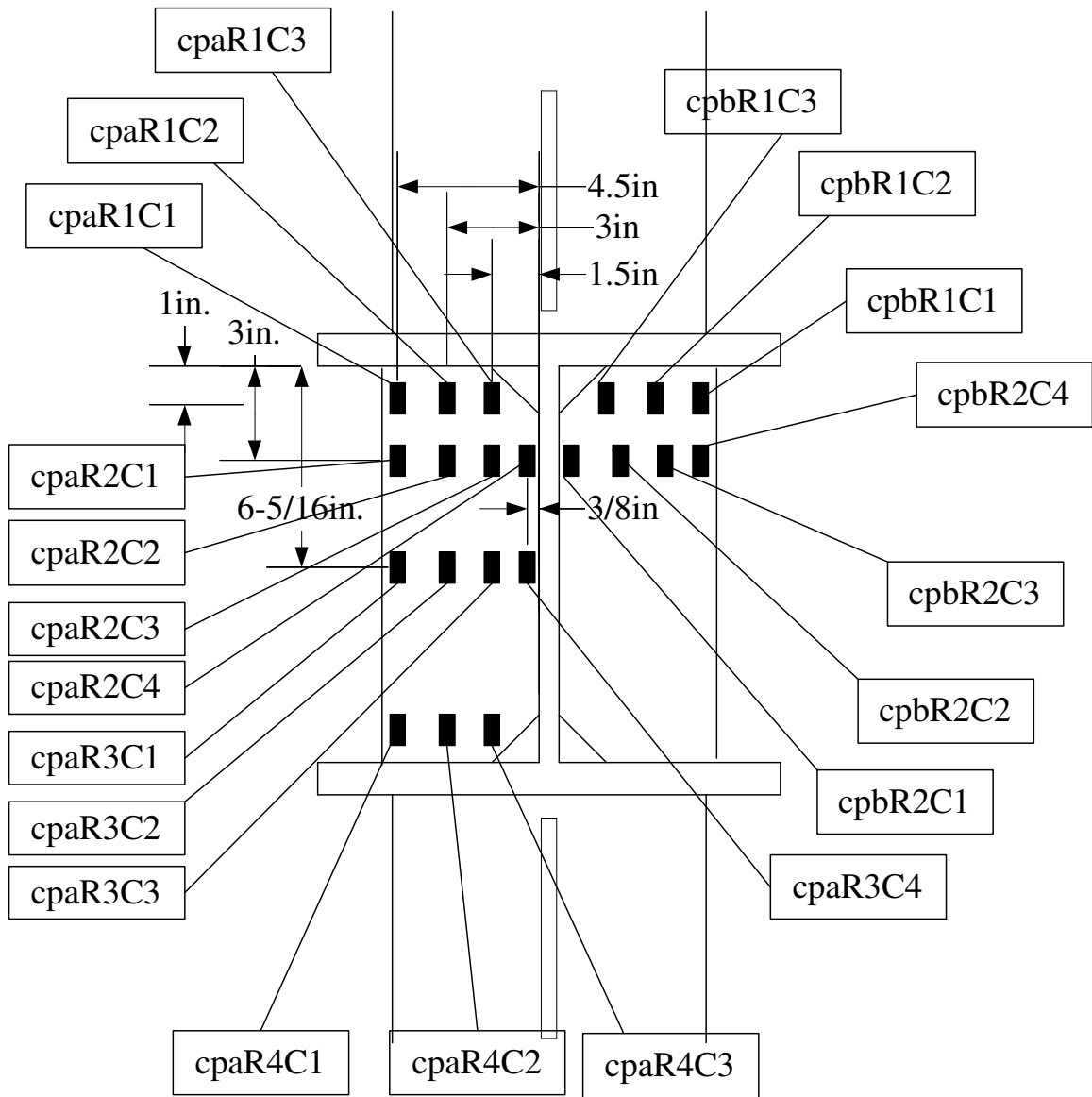
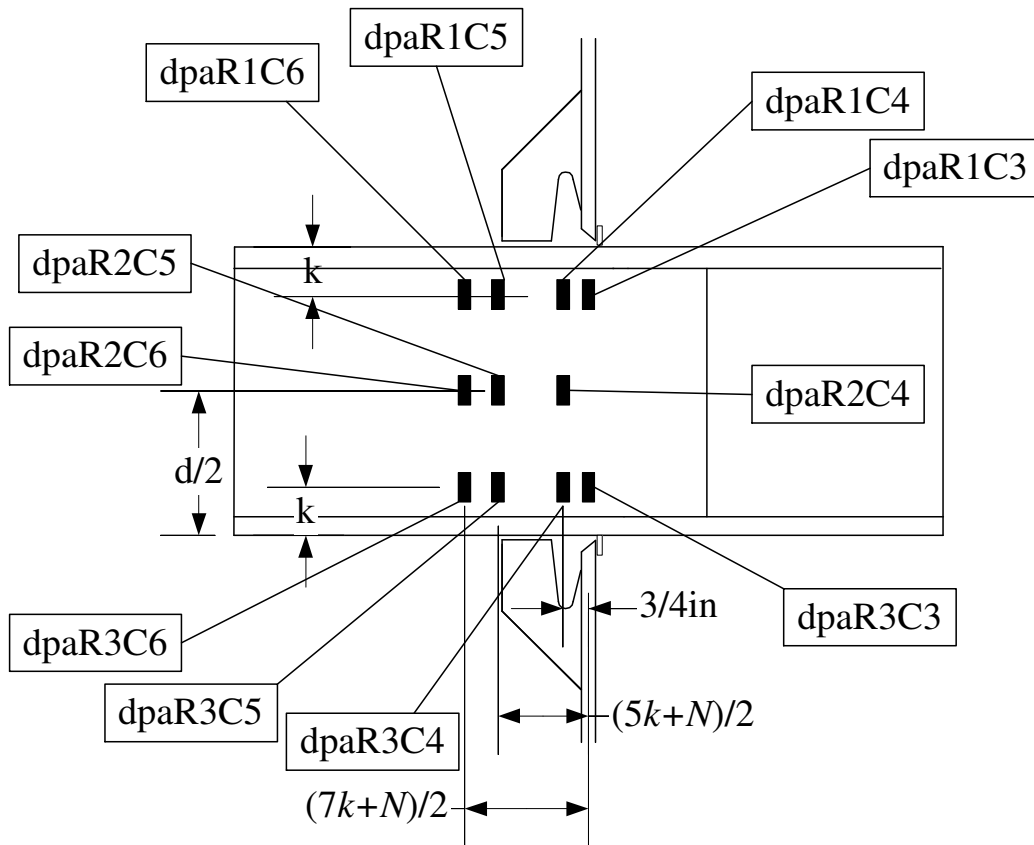


Figure A.3: Column Flange Strain Gage Names and Locations



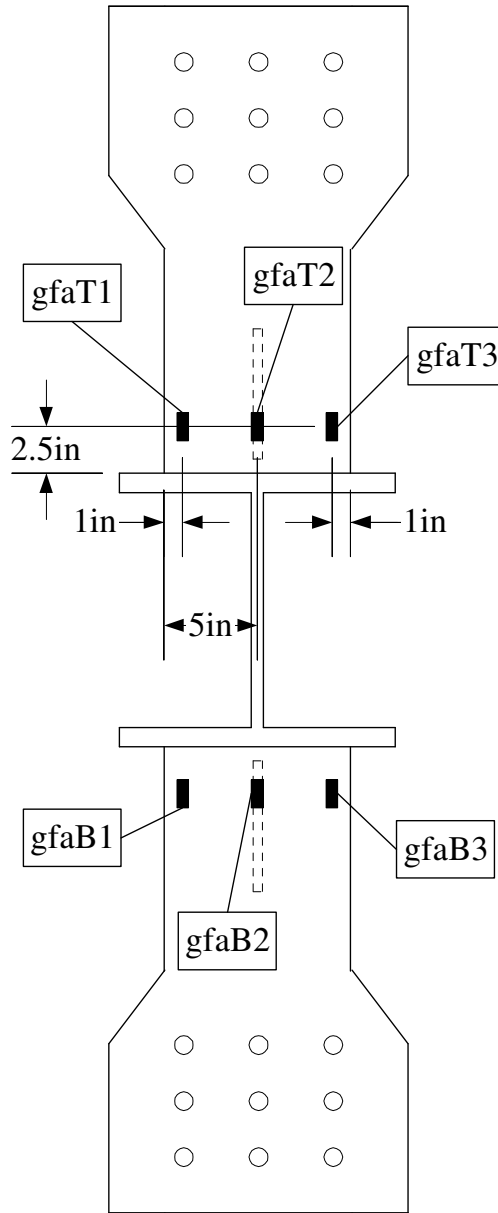
Gages on the opposite side of the continuity plates from what is shown above have the same gage names except they end with "B". For example, gage cpaR3C4 is on the side of the continuity plate shown, but gage cpaR3C4B is on the opposite side of the plate.

Figure A.4: Continuity Plate Strain Gage Names and Locations



The gages shown are on the A-side of the doubler plate detail. Gages on the doubler plate directly on the opposite side of the column web are named "dpb" instead of "dpa". The rest of the gage name is the same.

Figure A.5: Doubler Plate Strain Gage Names and Locations



The gages that are shown are on the A-side of the girder flanges (pull-plate). The gages directly on the opposite side of the pull-plates are labeled "gfb" instead of "gfa". The rest of the gage name is the same.

Figure A.6: Pull-Plate Strain Gage Names and Locations

- A.7 Load vs. Overall LVDT Displacement of Specimen 1-LFB
- A.8 Load vs. Flange LVDT Displacement of Specimen 1-LFB
- A.9 Load vs. Top Pull-Plate Gages of Specimen 1-LFB
- A.10 Load vs. Bottom Pull-Plate Gages of Specimen 1-LFB
- A.11 Load vs. Column Flange Gages in the Longitudinal Direction of Specimen 1-LFB
- A.12 Load vs. Column Flange Gages in the Transverse Direction of Specimen 1-LFB
- A.13 Load vs. Column Flange Gages in the xy Direction of Specimen 1-LFB
- A.14 Load vs. Overall LVDT Displacement of Specimen 2-LFB
- A.15 Load vs. Flange LVDT Displacement of Specimen 2-LFB
- A.16 Load vs. Top Pull-Plate Gages of Specimen 2-LFB
- A.17 Load vs. Bottom Pull-Plate Gages of Specimen 2-LFB
- A.18 Load vs. Column Flange Gages in the Longitudinal Direction of Specimen 2-LFB
- A.19 Load vs. Column Flange Gages in the Transverse Direction of Specimen 2-LFB
- A.20 Load vs. Column Flange Gages in the xy Direction of Specimen 2-LFB
- A.21 Load vs. Overall LVDT Displacement of Specimen 1-LWY
- A.22 Load vs. Flange LVDT Displacement of Specimen 1-LWY
- A.23 Load vs. Top Pull-Plate Gages of Specimen 1-LWY
- A.24 Load vs. Bottom Pull-Plate Gages of Specimen 1-LWY
- A.25 Load vs. Column Web K-Line Gages in Columns 3 and 4 of Specimen 1-LWY
- A.26 Load vs. Column Web K-Line Gages in Columns 5 and 6 of Specimen 1-LWY
- A.27 Load vs. Column Web Mid-Depth Gages of Specimen 1-LWY
- A.28 Load vs. Column Flange Gages in the Longitudinal Direction of Specimen 1-LWY
- A.29 Load vs. Column Flange Gages in the Transverse Direction of Specimen 1-LWY
- A.30 Load vs. Overall LVDT Displacement of Specimen 2-LWY
- A.31 Load vs. Flange LVDT Displacement of Specimen 2-LWY
- A.32 Load vs. Top Pull-Plate Gages of Specimen 2-LWY
- A.33 Load vs. Bottom Pull-Plate Gages of Specimen 2-LWY
- A.34 Load vs. Column Web K-Line Gages in Columns 3 and 4 of Specimen 2-LWY
- A.35 Load vs. Column Web K-Line Gages in Columns 5 and 6 of Specimen 2-LWY
- A.36 Load vs. Column Web Mid-Depth Gages of Specimen 2-LWY

- A.37 Load vs. Column Flange Gages in the Longitudinal Direction of Specimen 2-LWY
- A.38 Load vs. Column Flange Gages in the Transverse Direction of Specimen 2-LWY
- A.39 Load vs. Overall LVDT Displacement of Specimen 3-UNST
- A.40 Load vs. Flange LVDT Displacement of Specimen 3-UNST
- A.41 Load vs. Top Pull-Plate Gages of Specimen 3-UNST
- A.42 Load vs. Bottom Pull-Plate Gages of Specimen 3-UNST
- A.43 Load vs. Column Web K-Line Gages in Columns 3 and 4 of Specimen 3-UNST
- A.44 Load vs. Column Web K-Line Gages in Columns 5 and 6 of Specimen 3-UNST
- A.45 Load vs. Column Web Mid-Depth Gages of Specimen 3-UNST
- A.46 Load vs. Column Flange Gages in the Longitudinal Direction of Specimen 3-UNST
- A.47 Load vs. Column Flange Gages in the Transverse Direction of Specimen 3-UNST
- A.48 Load vs. Column Flange Gages in the xy Direction of Specimen 3-UNST
- A.49 Load vs. Overall LVDT Displacement of Specimen 1-HCP
- A.50 Load vs. Flange LVDT Displacement of Specimen 1-HCP
- A.51 Load vs. Top Pull-Plate Gages of Specimen 1-HCP
- A.52 Load vs. Bottom Pull-Plate Gages of Specimen 1-HCP
- A.53 Load vs. Column Web K-Line Gages in Columns 3 and 4 of Specimen 1-HCP
- A.54 Load vs. Column Web K-Line Gages in Columns 5 and 6 of Specimen 1-HCP
- A.55 Load vs. Column Web Mid-Depth Gages of Specimen 1-HCP
- A.56 Load vs. Column Flange Gages in the Longitudinal Direction of Specimen 1-HCP
- A.57 Load vs. Column Flange Gages in the Transverse Direction of Specimen 1-HCP
- A.58 Load vs. Column Flange Gages in the xy Direction of Specimen 1-HCP
- A.59 Load vs. Continuity Plate Gages in Rows 1 and 4 of Specimen 1-HCP
- A.60 Load vs. Continuity Plate Gages in Row 2 of Specimen 1-HCP
- A.61 Load vs. Continuity Plate Gages in Row 3 of Specimen 1-HCP
- A.62 Load vs. Overall LVDT Displacement of Specimen 1B-HCP
- A.63 Load vs. Flange LVDT Displacement of Specimen 1B-HCP
- A.64 Load vs. Top Pull-Plate Gages of Specimen 1B-HCP
- A.65 Load vs. Bottom Pull-Plate Gages of Specimen 1B-HCP

- A.66 Load vs. Column Web K-Line Gages in Columns 3 and 4 of Specimen 1B-HCP
- A.67 Load vs. Column Web K-Line Gages in Columns 5 and 6 of Specimen 1B-HCP
- A.68 Load vs. Column Web Mid-Depth Gages of Specimen 1B-HCP
- A.69 Load vs. Column Flange Gages in the Longitudinal Direction of Specimen 1B-HCP
- A.70 Load vs. Continuity Plate Gages in Row 1 of Specimen 1B-HCP
- A.71 Load vs. Continuity Plate Gages in Row 2 of Specimen 1B-HCP
- A.72 Load vs. Continuity Plate Gages in Row 3 of Specimen 1B-HCP
- A.73 Load vs. Overall LVDT Displacement of Specimen 1-FCP
- A.74 Load vs. Flange LVDT Displacement of Specimen 1-FCP
- A.75 Load vs. Top Pull-Plate Gages of Specimen 1-FCP
- A.76 Load vs. Bottom Pull-Plate Gages of Specimen 1-FCP
- A.77 Load vs. Column Web K-Line Gages in Columns 3 and 4 of Specimen 1-FCP
- A.78 Load vs. Column Web K-Line Gages in Columns 5 and 6 of Specimen 1-FCP
- A.79 Load vs. Column Web Mid-Depth Gages of Specimen 1-FCP
- A.80 Load vs. Column Flange Gages in the Longitudinal Direction of Specimen 1-FCP
- A.81 Load vs. Continuity Plate Gages in Row 1 of Specimen 1-FCP
- A.82 Load vs. Continuity Plate Gages in Row 2 of Specimen 1-FCP
- A.83 Load vs. Continuity Plate Gages in Row 3 of Specimen 1-FCP
- A.84 Load vs. Overall LVDT Displacement of Specimen 1-DP
- A.85 Load vs. Flange LVDT Displacement of Specimen 1-DP
- A.86 Load vs. Top Pull-Plate Gages of Specimen 1-DP
- A.87 Load vs. Bottom Pull-Plate Gages of Specimen 1-DP
- A.88 Load vs. Column Web K-Line Gages in Columns 3 and 4 of Specimen 1-DP
- A.89 Load vs. Column Web K-Line Gages in Columns 5 and 6 of Specimen 1-DP
- A.90 Load vs. Column Web Mid-Depth Gages of Specimen 1-DP
- A.91 Load vs. Column Flange Gages in the Longitudinal Direction of Specimen 1-DP
- A.92 Load vs. Doubler Plate Box Detail Gages in Columns 3 and 4 of Rows 1 and 3 of Specimen 1-DP
- A.93 Load vs. Doubler Plate Box Detail Gages in Columns 5 and 6 of Rows 1 and 3 of Specimen 1-DP

A.94 Load vs. Doublor Plate Box Detail Gages in Row 2of Specimen 1-DP

References

American Institute of Steel Construction (AISC) (1937). *A Manual for Architects, Engineers and Fabricators of Buildings and Other Steel Structures*, Third ed., AISC, New York, New York.

AISC (1953). *A Manual for Architects, Engineers and Fabricators of Buildings and Other Steel Structures*, Fifth ed., AISC, New York, New York.

AISC (1978). *Manual of Steel Construction – Allowable Stress Design*, Eighth ed., AISC, New York, New York.

AISC (1989). *Manual of Steel Construction – Allowable Stress Design*, Ninth ed., AISC, Chicago, Illinois.

AISC (1992). “Seismic Provisions for Structural Steel Buildings,” AISC, Chicago, Illinois.

AISC (1995). *Load and Resistance Factor Design Manual for Structural Steel Buildings*, Second ed., AISC, Chicago, Illinois.

AISC (1997). “Seismic Provisions for Structural Steel Buildings,” AISC, Chicago, Illinois.

AISC (1999a). *Stiffening of Wide-Flange Columns at Moment Connections: Wind and Seismic Applications*, Steel Design Guide Series 13, AISC, Chicago, Illinois.

AISC (1999b). *Load and Resistance Factor Design Specification for Structural Steel Buildings*, Third ed., AISC, Chicago, Illinois.

AISC k-line Advisory (1997). "AISC Advisory Statement on Mechanical Properties Near the Fillet of Wide Flange Shapes and Interim Recommendations January 10, 1997," *Modern Steel Construction*, February, pp. 18.

American Society for Testing and Materials (ASTM) (1984). "ASTM E18-84: Standard Test Methods for Rockwell Hardness and Rockwell Superficial Hardness of Metallic Materials," ASTM, Conshohocken, Pennsylvania.

ASTM (1985). "ASTM E8-85a: Tension Testing of Metallic Materials," ASTM, Conshohocken, Pennsylvania.

ASTM (1991). "ASTM E23-91: Standard Test Methods for Notched Bar Impact Testing of Metallic Materials," ASTM, Conshohocken, Pennsylvania.

ASTM (1998a). "ASTM A992/A992M: Standard Specification for Steel for Structural Shapes For Use in Building Framing," ASTM, Conshohocken, Pennsylvania.

ASTM (1998b). "ASTM A6/A6M: Standard Specification for General Requirements for Rolled Structural Steel Bars, Plates, Shapes, and Sheet Piling," ASTM, Conshohocken, Pennsylvania.

Barsom, J. M. and Pellegrino, J. V. (2000). "Failure Analysis of a Column k-Area Fracture," *Modern Steel Construction*, September, pp. 62-67.

Bjorhovde, R., Golland, L. J., and Benac, D. J. (1999). "Tests of Full-Scale Beam-to-Column Connections," Southwest Research Institute, San Antonio, Texas.

Cotton, S. C. Dexter, R. D., Hajjar, J. F., Ye, Y., Prochnow, S. D. (2001). "Column Stiffener Detailing and Panel Zone Behavior of Steel Moment Frame Connections,"

Report No. ST-01-1, Department of Civil Engineering, University of Minnesota, Minneapolis, Minnesota.

Dexter, R. J. and Melendrez, M. I. (2000). "Through-Thickness Properties of Column Flanges in Welded Moment Connections," *Journal of Structural Engineering*, ASCE, Vol. 126, No. 1, pp. 24-31.

Dexter, R. J., Graeser, M. D., Saari, W. K., Pascoe, C., Gardner, C. A., and Galambos, T. V. (2000). "Structural Shape Material Property Survey," Final Report for the Structural Shape Producers Council, University of Minnesota, Minneapolis, Minnesota.

El-Tawil, S., Mikesell, T., Vidarsson, E., and Kunnath, S. (1998). "Strength and Ductility of FR Welded-Bolted Connections," Report No. SAC/BD-98/01), Applied Technology Council, Redwood City, California.

Engelhardt, M. D. (1999). "Design of Reduced Beam Section Moment Connections," AISC North American Steel Construction Conference, Toronto, Ontario, May 19-21, 1999.

Engelhardt, M. D., Shuey, B. D., and Sabol, T. A. (1997). "Testing of Repaired Steel Moment Connections," Proceedings of the ASCE Structures Congress, Kempner, L, Brown, C. (eds.), Portland, Oregon, April 13-16, 1997, pp. 408-412.

FEMA (1995). "Steel Moment Frame Structures: Interim Guidelines," Report No. FEMA 267 (SAC-95-02), SAC Joint Venture, Sacramento, California.

FEMA (1996). "Interim Guidelines Advisory No. 1," Report No. FEMA 267A (SAC-96-03), SAC Joint Venture, Sacramento, California.

FEMA (2000a). "State-of-the-Art Report on Connection Performance," Report No. FEMA 335D, SAC Joint Venture, Sacramento, California.

FEMA. (2000b). "Recommended Seismic Design Criteria for New Moment-Resisting Steel Frame Structures," Report No. FEMA 350, SAC Joint Venture, Sacramento, California.

FEMA. (2000c). "Recommended Specifications for Moment-Resisting Steel Frames for Seismic Applications," Report No. FEMA 354, SAC Joint Venture, Sacramento, California.

FEMA. (2000d). "State of the Art Report Base Metals and Fracture," Report No. FEMA 355a, SAC Joint Venture, Sacramento, California.

FEMA. (2000e). "State of the Art Report on Joining and Inspection," Report No. FEMA 355B, SAC Joint Venture, Sacramento, California.

FEMA. (2000f). "State of the Art Report Connection Performance," Report No. FEMA 355D, SAC Joint Venture, Sacramento, California.

Fisher, J. W., Dexter, R. J., and Kaufmann, E. J. (1997). "Fracture Mechanics of Welded Structural Steel Connections", Report No. SAC 95-09, FEMA-288.

Graham, J. D., Sherbourne, A. N., Khabbaz, R. N., and Jensen, C. D. (1960). "Welded Interior Beam-to-Column Connections," Welding Research Council, Bulletin No. 63, pp. 1-28.

Goel, S. C., Stojadinovic, B., Lee, L. H., Margarian, A. G., Choi, J. H., Wongkaew, a., Reyher, B. P., and Lee, D. Y. (1998). "Conduct Parametric Tests of Unreinforced Connections," Preliminary Report to SAC, Task 7, Subtask 7.02, University of Michigan, Ann Arbor, Michigan.

Haaijer, G. (1958). "Plate Buckling in the Strain Hardening Range," *Proceedings of the ASCE*, Vol. 83, EM-2, pp. 1581.

Iwankiw, N. (1999). Personal communication, June 24, 1999.

Johnson, L.G. (1959a). "Tests on Welded Connections between I-Section Beams and Stanchions," *British Welding Journal*, Vol. 6, No. 1, pp. 38-46.

Johnson, L.G. (1959b). "Further Tests on Welded Connections between I-Section Beams and Stanchions," *British Welding Journal*, Vol. 6, No. 1, pp. 367-373.

Johnson, L.G. (1959c). "Compressive and Tensile Loading Tests on Joists with Web Stiffeners," *British Welding Journal*, Vol. 6, No. 1, pp. 411-420.

Kaufmann, E. J., Xue, M., Lu, L. W., and Fisher, J. W. (1996a). "Achieving Ductile Behavior of Moment Connections," *Modern Steel Construction*, January, pp. 30-39.

Kaufmann, E. J., Xue, M., Lu, L. W., and Fisher, J. W. (1996b). "Achieving Ductile Behavior of Moment Connections," *Modern Steel Construction*, June, pp. 38-42.

Leon, R. T., Hajjar, J. F., and Gustafson, M. A. (1998). "Seismic Response of Composite Moment-Resisting Connections. I: Performance," *Journal of Structural Engineering*, ASCE, Vol. 124, No. 8, pp. 868-876.

Parkes, E. W. (1952). "The Stress Distribution Near a Loading Point in a Uniform Flanged Beam," *Philosophical Transactions of the Royal Society*, Vol. 244A, pp. 417-467.

Popov, E. P., Amin, N. R., Louie, J. J. C., and Stephen, R. M. (1986). "Cyclic Behavior of Large Beam-Column Assemblies," *Engineering Journal*, AISC, Vol. 23, No. 1, pp. 9-23.

Ricles, J. M., Mao, L., Kaufmann, E. J., Lu, L., and Fisher, J. W. (2000). "Development and Evaluation of Improved Details for Ductile Welded Unreinforced Flange Connections," SAC BD 00-24, SAC Joint Venture, Sacramento, California.

Roeder, C. W. (1997). "An Evaluation of Cracking Observed in Steel Moment Frames," Proceedings of the ASCE Structures Congress, Kempner, L., Brown, C. (eds.), Portland, Oregon, April 13-16, 1997, ASCE, New York, New York, pp. 767-771.

Roeder, C. W. (2000). "Connection Performance State of the Art Report," University of Washington, Seattle, Washington.

SAC Joint Venture (SAC) (1996). "Technical Report: Experimental Investigations of Beam-Column Subassemblages," Report No. SAC-96-01, SAC Joint Venture, Sacramento, California.

Salmon, C. G., and Johnson J. E. (1996). *Steel Structures: Design and Behavior, Emphasizing Load and Resistance Factor Design*, Fourth ed., Harper Collins Publishers Inc., New York, New York.

Sherbourne, A. N., and Jensen, C. D. (1957). "Direct Welded Beam Column Connections," Report. No. 233.12, Fritz Laboratory, Lehigh University, Bethlehem, Pennsylvania.

Structural Stability Research Council (SSRC) Task Group. (1998). "SSRC Technical Memorandum No. 7: Tension Testing," SSRC, Bethlehem, Pennsylvania.

Stojadinovic, B., Goel, S., and Lee, K. (1999). "Welded Steel Moment Connections – Old and New," *Structural Engineering in the 21st Century*, Proceedings of the ASCE Structures Congress, Avenet, R. R. and Alawady, M. (eds.), New Orleans, Louisiana, April 18-21, 1999, ASCE, Reston, Virginia, pp. 789-792.

Tide, R. H. (1999). "Evaluation of Steel Properties and Cracking in the 'k' -area of W Shapes," *Engineering Structures*, Vol. 22, pp. 128-124.

Tremblay, R., Timler, P., Bruneau, M., and Filiatrault, A. (1995). "Performance of Steel Structures during the 1994 Northridge Earthquake," *Canadian Journal of Civil Engineering*, Vol. 22, pp. 338-360.

Uang, C. M., Yu, Q.S., and Bondad, D. (1998). "Dynamic Testing of Pre-Northridge and Haunch-Repaired Steel Moment Connections," *Research on the Northridge, California Earthquake of January 17, 1994*, Proceedings of the NEHRP Conference and Workshop, NEHRP, Vol. III-B, pp. 790-737.

Wood, R. H. (1955). "Yield Line Theory," Research Paper No. 22, Building Research Station.

Ye, Y., Hajjar, J. F., Dexter, R. D., Prochnow, S. C., Cotton, S. C. (2000). "Nonlinear Analysis of Continuity Plate and Doubler Plate Details in Steel Moment Frame Connections," Report No. ST-00-3, Department of Civil Engineering, University of Minnesota, Minneapolis, Minnesota.

Yee, R. K., Paterson, S. R., and Egan, G. R. (1998). "Engineering Evaluations of Column Continuity Plate Detail Design and Welding Issues in Welded Steel Moment Frame Connections," *Welding for Seismic Zones in New Zealand*, Aptech Engineering Services, Inc., Sunnyvale, California.